THESIS FOR THE DEGREE OF DOCTOR OF PHILOSOPHY

Characterising turbulent ship wakes from an environmental impact perspective

AMANDA T. NYLUND

Department of Mechanics and Maritime Sciences

CHALMERS UNIVERSITY OF TECHNOLOGY

Gothenburg, Sweden 2023

Characterising turbulent ship wakes from an environmental impact perspective

AMANDA T. NYLUND
ISBN 978-91-7905-898-2

Doctoral Thesis at Chalmers University of Technology
Serial number: 5364
ISSN 0346-718X

Department of Mechanics and Maritime Sciences
Chalmers University of Technology
SE-412 96 Gothenburg
Sweden
Telephone + 46 (0)31-772 1000

Cover:
The top figure is an echogram of the bubble cloud of a turbulent wake, observed from below by an Acoustic Doppler Current Profiler (ADCP). The bottom figure is the calculated turbulent kinetic energy dissipation rate (ε) for the same wake, indicating the vertical extent and duration of the ship-induced turbulence. The water depth is 30 m. For more details see Figure 3 in **Paper I**.

Printed by Chalmers digitaltryck.
Gothenburg, Sweden 2023

ABSTRACT

The world's oceans, especially coastal areas, are intensively trafficked by ships. All these ships exert pressure on the marine environment, through emission to the atmosphere, discharges of pollutants to the water, and physical disturbance through energy input. Of these impacts, energy pollution from shipping has received the least attention. Especially the impact of ship-induced turbulence in the wake, which is induced by the hull friction and propeller, and remains for up to 15 minutes. The turbulent wake can impact the spread of contaminants, affect air-sea gas exchange, physically disturb plankton, and potentially impact local biogeochemistry through increased entrainment and vertical mixing. To assess these impacts, an understanding of the turbulent wake development and interaction with surface ocean stratification, is essential. However, characterisation of the turbulent wake development in time and space, especially in stratified conditions, is challenging and requires an interdisciplinary approach.

The aim of this thesis is to advance the understanding of turbulent wake development from an environmental impact perspective. The intensity and spatiotemporal extent of the turbulent wake, and its impact, have been investigated through a combination of *in situ* and *ex situ* observations, and Computational Fluid Dynamic (CFD) modelling of ships in full-scale. The unique dataset of several hundred *in situ* turbulent wake observations, showed large variation in spatiotemporal extent and intensity. Wake depths can reach down to 30 m, and the turbulent intensities in the near wake are 1–3 orders of magnitude higher than generally observed in the upper ocean surface layer. In addition, during stratified conditions ship-induced turbulence entrain water from below the pycnocline, with implications for local nutrient input and primary production in the ocean surface layer. In addition, ship-passages were observed to frequently trigger large methane emissions in an estuarine shipping lane.

The results highlight the importance of addressing ship-induced turbulence in marine environmental management. Intensively trafficked coastal areas should be considered anthropogenically impacted, even unnatural, with respect to turbulence. The interdisciplinary approach applied in this thesis, is a first step towards a holistic assessment of the environmental impact of the turbulent wake.

SVENSK SAMMANFATTNING

Världens hav, speciellt kustnära områden, är intensivt trafikerade av fartyg. Alla dessa fartyg påverkar den marina miljön via luftutsläpp till atmosfären, utsläpp av olika föroreningar till vattnet, och fysisk påverkan genom tillförsel av energi. Av dessa olika typer av påverkan, så har tillförseln av energi från fartyg studerats minst. Det gäller framför allt påverkan från fartygsinducerad omblandning i kölvattnet (turbulenta vaken), vilken genereras av friktion från skrovet och propellern, och kan bestå i upp till 15 minuter. Den turbulenta vaken kan påverka hur föroreningar sprids, gasutbytet mellan hav och atmosfär, den kan utsätta plankton för fysisk påverkan, och kan potentiellt påverka lokal biogeokemi genom en ökad vertikal omblandning och uppblandning av näringsrikt djupvatten. För att uppskatta dessa olika typer av påverkan, så krävs förståelse för hur den turbulenta vaken utvecklas över tid och hur vaken interagerar med ett skiktat ytvattnet. Att karaktärisera den turbulenta vakens utbredning i tid och rum är dock komplicerat, speciellt under skiktade förhållanden, och kräver ett tvärvetenskapligt tillvägagångssätt.

Syftet med denna avhandling är att öka förståelsen för den turbulenta vakens utveckling utifrån ett miljöpåverkansperspektiv. Vakens intensitet och utbredning har studerats genom en kombination av *in situ* och *ex situ* observationer, och beräkningsströmningsdynamik (CFD) modellering av fartyg i verklig skala. Det unika datasetet av hundratals *in situ* observationer av turbulenta vakar, visade stor variation av intensitet och utbredning. Vakar kan nå ner till 30 m djup och den turbulenta intensiteten i vakområdet närmast fartyget är 1–3 storleksordningar större än vad som vanligtvis uppmäts i den övre delen av vattenmassan. Under skiktade förhållanden så orsakar den turbulenta vaken uppblandning av djupare vatten vid språngskiktet, vilket lokalt kan ha betydelse för ytvattnets närsaltstillförsel och primärproduktion. Utöver detta, så har fartyg observerats att frekvent inducera stora utsläpp av metan i en kustnära farled.

Resultaten presenterade i denna avhandling, belyser vikten av att inkludera fartygsinducerad turbulens i marin miljöförvaltning. Kustnära områden med intensiv fartygstrafik bör anses vara utsatta för mänsklig påverkan, och onaturliga med avseende på turbulens. Det interdisciplinära arbetssätt som använts, är ett första steg mot en holistisk bedömning av miljöpåverkan från den turbulenta fartygsvaken.

ACKNOWLEDGEMENTS

This thesis could not have been written without the support from my supervisors, co-authors, colleagues, friends, and family. First, I would like to thank my main supervisor Ida-Maja, because this thesis would probably never have started nor ended, without your endless support and determination. I am so grateful that I have been on this journey with you. I would also like to thank my co-supervisors Anders, for always being positive and sharing your knowledge, and Lars, for your honest opinions and generous support. I feel really lucky to have been working in a team with you. I would also like to thank Rickard, for the great support in my work and our interesting discussions. I also want to thank my examiner Sverker, for his support and relevant critique.

I want to thank all my co-authors for taking a dive into turbulent wake studies with me. Ulf, for introducing me to remote sensing and always making me smile. Alexander, Igor, and Debabrota, for developing the deep learning model, and being ever patient in answering my questions. Martin and Göran, for the joint effort during the field work in Öresund. Johan, Kent, Jukka-Pekka, and Vladimir, for increasing my knowledge about the atmospheric side of things.

I also want to thank all my colleagues at the division of Maritime Studies, for your support and input through the years. I would like to especially thank my junior research colleagues, past and present, for making my days at the office so enjoyable! A special thanks to my roomie Anna L-H, for being so sensible and kind, and for sharing our Arctic adventure. A huge thank you to Elin M, for being my emotional support and making my life a million times better. I am so happy that I could share this time with you. A huge tank you to Anna K, Anders, Jannik, Katrin, and Marco, for helping me survive the pandemic and for being my found family. Thank you also to Adam and Marcus, for fulfilling my dream of going to the Arctic.

I want to thank my amazing family, for your endless love and support, and for brightening my day every day. Mum and dad, for always being there for me. Erland and Siri, for your help and encouragement, I am so lucky to be your sister. This would not have been possible without you! Thank you Lotta for being my forever partner in crime. I want to thank my grandmother, for your encouragement and inspiration, my aunt for all the great time we've spent together the past year, my uncle and cousins for bringing the life to the party, and all my extended family. Thank you to everyone at Mannakull, for letting me be part of your family.

Thank you Elin Ö, for being there when I need it the most, having you in my life makes everything better. Astrid and Anna-Li, for being with me from the start of this journey. Thank you, Amanda, Gabriella, and Elin H, for our epic adventures that have made me survive the past two years. Thank you, Karin B and Sigrid, for your love and support, even when times are rough.

I am so grateful for having all of you in my life!

FUNDING

Paper I: Acknowledgment of funding for the OCEANSensor project by the Research Council of Norway (project number 284628) and co-funding by the European Union 2020 Research and Innovation Program, as part of the MarTERA Program.

Paper II: Acknowledgement of funding from the Area of Advance Transport, Chalmers University of Technology.

Paper III: Acknowledgement of funding to the European Union's Horizon 2020 research and innovation programme Evaluation, control and Mitigation of the EnviRonmental impacts of shippinG Emissions (EMERGE) [grant agreement No 874990], the Swedish Agency for Marine and Water Management [grant agreement No 810-23] and Chalmers Area of Advance Transport, and OCEANSensor, EU-Martera [project nr: 284628]. The computations were enabled by resources provided by the Swedish National Infrastructure for Computing (SNIC) at NSC partially funded by the Swedish Research Council through grant agreement no. 2018-05973.

Paper IV: Acknowledgement of funding to the Swedish Agency for Marine and Water Management [grant agreement No 810-23] and Chalmers Area of Advance Transport. The computations were enabled by resources provided by the Swedish National Infrastructure for Computing (SNIC) at NSC partially funded by the Swedish Research Council through grant agreement no. 2018-05973. Acknowledge of support from InfraVis for providing application expertise for visualisation through Swedish Research Council grant 2021-00181.

LIST OF PUBLICATIONS

PAPER I

Nylund, A. T., Arnebog, L., Tengberg, A., Mallast, U. & Hassellöv, I. M. 2021. In situ observations of turbulent ship wakes and their spatiotemporal extent. *Ocean Science*, 17, 1285–1302.

Author contribution:
I-M. Hassellöv, **A. T. N.**, L. Arneborg and A. Tengberg conceptualised and conducted the in situ field measurements and consecutive analysis and visualisation. **A. T. N.** developed the code used in the analysis, with contribution from L. Arneborg. U. Mallast conducted the data curation and formal analysis of the satellite images, with contribution from **A. T. N.**. The manuscript was prepared by **A. T. N.** with contributions from all co-authors.

PAPER II

Ryazanov, I., **Nylund, A. T**., Basu, D., Hassellöv, I.-M. & Schliep, A. 2021. Deep Learning for Deep Waters: An Expert-in-the-Loop Machine Learning Framework for Marine Sciences. *Journal of Marine Science and Engineering,* 9**,** 169.

Author contribution:
I.R. and **A.T.N.** contributed equally to this work. A.S. and I.-M.H. conceived and supervised the study. All authors contributed to the design of the study. **A.T.N**. and I.-M.H. acquired the acoustic data, and **A.T.N**. performed the data annotation. I.R. and D.B. developed the method, the testing procedure and performed data analysis; the method was implemented by I.R. under supervision by D.B. The initial draft was written by I.R. and **A.T.N**. All authors discussed, read, edited and approved the article. All authors have read and agreed to the published version of the manuscript.

PAPER III

Nylund, A. T., Hassellöv, I-M., Tengberg, A., Bensow, R., Broström, G., Hassellöv, M., & Arneborg, L.. Hydrographical implications of ship-induced turbulence in stratified waters studied through field observations and CFD modelling. (To be submitted to Frontiers in Marine Science special issue: *Advances in Ship Wake Studies*)

Author contribution:
All authors contributed to the conceptualization, methodology, and formal analysis of the paper. **A.T.N**, I-M.H., A.T., G.B., and M.H conducted the field work. **A.T.N**, R.B., and L.A visualized the data. **A.T.N.** wrote the original draft, which was reviewed and edited by all authors. G.B., M.H, I-M.H., and A.T. were responsible for the funding acquisition, modelling resources were provided by R.B. and field equipment resources by L.A., G.B., M.H, A.T, and I-M.H. **A.T.N.** was supervised by I-M.H., A.T., and L.A.

PAPER IV

Nylund, A. T., Mellqvist, J., Conde, V., Salo, K., Bensow, R., Arnebog, L., Jalkanen, J-P., Tengberg, A., & Hassellöv, I. M.. Coastal methane emissions triggered by ship passages. (*Draft*)

Author contribution:
J.M., I-M.H. and R.B. were responsible for the conceptualization of the study. **A.T.N**, J.M., V.C., R.B, K.S, J-P.J., I-M.H., and L.A. developed and designed the methodology. J.M., V.C., and K.S. conducted the field work. **A.T.N**, J.M., V.C., and J-P.J. developed the software and code. **A.T.N**., J.M., V.C., L.A. and R.B conducted the formal analysis. Visualization of the data was made by **A.T.N** and R.B. in dialogue with I-M.H., L.A., J.M., and V.C. **A.T.N.** wrote the original draft, which was reviewed and edited by all authors. Funding was acquired by I-M.H., J.M., R.B. and A.T. modelling resources provided by R.B and J-P.J., and field work resources by J.M., V.C., K.S., L.A. A.T. and I.-M.H. **A.T.N.** was supervised by I-M.H., L.A., and A.T.

OTHER RELEVANT PUBLICATIONS, NOT INCLUDED IN THE THESIS

Ytreberg, E., Hassellöv, I.-M., **Nylund, A. T.**, Hedblom, M., Al-Handal, A. Y. & Wulff, A. 2019. Effects of scrubber washwater discharge on microplankton in the Baltic Sea. *Marine Pollution Bulletin,* 145**,** 316-324.

Nylund, A. T., Bensow, R., Liefvendahl, M., Eslamdoost, A., Arneborg, L., Hassellöv, I.-M., Tengberg, A. & Broström, G. 2021. Modellering av omblandning i fartygs kölvatten, för ökad förståelse av belastning på havsmiljön till följd av utsläpp från fartyg. Uppdragsrapport för Havs- och vattenmyndigheten, 2020. Projekt: Miljövänligare sjöfart Dnr 796-20.

Ytreberg, E., Karlberg, M., Hassellöv, I.-M., Hedblom, M., **Nylund, A. T.**, Salo, K., Imberg, H., Turner, D., Tripp, L., Yong, J. & Wulff, A. 2021. Effects of seawater scrubbing on a microplanktonic community during a summer-bloom in the Baltic Sea. *Environmental Pollution*, 291, 118251.

Snoeijs-Leijonmalm, P. and the SAS-Oden 2021 Scientific Party (2022). Expedition Report SWEDARCTIC Synoptic Arctic Survey 2021 with icebreaker Oden. Swedish Polar Research Secretariat. 300 pp.

Prytherch, J., Murto, S., Brown, I., Ulfsbo, A., Thornton, B., Brüchert, V., Tjernström, M., Lunde Hermansson, A., **Nylund, A. T.**, Holthusen, L. 2023. Central Arctic Ocean surface-atmosphere exchange of CO2 and CH4 constrained by direct measurements. (*Accepted for interactive public peer review in Biogeoscience, 2023-05-19, bg-2023-82*)

ABBREVIATIONS

ADCP	Acoustic Doppler Current Profiler
AIS	Automatic Identification System, a tracking system for ships.
AUV	Autonomous Underwater Vehicle
CFD model	In this thesis, CFD model refers to a high resolution Computational Fluid Dynamic (CFD) model used for optimising the ship hull and propeller design, which models the turbulent wake up to a few ship lengths behind the ship.
CNN	Convolutional Neural Network
CRDS	Cavity Ring-Down Spectrometer
CTD	An instrument used to measure Conductivity, Temperature and Depth
DDES	Delayed Detached Eddy Simulation
ε	Turbulent kinetic energy dissipation rate
EC	Eddy-Covariance
EU	European Union
FNR	False Negative Rate
GMM	Gaussian Mixture Model
HELCOM	Baltic Marine Environment Protection Commission, also the Helsinki Commission
IMO	International Maritime Organisation
IR	Infrared
MBES	Multibeam Echo Sounder
ML	Machine Learning
RANS	Reynolds-averaging Navier-Stokes model
RoPax	A roll-on/roll-off and passenger vessel, transporting vessels, cargo, and passengers.
RoRo	A roll-on/roll-off vessel, transporting cargo
ROV	Remotely Operated Vehicle
SAR	Surface aperture radar
SST	Sea Surface Temperature
STEAM	Ship Traffic Emission Assessment Model

TABLE OF CONTENTS

1 INTRODUCTION

The shipping industry is a vital part of the global economy (Millefiori et al., 2021, UNCTAD, 2022), and intense ship traffic is prevalent in coastal regions around the world (Figure 1) (Fu et al., 2017, Corbett et al., 1999). This intensive shipping gives rise to a multitude of environmental pressures and is one of the anthropogenic stressor categories with the largest impact in coastal marine environments (Halpern et al., 2019). Ships can be compared to floating industries, and their environmental pressures include air emissions of greenhouse gases and particulate matter (Corbett et al., 1999, Balcombe et al., 2019), direct discharges of pollutants, contaminants, and acidifying substances to the marine environment (Andersson et al., 2016, Moldanová et al., 2018, Hassellöv et al., 2019, Jalkanen et al., 2021), and different types of physical disturbances such as underwater noise (Duarte et al., 2021, Popper and Hawkins, 2016) and ship-induced waves and turbulence (Kelpšaite et al., 2009, Soomere, 2005, Soomere and Kask, 2003, Gabel et al., 2017, Jürgensen, 1991)(**Paper I**, **Paper III**). Of these different pressures, ship-induced turbulence has received little attention, and there are large knowledge gaps regarding its extent, intensity, and potential impacts. Still, ship-induced turbulence should be considered a type of anthropogenic energy pollution (European Parliament, 2008, Soomere, 2005), and should be included in holistic assessments of the environmental impact from shipping.

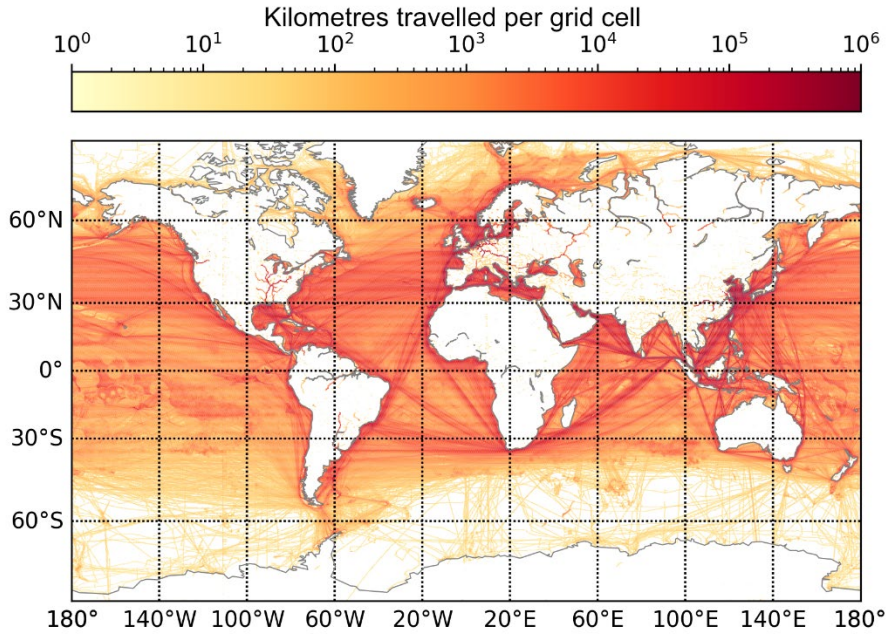

Figure 1. Global ship traffic density based on AIS data from 2022 (**Paper IV**), derive using the Ship Traffic Emission Assessment Model (STEAM) (Jalkanen et al., 2009). The colour bar indicates the number of kilometres travelled every year in each 0.1° x 0.1° grid cell. Assuming travels in a north south direction of the grid cell, values of 10^4 and 10^6 km travelled y^{-1} correspond to approximately 250 and 2.5 passages day^{-1} respectively.

When a ship moves through water, the ship's propeller and hull friction induce turbulence in a wake behind the vessel (NDRC, 1946, Trevorrow et al., 1994, Soloviev et al., 2010, Voropayev et al., 2012, Francisco et al., 2017, Golbraikh and Beegle-Krause, 2020). Previous studies have found that the turbulent wake can be sustained for 10–30 minutes, expand to widths of 100–250 m, and reach depths of 10–18 m (Table 1). Thus,

shipping contributes with turbulence input to the upper ocean surface layer. In areas with intense ship traffic and low wind- and tide-induced turbulence, the relative contribution from shipping could be substantial (**Paper I**). Previous studies of ship wakes have been performed in a diverse set of scientific fields (Figure *2*).

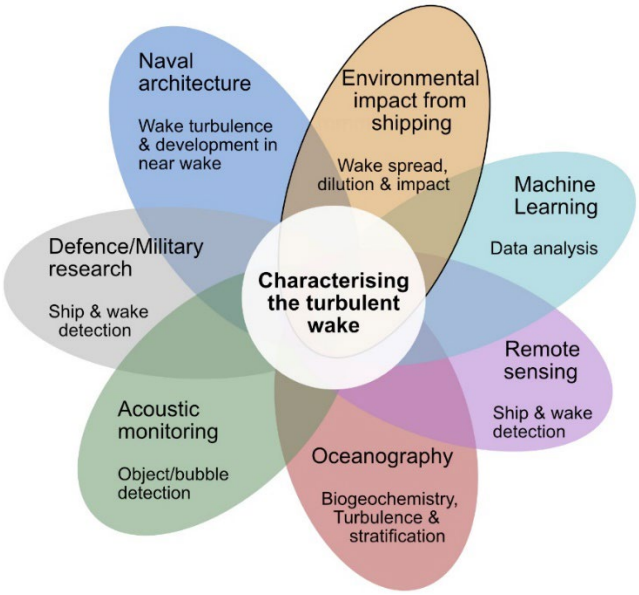

Figure 2. Scientific fields relevant for turbulent wake characterisation.

These studies have mainly focused on wake detection (Smirnov et al., 2005, Liefvendahl and Wikström, 2016, NDRC, 1946), the dilution of pollutants in the wake region (Loehr et al., 2001, US-EPA, 2002, Katz et al., 2003, Golbraikh and Beegle-Krause, 2020, Chou, 1996, Lewis, 1985, Byrne et al., 1988, Situ and Brown, 2013), and erosion and turbidity induced by ship-induced surface waves in the Kelvin wake pattern (Figure 3a) (Kelpšaite et al., 2009, Soomere, 2005, Soomere and Kask, 2003, Gabel et al., 2017). Jürgensen (1991) was the first to consider the direct environmental impact of the ship induced turbulence and investigated how the vertical mixing induced by the turbulent wake affected local hydrographical conditions through a deepening of the surface mixed layer, i.e., affecting water column stratification. Since then, field observations of turbulent wakes penetrating the stratification (Loehr et al., 2001) and increasing the stratification depth (Lindholm et al., 2001) have been made. Turbulent intensities and durations similar to a ship's turbulent wake have been found to increase plankton mortality, potentially impacting nutrient availability in areas with intense ship traffic (Bickel et al., 2011, Garrison and Tang, 2014). The bubbles and turbulence in the wake region can also impact air-sea gas exchange (Weber et al., 2005, Emerson and Bushinsky, 2016)(**Paper IV**).

Despite awareness of the potential impacts of ship-induced turbulence, there are no available studies where wake turbulence intensities have been quantified *in situ* for full-scale ships (Carrica et al., 1999, Parmhed and Svennberg, 2006, Ermakov and Kapustin, 2010, Golbraikh and Beegle-Krause, 2020, Kouzoubov et al., 2014). Moreover, few studies reporting results on the turbulent wake extent have been conducted in conditions where the interaction between the turbulent wake and stratification could be assessed (Table 1). Stratification can both affect and be affected by the turbulent wake (Lindholm et al., 2001, Jürgensen, 1991, Jacobs, 2020, Merritt, 1972, Watson et al., 1992, Lin and Pao, 1979). Thus, for the wake characterisation to be representative for

naturally stratified coastal environments, where shipping often is intensive, the interaction between the turbulent wake and stratification needs to be addressed. There are estimates of the wake turbulence from model-scale laboratory experiments and numerical modelling (e.g. (Milgram et al., 1993, Hoekstra and Ligtelijn, 1991, Loberto, 2007, Wall and Paterson, 2020)). However, the model scale results are not directly applicable for full-scale ships in natural conditions, and numerical models of turbulent ship wakes in stratified conditions is a field currently in development (Wall and Paterson, 2020). In summary, there is currently no characterisation of the turbulent wake that allow for estimations of the environmental impact of ship-induced turbulence from full-sized ships in natural stratified conditions (Wall and Paterson, 2020, Soomere, 2007, Golbraikh and Beegle-Krause, 2020).

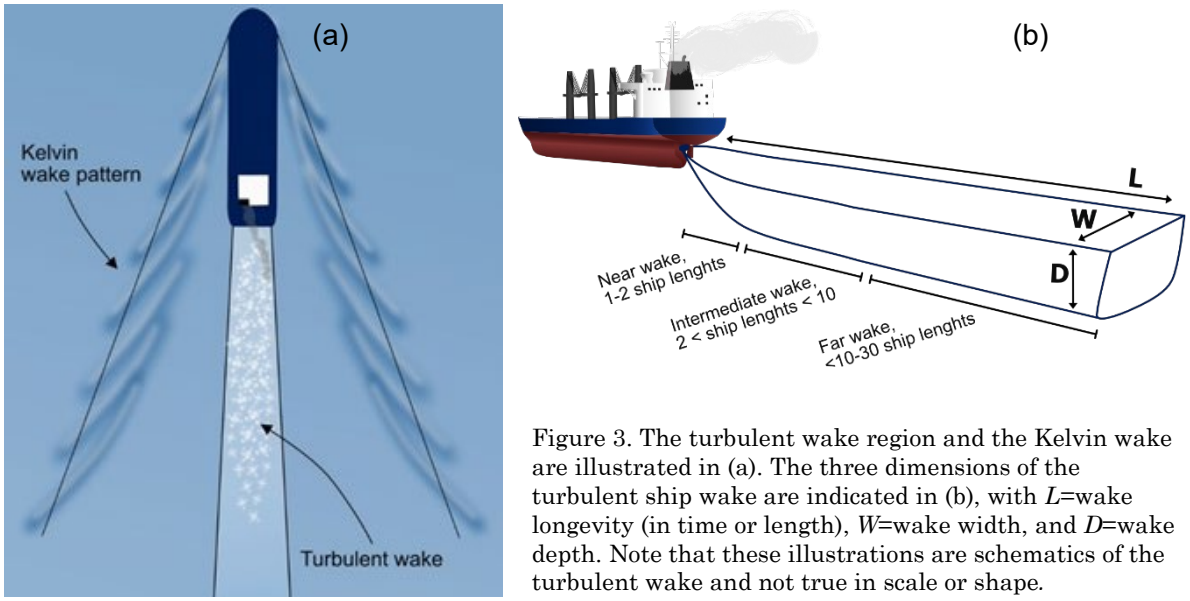

Figure 3. The turbulent wake region and the Kelvin wake are illustrated in (a). The three dimensions of the turbulent ship wake are indicated in (b), with *L*=wake longevity (in time or length), *W*=wake width, and *D*=wake depth. Note that these illustrations are schematics of the turbulent wake and not true in scale or shape.

The limited amount of *in situ* observations and full-scale numerical modelling estimates of the turbulent wake development and intensity, may be related to methodological challenges. Conducting *in situ* observations in the turbulent wake of a large vessel is very challenging (Kouzoubov et al., 2014), and many of the commonly used instruments, sensor platforms, and methodological approaches, are not feasible, or do not capture all the relevant spatiotemporal scales. The turbulent wake needs to be observed in three dimensions (depth, width, length/time) at spatial scales of µm to tens of kilometres, and temporal scales of seconds to hours (Table 1). Hence, observing the entire extent of the turbulent wake development and its impact, requires an interdisciplinary approach, where methodologies from different scientific fields are combined (Figure 2).

The spatiotemporal scales of the turbulent wake are also difficult to model, and likewise require a combination of different modelling approaches. There are available high resolution Computational Fluid Dynamic (CFD) models of the turbulent wake region closest to the ship (near wake) (Figure 3) (Wall and Paterson, 2020, Fujimura et al., 2016, Esmaeilpour et al., 2016), but CFD models are computationally demanding (Wall and Paterson, 2020, Fujimura et al., 2016) and have therefore seldom been run to simulate more than 1–2 ship lengths aft the vessel. On the other side of the spectrum, there are regional oceanographic models for simulating turbulent and biogeochemical processes in the ocean (e.g., Daewel et al. (2022)). However, even the high-resolution regional oceanographic models have a resolution of 1–10 km, which is too coarse to

capture the spatiotemporal scales of the turbulent wake (Table 1). Semiempirical models have been used to estimate the turbulent wake development (Katz et al., 2003, Voropayev et al., 2012, Milgram et al., 1993, Dubrovin et al., 2011, Chou, 1996, Tennekes and Lumley, 1972), but their reliability and applicability is dependent on the data they are derived from and are thus limited by the low availability of *in situ* observations. Consequently, to characterise the turbulent wake development from an environmental impact perspective, there is a need to develop possible methodological approaches to observe and model the entire extent of the turbulent wake.

1.1 AIM

The aim of this thesis is to provide a characterisation of the turbulent wake, covering the spatiotemporal scales relevant to assess the impact of ship-induced turbulence on pollutant dispersion, air-sea gas exchange, biogeochemistry, hydrography, biota/ecology, and as a source of energy pollution. Further, to investigate the environmental impact of ship-induced turbulence in areas of intense ship traffic, with respect to stratification and entrainment, and air-sea gas exchange of methane (CH_4).

1.2 RESEARCH QUESTIONS

The specific objectives and research questions are:

1) To review, test, and develop suitable methodologies and approaches for detecting and characterising turbulent ship wakes and their impact.

    - RQ1a: Which available methodologies are suitable for observing turbulent ship wakes and their impact?
    - RQ1b: To what extent can machine learning models be trained to accurately detect ship wakes in acoustic data, with only a limited dataset to train on?

2) Characterise the turbulent wake development with respect to spatiotemporal scales and turbulent intensity, for stratified and non-stratified conditions, using *in situ* observations and modelling.

    - RQ2a: What is the spatiotemporal extent and intensity of turbulent ship wakes?
    - RQ2b: What are the effects of the interaction between the ship's turbulent wake and stratification?

3) Quantify the impact of ship passages in coastal shipping lanes with respect to energy pollution and ship-induced methane emissions.
    - RQ3a: How does the quantity and distribution of ship-induced turbulent mixing compare to the natural wind driven mixing?
    - RQ3b: Which ship-related and natural processes govern the magnitude and frequency of ship-induced methane emissions in coastal/estuarine shipping lanes?

The first objective is addressed in all the appended papers, with **Paper II** specifically focusing on RQ1b. The second objective is addressed in **Paper I** and **Paper III**. The research questions of the third objective are addressed in **Paper III** (RQ3a) and **Paper IV** (RQ3b).

2 BACKGROUND

Characterising the turbulent ship wake from an environmental impact perspective requires an interdisciplinary approach and insight into several different scientific fields (Figure 2). This chapter will present a summary of what previous studies within relevant fields have shown regarding turbulent wake development and its potential environmental impact. First, a description of the current knowledge regarding the turbulent wake's extent and intensity will be provided. It will be followed by a summary of the hydrographic and biogeochemical processes in the surface ocean relevant for the development and impact of turbulent ship wakes. The final section will give a brief overview of environmental impact from shipping and describe the direct and indirect impacts of ship-induced turbulence on hydrographic and biogeochemical processes in the marine environment.

2.1 TURBULENT SHIP WAKES

A ship moving through water will create a wake, which consists of surface waves diverging in a V-shape behind the ship (Kelvin wake pattern), and a turbulent wake trailing behind the vessel (Figure 3a) (Stanic et al., 2009). The focus of this thesis is the turbulent wake, which is induced by the ship's propeller and hull friction and characterised by intense turbulence and a dense bubble cloud (NDRC, 1946, Trevorrow et al., 1994, Soloviev et al., 2010, Voropayev et al., 2012, Francisco et al., 2017, Golbraikh and Beegle-Krause, 2020). The turbulent wake can be divided into three regions (Figure 3b), which are governed by different physical processes. The near wake is characterised by strong and dynamic turbulence and can be considered a turbulence-production phase (Reed and Milgram, 2002, Fujimura et al., 2016, Chou, 1996). The far wake is the decay-phase and has a more stable turbulence field. Lastly, the intermediate wake is the transition stage between the near and far wake. The turbulent wake depth, width, longevity (Figure 3b), and intensity depend on the ship's geometry, speed, and manoeuvring: as well as environmental conditions such as water column stratification, currents, and waves (Loehr et al., 2001, Voropayev et al., 2012, Somero et al., 2018).

Although all these ship specific and environmental parameters are known to impact the turbulent wake, their interdependence and respective importance in governing the spatiotemporal extent and intensity of the turbulent wake, are not well understood. This section will provide an overview of available field observations and modelling estimates related to the characterisation of the turbulent wake extent and intensity.

2.1.1 Previous studies of turbulent ship wakes

Turbulent wakes have been studied for a variety of purposes, focusing on different aspects of the wake, and using different methodological approaches. Initially, ship wakes were mainly studied for military purposes with the aim of detecting or identifying ships through wake signals such as surface waves or the bubble cloud of the turbulent wake (Smirnov et al., 2005, Liefvendahl and Wikström, 2016, NDRC, 1946). Theoretical models of turbulent wake development in idealised conditions have also been derived for surface ships and submarines (e.g. (Tennekes and Lumley, 1972)), which have been verified using tank experiments with model-scale ships (Hoekstra and Aalbers, 1997, Milgram et al., 1993). However, publicly available published *in situ* measurements of the turbulent wake of real-size ships are almost non-existent (Carrica et al., 1999, Parmhed and Svennberg, 2006, Ermakov and Kapustin, 2010, Golbraikh and Beegle-Krause,

2020, Kouzoubov et al., 2014). Since the 1980s, turbulent ship wakes have also been studied from an environmental perspective, with a focus on the dilution of waste or contaminants discharged from the ship in the wake (Loehr et al., 2001, US-EPA, 2002) (Katz et al., 2003, Golbraikh and Beegle-Krause, 2020, Chou, 1996, Lewis, 1985, Byrne et al., 1988, Situ and Brown, 2013). Although these previous studies have recognized the importance of the turbulent wake, no studies have observed the wake turbulence directly. Instead, observations of bubbles in the wake, or dye added to the wake, have been used as proxies for the extent of the turbulent wake and its impact (Stanic et al., 2009, Trevorrow et al., 1994).

Previous field observations report wake depths between 3–18 m, wake widths of 10–500 m, and wake lengths of 1.5–60 min/0.5–22 km (Table 1). The observed values span over large ranges, which is to be expected, as the ships inducing the observed wakes varied greatly in size, and different observational methods were used in the studies. Still, the total number of different ship types is low, where naval vessels and cruise ships are the most studied, hence the observations in Table 1 might not be representative for all ship types. Most previous studies were also conducted in near idealised hydrographical conditions, in calm weather without stratification, and thus not necessarily representative for stratified or windy conditions.

Observations of wake development from field and model-scale experiments have also been used to express the wake width and/or depth as a function of wake length/age (Katz et al., 2003, Golbraikh and Beegle-Krause, 2020, Golbraikh et al., 2013, Dubrovin et al., 2011, Voropayev et al., 2012, Hoekstra and Ligtelijn, 1991). The wake width has been observed to relate to the distance aft of the ship according to a power law increase, with observed and modelled exponents ranging from 0.18–0.31 (Dubrovin et al., 2011, Katz et al., 2003, Hoekstra and Ligtelijn, 1991). A similar power law increase in wake width over time has also been observed, with an exponent of 0.4 (Ermakov and Kapustin, 2010). Golbraikh and Beegle-Krause (2020) reported ratios of wake depths/ship draught, ranging from 1.42–3 for different ship types.

Measurements of the turbulence intensity and decay in the wake region of a full-size ship are lacking (Ermakov and Kapustin, 2010, Golbraikh and Beegle-Krause, 2020, Kouzoubov et al., 2014, Wall, 2021). However, the turbulent wake extent and intensity have been estimated using numerical modelling and experiments with model-scale ships and propellers (Milgram et al., 1993, Hoekstra and Ligtelijn, 1991, Loberto, 2007, Wall and Paterson, 2020). Measurements of turbulent kinetic energy dissipation rate (ε) in the wake of different self-propelled ship types of model scale (Hoekstra and Ligtelijn, 1991), were found to have an exponential ε decay rate of (-4/5) (Milgram et al., 1993). Voropayev et al. (2012) reported the wake turbulence in their model study to be sustained for 10–15 ship lengths behind the ship and subsiding after ~30 ship lengths.

Table 1. Summary of previous studies with field observations of the turbulent wake of full-sized ships. The observed wake proxies were bubbles, the thermal signal from the wake, and the concentration/dilution of dye released in the wake.

Study	Wake proxy	Wake depth [m]	Wake length [km]	Wake duration [min]	Wake width [m]	Number and type of vessels	Ship length [m]	Ship draught [m]	Ship width [m]	Ship speed [knots]	Propulsion system	Hydrographic conditions
(Trevorrow et al., 1994)	Bubble	7–12	2.8*	7.5	66	3 naval vessels, 2 different types	39.7–64.5	4.3–5.5	9.46–12.2	5, 10	2 Single screw, 1 Twin screw	Calm, well mixed, no stratification
(Francisco et al., 2017)	Bubble	6–12	0.5*	1.5		2 small passenger ships	37.7, 41.8	1.3, 1.1	7.5, 7.7		1 Propeller/ 1 Water jet	
(Soloviev et al., 2010)	Bubble	10–18	4–10*	10–30	100–200	2 container ships	148	8.51, 7.2	23.43, 25.63	Decelerating, 11.3	Single screw	
(Soloviev et al., 2012)	Bubble	7				1 cargo ship	128	7.3	21	5.8		
(Gilman et al., 2011)	Thermal/ Bubble				100–250	1 cruise ship	311	11.7	38.6		3 Propellers	
(Ermakov and Kapustin, 2010)	Bubble	4–8	3.7–5.5*	10–15	40–80	1 small passenger ship	20		6		Twin screw	Coastal, calm, pycnocline 13-15 m
(Weber et al., 2005)	Bubble	8	6	15		1 research vessel	61	4.1		6.4	Twin screw	Calm, low current. pycnocline 7.5 m.
(Stanic et al., 2009)	Bubble		1.5–2	19	10	1 naval/research vessel	39.9	1.5	8.1	12 & 15	2 Water jets	Water depth 35 m.
(NDRC, 1946)	Bubble/ Thermal	3–10	11–22*	30–40/ 10–60	91/46	**2 naval yachts, 3 destroyers	31.7–38.7	3.6	7	3.5–11	Single screw	Wake width observed during calm sea
(Loehr et al., 2001) ¤	Bubble	12–18	5.5	12–17	76–155	2 large cruise vessels	220, 261.3	7.5, 8.1	32, 32.28	7.5, 12	Twin screw	Stratification, shear, strong tidal currents
(US-EPA, 2002) ¤	Dye dilution	12–18			40–500	4 large cruise vessels	260–311	7.5–8.8	31.4–36.8	9–19	Twin screw (one 3 screw)	
(Kouzoubov et al., 2014)	Bubble	5			20	1 research vessel	25	3	7.2	8		Coastal, water depth 15 m.
(Katz et al., 2003)	Dye dilution	8–10	Min 3		40–44	1 navy frigate	129.9	6.7	13.7	8, 15	Single screw	Upper mixed layer depth 20 m, coastal

*Calculated based on temporal longevity and a ship speed of 12 knots

**Vessel information only available for the 2 yachts, speed only know for the destroyers

¤ Report, not peer reviewed

2.1.2 Parameters governing the turbulent wake development

Characterising and observing the turbulent wake *in situ* is complex, as the wake development depends on both the ship design and operation, and the hydrographic conditions (Loehr et al., 2001, Voropayev et al., 2012, Somero et al., 2018) (Stanic et al., 2009). As reviewed in the previous section, the ship size has previously been related to the wake expansion (Katz et al., 2003, Golbraikh and Beegle-Krause, 2020, Golbraikh et al., 2013, Dubrovin et al., 2011, Voropayev et al., 2012, Hoekstra and Ligtelijn, 1991), and wake water dilution to ship speed (Lewis, 1985). However, the interdependence and relative importance of ship-related and environmental parameters have not been well investigated.

Most previous studies have mainly considered ship size in terms of length, width, and draught. Yet, ship type is also important to consider, as hull shape, design speed, and propeller configuration impact the ship's displacement and drag. The propeller configuration has been observed to impact the turbulent wake development, as ships with twin-screw propellers produce two propeller vortices instead of one (Marmorino and Trump, 1996, Weber et al., 2005). The manoeuvring of the ship will also impact the wake development, as the speed and direction of the energy input to the wake will differ.

Model-scale experiments and numerical modelling results have shown that the turbulent wake development is affected by stratification, by a dampening of the vertical expansion and increasing the horizontal expansion (Merritt, 1972, Lin and Pao, 1979, Brucker and Sarkar, 2010, Jacobs, 2020, Voropayev et al., 2012). In stratified conditions, the turbulent wake can entrain denser water from below the stratification (Lindholm et al., 2001, Loehr et al., 2001, Jürgensen, 1991), which will impact the wake water density, and thereby the wake development, compared to non-stratified conditions (Jacobs, 2020, Merritt, 1972). Strong currents and shear can also impact the wake development (Benilov et al., 2001, Loehr et al., 2001, Somero et al., 2018). As few previous wake studies have been conducted in stratified conditions with full-scale ships, there is a knowledge gap regarding the interaction between stratification, and the turbulent wake development in natural conditions.

2.2 NATURAL PROCESSES IN SURFACE AND COASTAL OCEANS POTENTIALLY AFFECTED BY SHIP-INDUCED TURBULENCE

For the study of the turbulent wake and its impacts, the top 30–40 m of the water column is of most interest, as it is within this range the turbulent wake can have a direct impact (**Paper I**, **Paper III**). This subchapter provides an overview of the hydrographical and environmental conditions most relevant when discussing the development and impact of turbulent ship wakes. The naturally occurring turbulent intensities in the surface ocean, are described, along with water column stratification and its role in nutrient availability in the surface layer, and biogeochemical processes related to air-sea gas exchange. As **Paper IV** studies ship-triggered release of CH_4, a brief overview of CH_4 emissions from coastal and estuarine areas is included. How turbulent wakes impact and interact with these processes are described in section 2.3.

2.2.1 Hydrographic and biogeochemical processes in surface and coastal oceans

In the surface ocean, turbulence can be induced by wind, waves, currents, and tides (Thorpe, 2007). As the field observations included in this thesis are from the Baltic Sea,

where there are no tides and turbulence in the surface layer is mainly induced by wind-driven mixing and surface waves (Reissmann et al., 2009), tidal effects will not be included here.

In this thesis, turbulence intensities and water column mixing have been quantified and discussed in terms of ε, a parameter indicating the amount of kinetic energy from large scale velocity shear that dissipates at smaller scales and thus contribute to mixing (Franks et al., 2022). Observed open ocean ε intensities in the top 30–40 m, range between 10^{-8}–10^{-6} m^2 s^{-3}, and seldom reach 10^{-5} m^2 s^{-3} (Fuchs and Gerbi, 2016, Franks et al., 2022). In the surface layer, where wind and breaking waves increase the turbulence, the values are higher at 10^{-5}–10^{-3} m^2 s^{-3} (Fuchs and Gerbi, 2016). In the Baltic Sea, the maximum observed near-surface values of ε have been reported to be around 10^{-5} m^2 s^{-3} (Lass et al., 2003, Zülicke et al., 1998). In addition to field observations, the wind induced ε (ε_{wind}) at different depth can be estimated from the law of the wall (Thorpe, 2007), according to Equation 1:

$$\varepsilon_{wind} = \frac{\sqrt{(c_d \cdot \rho_{air} \cdot u_{wind}^2)/\rho_{water}}^3}{\kappa \cdot z} \qquad \text{(Eq. 1)}$$

where c_d is the drag coefficient for wind stress, ρ_{air} is the air density, u_{wind} is the wind speed, ρ_{water} is the water density, κ is the Von Kármán constant (0.4), and z is the distance to the surface. Figure 3 shows a simplified estimate of ε_{wind} for three different wind speeds. This estimate is representative for the region unaffected by breaking waves, as waves have a large effect on turbulence intensities down to 1–2 significant wave heights below the surface (Umlauf and Burchard, 2003).

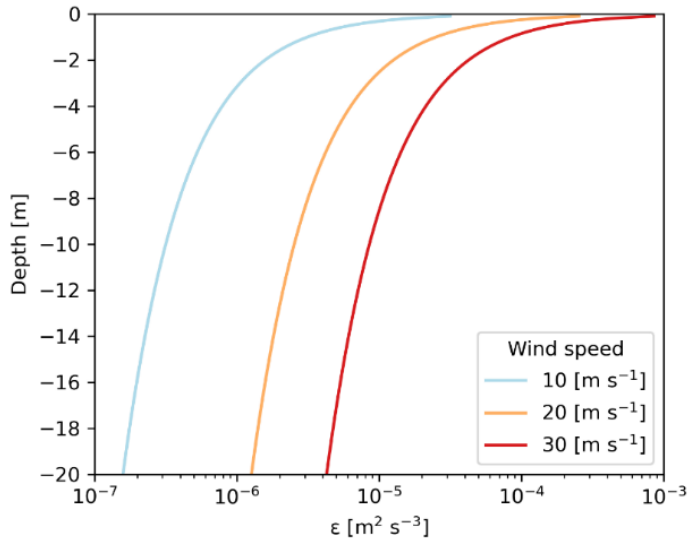

Figure 4. Simplified estimate of wind-induced ε over depth, for three different wind speeds, based on Equation 1. The drag coefficient (c_d) is simplified to 0.001, air density estimated to 1.2 kg m^{-3}, water density set to 1025 kg m^{-3} (brackish conditions), and κ = 0.4. The effect of wind-induced breaking waves is not included.

The water column stratification describes how the water density changes with depth: if there are large density gradients over short distance, there is a strong stratification (pycnocline) and if there are no density gradients the water is non-stratified (homogenous) (Thorpe, 2007). Water density is affected by temperature and salinity, where a water mass with low salinity and high temperature will be lighter than a water mass with cold and salty water (Thorpe, 2007). The pycnocline in the Baltic Sea is mainly governed by large salinity gradients, both on a regional horizontal scale (from the northern Bothnian Bay to the Skagerrak on the Swedish west coast) and locally over depth, with densities ranging from 3–35 g kg^{-1} (Stigebrandt, 2001, Leppäranta and

Myrberg, 2009, Reissmann et al., 2009). There are also large temperature gradients over depth, which give rise to a seasonal thermal stratification (thermocline) near the surface during summer (Stigebrandt, 2001, Leppäranta and Myrberg, 2009, Reissmann et al., 2009). On the Swedish west coast, including the study sites outside Gothenburg and in Oresund, there is usually a strong pycnocline at 10–20 m depth and a shallower seasonal thermocline (Reissmann et al., 2009).

In a stratified water mass, internal waves can occur. Internal waves are similar to surface waves, but they move along the pycnocline instead of the air-sea interface (Thorpe, 2007). Internal waves are induced by tidal forcing, topography, wind, and atmospheric pressure gradients (Reissmann et al., 2009, Thorpe, 2007, Inall et al., 2021). Propagating internal waves do not usually induce strong vertical mixing across the pycnocline (diapycnal mixing), but simply moves the interface up and down in a wave motion (Thorpe, 2007). However, if the internal waves break, they diapycnal mixing will occur, and internal waves are an important source of turbulence below the surface mixed layer in the open ocean (Reissmann et al., 2009, Thorpe, 2007).

It takes more energy to mix a stratified water mass compared to a homogenous water mass, as the deeper denser water needs to be moved above lighter water, which creates an increase in potential energy and requires work (Thorpe, 2007). A strong stratification will therefore decrease the vertical exchange of gases and nutrients across the stratification, as only intense turbulence can mix the two water masses (Reissmann et al., 2009). The light surface layer (euphotic zone) has a high primary production rate, and without any input of nutrients the bioavailable nutrients in the surface water will eventually be depleted. The water below the stratification usually contains more nutrients, as organic matter sinking to the sea floor will be remineralised and release nutrients to the bottom water (Rippeth et al., 2009, Snoeijs-Leijonmalm and Andrén, 2017). The nutrient consumption is also lower in the deeper parts of the water column, as the light availability limits the primary production. As the remineralisation process also consumes oxygen, the bottom water usually contains lower concentration of dissolved oxygen compared to the surface water.

During periods of strong wind, upwelling events can occur near costs, were large amounts of nutrient rich water from below the stratification is brought up to the surface (Reissmann et al., 2009). In the Baltic Sea, the stratification is the strongest and the wind-induced turbulence the weakest, during the summer months (Reissmann et al., 2009). Hence, mixing across the stratification during the summer season is usually limited. Strong stratification and weak vertical mixing can thus lead to low/no oxygen (hypoxia/anoxia) below the stratification, and low nutrient concentrations in the water above the stratification (Reissmann et al., 2009, Snoeijs-Leijonmalm and Andrén, 2017).

Air-sea gas exchange is an important part of the biogeochemical cycles in the ocean, governed both by physical processes affecting the gas transfer rate, and by biological processes such as photosynthesis and respiration. The gas transfer rate is affected by turbulence, which affects the diffusion rate over the air-sea boundary layer (e.g. (Wanninkhof et al., 2009)), and the presence of bubbles in the water (Emerson and Bushinsky, 2016, Liang, 2020). The biological processes affect air-sea gas exchange through photosynthesis, during which carbon dioxide (CO_2) is taken up from the atmosphere and converted into oxygen (O_2) and organic matter (Rippeth et al., 2014, Snoeijs-Leijonmalm and Andrén, 2017). If nitrogen fixing cyanobacteria are present,

atmospheric nitrogen (N_2) can also be taken up from the atmosphere. The organic matter will eventually sink to the sea floor, and either be buried in the sediment, and permanently remove CO_2 from the atmosphere, or be remineralised through microbial aerobic or anaerobic respiration. If remineralised, inorganic CO_2 will be released to the water, which can be transported back to the atmosphere through diffusion or vertical mixing. In aerobic conditions O_2 will be used as the oxidising agent, in near anaerobic conditions denitrification will take over and nitrogen gas (N_2) will be released, and in anaerobic conditions, methanogenesis can occur, during which hydrogen (H_2) is consumed and methane (CH_4) is released (Snoeijs-Leijonmalm and Andrén, 2017, Nilsson et al., 2019, Nilsson et al., 2021).

2.2.2 Estuarine and coastal methane emissions

CH_4 is a potent greenhouse gas (Saunois et al., 2020, IPCC, 2022), and estuarine and coastal areas are important sources of natural methane emissions (Rosentreter et al., 2021, Lohrberg et al., 2020, Weber et al., 2019, Wallenius et al., 2021). CH_4 is emitted to the atmosphere via diffusive gas transfer or the release of CH_4 bubble clouds (ebullition) (Weber et al., 2019). Shallow water depth (< 10 m) and a well-mixed water column increase the flux of CH_4 to the atmosphere (Shakhova et al., 2014, Borges et al., 2018, Borges et al., 2016, Zang et al., 2020, Bonaglia et al., 2022). Ebullition occurs in areas where there is a high biogenic production of CH_4 or reserves of fossil natural gas in the sediment, and the ebullitive flux can be much higher than the diffusive flux. Biogenic CH_4 is mainly produced by methanogenic archaea in the deeper anoxic parts of the sediment (Wallenius et al., 2021), and the production increases with high temperature (Borges et al., 2016, Wilkinson et al., 2015), a high sediment content of reactive organic material (Egger et al., 2018, Humborg et al., 2019, Egger et al., 2016), and low salinity (Egger et al., 2018, Wallenius et al., 2021, Egger et al., 2016).

The occurrence and magnitude of ebullition events are difficult to observe and assess, as they often occur episodically, and are easily missed (Lohrberg et al., 2020, Maeck et al., 2014, Humborg et al., 2019, Römer et al., 2016, Thornton et al., 2020). The processes governing CH_4 emissions to the atmosphere are not fully understood, but pressure changes have been shown to trigger ebullition events (Mattson and Likens, 1990, Römer et al., 2016, Hofmann et al., 2010, Maeck et al., 2014, Wilkinson et al., 2015, Lohrberg et al., 2020, von Deimling et al., 2010).

Current estimates of CH_4 emissions from estuarine and coastal areas range between 0.02–0.64 mmol m^{-2} day^{-1} (Middelburg et al., 2002, Bonaglia et al., 2022, Liu et al., 2022, Borges et al., 2016, Borges et al., 2018, Bussmann et al., 2021, Zang et al., 2020, Mao et al., 2022), and for continental shelfs reported estimates range from 0.002–0.053 mmol m^{-2} day^{-1}) (Liu et al., 2022, Sun et al., 2018, Bange et al., 1994, Yang et al., 2010). Emission estimates from shallow coastal estuaries and bays around the Baltic Sea have an upper range of (~1-33 mmol m^{-2} day^{-1}) (Gutiérrez-Loza et al., 2019, Humborg et al., 2019, Myllykangas et al., 2020, Myllykangas, 2020, Bange et al., 1994), and an average lower range of 0.0007–0.345 mmol m^{-2} day^{-1} (Myllykangas, 2020, Steinle et al., 2017, Gülzow et al., 2013, Bussmann et al., 2021, Lundevall-Zara et al., 2021, Roth et al., 2022).

2.3 Environmental impact from shipping and ship-induced turbulence

There is almost no part of the global ocean free from ship traffic, and the traffic intensity is especially high in coastal areas (Figure 1). All ships in the global fleet impact the

marine environment in many ways, and shipping is one of the largest anthropogenic stressor categories in marine coastal areas (Halpern et al., 2019). The Baltic Sea is one of the most intensively trafficked areas in the world (HELCOM, 2010, Swedish Maritime Administration, 2015), with traffic densities of 30 000–50 000 ships y^{-1} in the major shipping lanes, corresponding to a ship passage every 10–20 minutes on average (HELCOM, 2023).

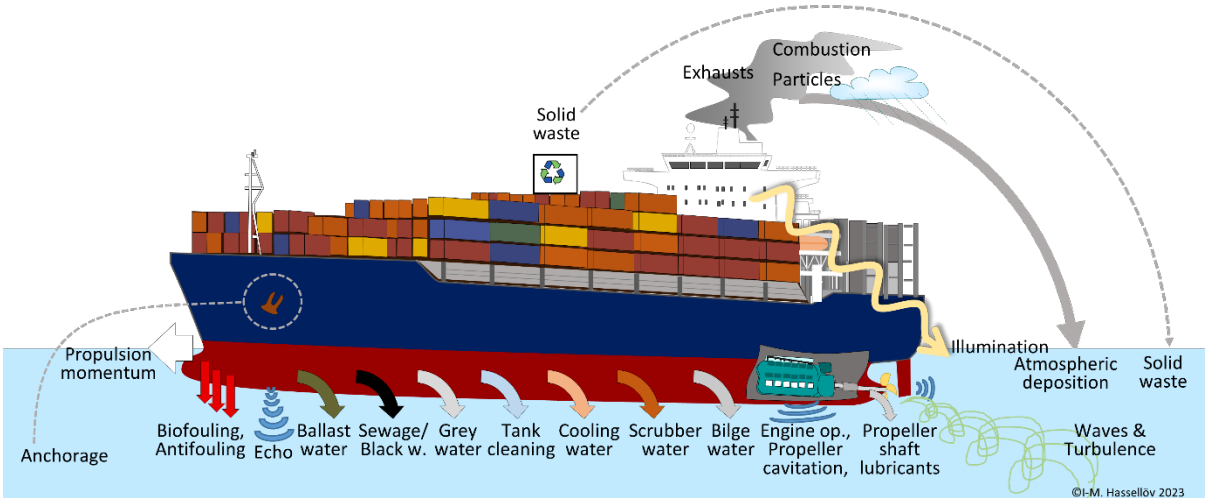

Figure 5. Illustration of environmental impacts from shipping. Figure credit: Ida-Maja Hassellöv, 2023.

A ship in operation discharges a multitude of different pollutants and induce physical disturbance (Andersson et al., 2016, Moldanová et al., 2018, Hassellöv et al., 2019, Jalkanen et al., 2020). A detailed description of all different impacts from shipping is beyond the scope of this thesis, but a summary is presented in Figure 5. The most well-known impact is likely the air emissions of greenhouse gases and particulate matter from the ship's fuel combustion. However, there is also a direct release of pollutants to the marine environment, from bilge-, grey-, black-, and ballast water, solid food waste, tank cleaning, antifouling paints, and wash water from exhaust gas cleaning systems (scrubbers), which will all end up in the ship's turbulent wake (Jalkanen et al., 2020). The final category of impacts is physical disturbances, which includes effects on the sea floor from anchorage, light pollution, underwater noise from the engine, propeller and echosounder, and ship induced turbulence and waves. The study of physical disturbances from shipping have mainly focused on underwater noise (Duarte et al., 2021, Popper and Hawkins, 2016) and ship-induced resuspension and erosion due to ship waves (Kelpšaite et al., 2009, Soomere, 2005, Soomere and Kask, 2003, Gabel et al., 2017). The study of environmental impact from ship-induced turbulence itself, was pioneered by Jürgensen (1991), but has since then been overlooked.

Turbulent ship wakes impact the marine environment in several ways (Figure 6). The turbulence can have a direct impact on plankton mortality (Bickel et al., 2011, Garrison and Tang, 2014), affect air-sea gas exchange (Weber et al., 2005, Emerson and Bushinsky, 2016)(**Paper IV**), increase erosion and turbidity in shallow areas (Kelpšaite et al., 2009, Soomere, 2005, Soomere and Kask, 2003), and govern the spread of pollutants discharged in the wake region (Chou, 1996, Loehr et al., 2001, US-EPA, 2002, Katz et al., 2003, Golbraikh and Beegle-Krause, 2020). In addition, the vertical mixing induced by the turbulent wake has the potential to affect stratification and nutrient availability (**Paper III**) (Lindholm et al., 2001, Jürgensen, 1991). Considering all these

different impacts, ship-induced turbulence has the potential to affect local/regional hydrography and biogeochemical cycles, especially in areas with intense ship traffic.

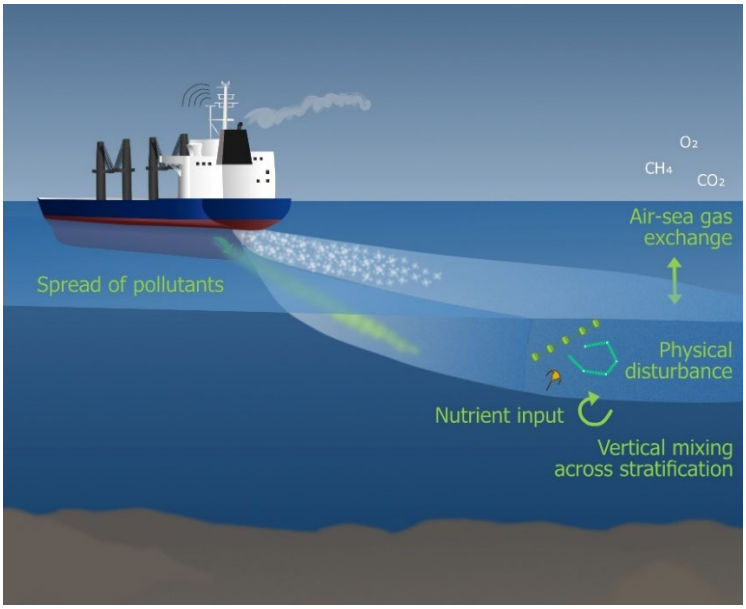

Figure 6. Environmental impacts from a turbulent ship wake.

Studies of environmental impact relating to the turbulent wake has mainly been focused on how the wake turbulence govern the spread of pollutants discharged in the turbulent wake. A reliable estimate of the concentration and fate of a pollutant, requires understanding of the turbulent wake development (US-EPA, 2002, Katz et al., 2003, Situ and Brown, 2013, Golbraikh and Beegle-Krause, 2020). The intensity and expansion of the turbulent wake will affect how quickly the pollutant will be diluted, as well as at which depths the contaminant will spread. A reliable estimate of the vertical distribution is especially important, as the horizontal dispersion is affected by currents, which can vary in strength and direction at different depths.

The turbulent wake can also directly impact the marine organisms. The episodic intense turbulence in the ship wake have a duration and magnitude shown to negatively affect plankton mortality (Bickel et al., 2011, Garrison and Tang, 2014). Bickel et al. (2011) made *in situ* observations of copepods in a shipping lane and found that the percentage of copepod carcases was 28 % higher in the shipping lane compared to undisturbed areas. These observations were supported by their laboratory experiments, which showed a linear increase in fraction of copepod carcases with increasing ε levels, reaching 30–60 % for their highest tested ε levels $2.24 \cdot 10^{-4}$ m^2 s^{-3} during 30 s. A similar laboratory study investigated the effect of ship-wake like turbulence for two diatom species, and found that 45 s of exposure of ε levels $2.5 \cdot 10^{-4}$ m^2 s^{-3}, reduced the abundance up to 32 % and increased the fraction of dead cells with 22 %. The high intensity and deep penetration of the turbulent wake, distinguishes it from naturally induced turbulence (**Paper I**, **Paper III**), and it is very difficult for plankton to avoid or adjust to (Bickel et al., 2011, Garrison and Tang, 2014, Franks et al., 2022). An increase in plankton mortality will affect food availability at higher trophic levels and increase nutrient availability for phytoplankton and the microbial loop (Bickel et al., 2011, Garrison and Tang, 2014). Consequently, shipping lanes and intensive ship traffic areas

should be considered as distinct, highly turbulent environments with a higher plankton mortality and nutrient availability compared to surrounding water.

The turbulent wake can also impact local biogeochemistry in stratified waters directly. If a water column have a stratification at a depth similar to the turbulent wake depth, ship-induced mixing have been found to increase the stratification depth and to entrain water from below the stratification to the upper surface layer (**Paper III**) (Lindholm et al., 2001, Jürgensen, 1991, Jacobs, 2020, Merritt, 1972). The ship-induced entrainment can bring nutrient rich water from below the stratification to the upper surface layer. Ships can also induce internal waves (Jacobs, 2020, Watson et al., 1992, Lin and Pao, 1979), which cause vertical mixing across the stratification when they break or lose their energy in other ways (Thorpe, 2007). In stratified waters with intense ship traffic, the repeated ship passages thus have the potential to affect local biogeochemistry and hydrography. In marine systems without tides or strong currents, like the Baltic Sea, the nutrient supply to the upper surface layer is dependent on vertical mixing induced by wind (Reissmann et al., 2009). In such systems, ship-induced turbulence could contribute with an important part of the vertical mixing in areas with intense ship traffic (**Paper I**).

Finally, the turbulent and bubbly wake can also impact air-sea gas exchange (Weber et al., 2005, Emerson and Bushinsky, 2016)(**Paper IV**). Diffusive gas transfer over the air-sea interface is dependent on the turbulent intensity just below the sea surface, and the transfer rate will increase with increased turbulence (Fredriksson et al., 2016, Wanninkhof et al., 2009). The large bubbles in the turbulent wake can also increase the air-sea gas transfer (Liang, 2020, Emerson and Bushinsky, 2016). Hence, the area affected by the turbulent and bubble wake will likely have an increased air-sea gas-exchange, which should be taken into consideration when estimating air-sea gas fluxes in areas with intense ship traffic.

3 THEORY

Several scientific fields apply methodologies relevant for turbulent wake characterisation (Figure 2) and an interdisciplinary approach is necessary to capture the different aspects of the turbulent wake and its impacts. Multiple methods can be used to observe or model the turbulent wake, but none of the currently available methodologies can capture the entire wake development at all relevant temporal and spatial scales. The wake depth, width, and length need to be observed at temporal scales of seconds to hours, and spatial scales of millimetres to tens of kilometres (Table 1). In addition to the wide range of spatiotemporal scales, the characterisation of the turbulent wake development from an environmental perspective also requires knowledge about ocean systems and the shipping industry. This chapter provides an overview of methodologies relevant for characterising the turbulent wake and its impact. It includes descriptions of instruments and sensors able to observe the turbulent wake and/or its impact and different sensor platforms that can be used to deploy the sensors *in situ*. A summary of how machine learning (ML) and numerical modelling can be used in turbulent wake studies, is also included.

3.1 FIELD OBSERVATIONS OF TURBULENT SHIP WAKES AND THEIR IMPACT

There are several types of methodological approaches and instruments that can be used to measure turbulence and its impact *in situ*. The wake's spatiotemporal scales and the practical challenges involved when sampling behind a ship means that not all approaches are suitable for studying turbulent ship wake development and impact. This section will present an overview of the feasibility of the most relevant *in situ* and *ex situ* methodologies and instruments suitable for turbulent wake studies. The focus will be on acoustic instruments and remote sensing but will also mention the release of tracers in the wake region, turbulence sensors, ship tracking, and conductivity, temperature, depth (CTD) observations of stratification. The main points of this section are summarised in Table 2.

3.1.1 Acoustic instruments

Acoustic instruments use the reflection of sound to detect objects and surfaces (targets) in the water column. The strength of the reflected signal (echo amplitude) provides information about the detected target and can be visualised as an echogram. As bubbles reflect sound more effectively than water, the bubble cloud of the turbulent wake will be clearly visible in the echogram (see Figure 7 for example) (NDRC, 1946, Trevorrow et al., 1994, Marmorino and Trump, 1996, Weber et al., 2005, Ermakov and Kapustin, 2010, Francisco et al., 2017). The signal strength of bubble targets is the highest when the sonar frequency coincides with the bubble resonance frequency, where higher frequencies resonate with smaller bubbles and lower frequencies with larger bubbles (Trevorrow et al., 1994, Kouzoubov et al., 2014, Liefvendahl and Wikström, 2016). The optimal frequency for observing the bubble wake development, is the resonance frequency for a bubble size small enough to be retained by the turbulence (Trevorrow et al., 1994, Stanic et al., 2009), but large enough not to dissipate too quickly. Bubble wakes have been observed using frequencies between 83–1000 kHz, and frequencies between 200–500 kHz have been found most suitable (Francisco et al., 2017, Kouzoubov et al., 2014, Soloviev et al., 2010, Trevorrow et al., 1994, Weber et al., 2005)(**Paper III**).

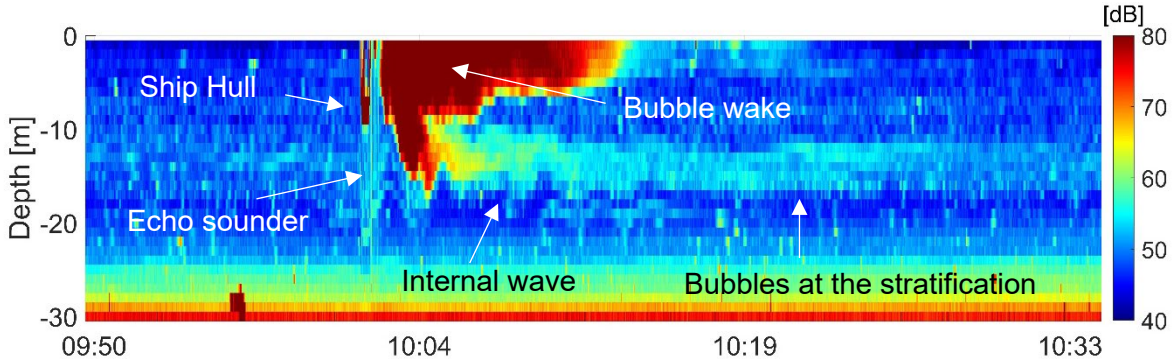

Figure 7. Example of an echogram with a clear bubble wake detected with a Signature 500 ADCP. The x-axis indicate time [hh:mm] and the colour bar indicates signal strength in dB. Red values indicate high signal strength and thus high bubble intensity. The U-shape in front of the wake is the signal of the ship hull, indicating that the ship inducing the wake had a draught of ca 8 m. The thin vertical line at the aft of the ship hull, is the signal from the ship's echo sounder. There is also a small ship-induced internal wave at the stratification and a trailing bubble wake "trapped" along the stratification.

The bubble wake can be used as a proxy for the turbulent wake, as turbulence traps the bubbles in the wake by counteracting their positive buoyancy (Stanic et al., 2009, Trevorrow et al., 1994). Still, as the bubbles will eventually disappear and either float up to the surface or dissipate (Carrica et al., 1998, Ermakov and Kapustin, 2010), the bubble wake does not fully reflect turbulent wake extent (Golbraikh and Beegle-Krause, 2020). Moreover, the bubble wake cannot be used to quantify the intensity of the turbulent wake or the ship-induced vertical mixing. However, one type of acoustic instrument can be used to estimate turbulence, namely acoustic doppler current profilers (ADCPs) (Wiles et al., 2006, Lucas et al., 2014, Togneri et al., 2017). ADCPs typically have 3–4 slanted beams and some even have a vertical beam. The instrument uses doppler shift to make high resolution continuous observations of velocities along each beam. From the current velocity observations, ε can be calculated using the structure function method (Lucas et al., 2014). ε provides a measure of the wake induced turbulent intensity at small scales and in a stably stratified fluid it can also be used to estimate water column mixing. The structure function method assumes that the most energetic turbulent length scales in the so-called inertial subrange are captured by the depth resolution of the velocity observations (bin size). For a bin size of 1 m the turbulence therefore needs to be strong enough for the largest vertical eddy scales to be 2–3 m. Even though the turbulence in ship wakes is strong, this requirement may not always be fulfilled in the stratified parts of the water column.

A major advantage of acoustic instruments is that they are non-invasive and can be deployed at a distance from the passing ship (Colbo et al., 2014). The reach of the instrument depends on the frequency used, where a 500 kHz instrument has a reach of around 60 m, which is sufficient to capture the wakes vertical extent (Table 1). Acoustic instruments can also be used to estimate water column stratification (e.g. (Stranne et al., 2018, Lavery et al., 2010, Muchowski et al., 2022, Brenner et al., 2023)), which is useful when studying the interaction between stratification and the turbulent wake. There are also promising methods to estimate ε directly from acoustic backscatter strength in stratified water (Muchowski et al., 2022). It is worth noting that most available acoustic instruments have been optimised to avoid measuring the ship wake, and no focus has been on developing instrumentation for *in situ* wake measurements.

Table 2. Summary of different acoustic instruments, shear probes, and remote sensing methods. The spatial resolution (res.) **Line** means that either a depth or width profile is possible, while **Profile** indicates that a depth profile is the only option. A continuous temporal resolution will add the width or length dimension to the wake observation. The wake resolution is given by the combination of the spatial and temporal resolution and a 3D observation is only possible if depth, width, and length can be observed simultaneously. The 2D wake resolution always corresponds to depth or width + length (i.e., time), except for the remote sensing cases which is length + width. For the drone case, both the spatial and temporal resolution gives the length dimension, hence the wake resolution is only 2D, despite continuous observations. The advantages, disadvantages, and comments are to large extent based on the results and experiences from the work presented in the appended papers and are further motivated and discussed in section 6.6.

	Acoustic instruments			**Shear probes**	**Remote sensing**	
	Acoustic Doppler Current Profiler (ADCP)	**Echo Sounder or Sonar**	**Multibeam Echo Sounder (MBES)**	**Microstructure shear probe profiler (MSP)**	**Satellite imagery**	**Aerial drone imagery**
Tested	Paper I, II, III	Paper I, II, III	no	no	Paper I	no
Spatial res.	Line	Line	Area*	Profile	Area**	Area**
Temporal res.	Continuous	Continuous	Continuous	Discrete	Discrete	Continuous
Wake res.	2D	2D	3D	1D (depth)***	2D**	2D**
Wake region	Entire	Entire	Entire	Far (intermediate)	Entire	Entire
Measured parameter	Current velocity, signal strength	Signal strength	Signal strength	ε	Sea surface temperature (SST), Synthetic Aperture Radar	
Wake proxy	Turbulence, internal waves, bubbles	Internal waves, bubbles, stratification	Internal waves, bubbles, stratification	Turbulence	Thermal wake, surface wake (Kelvin wake)	Thermal and surface wake
Advantages	Continuous, long-term, feasible, nonintrusive, turbulent & bubble wake, reliable vertical extent.	Continuous, long-term, feasible, non-intrusive, reliable vertical extent.	The only method which can provide a 3D view of bubble wake development.	High-resolution small-scale turbulence measurements	Captures large spatiotemporal scales. Freely available. SST shows the effect of mixing.	Continuous observations which can be combined with underwater observations.
Disadvantages	Limited spatial resolution, requires close ship passages, risk of instrument loss, interference with ship echo-sounder and bow wave. Sidelobe interference close to surface.	Same as for ADCP, except ship interference is not a problem. Cannot currently quantify wake turbulence, but new methods are emerging. Sidelobe interference.	Cannot quantify wake turbulence. Large data files. Ships must pass close, risk of instrument loss, depth limit. Sidelobe interference.	Difficult to get in position quickly enough to deploy instruments in the near wake, unless sampled from wake-inducing ship, in which case there is risk of the instrument colliding with the propeller.	No vertical dimension. Require cloud free conditions. Temporal snapshot, low data frequency. Reliability not as good near coast.	No vertical dimension. Practically and sometimes legally difficult to operate in open waters and shipping lanes.
Comment	Fixed bottom mounted setup preferrable to moorings, which are affected by waves, and to ship-hull mounted instruments, as the research ship can affect wake observations and the vertical extent is more reliably observed from below.			Complements the ADCP turbulence estimates.	Not suitable due to cloud disturbance and low temporal resolution.	Suitable scales for turbulent wake observations.

*Depth **and** width. **Length **and** width, ***With a slight horizontal shift as the probe falls with a speed of ca 1 m s^{-1}.

Of the acoustic instruments, only multibeam echosounders can observe the wake in 3D (Soloviev et al., 2012, Weber et al., 2005) (Table 2). Their multiple acoustic beams are arranged in a fan shape measuring a cross-section/area of the water column, and with a moving target or instrument, continuous observations of wake depth, width, and length are possible. The ADCP, sonar, and echosounder observe a profile/line of the wake over time, providing continuous observations for two of the three dimensions depth, width, and length. Which dimensions depend on the sensor platform configuration (see section 3.2 and Table 3). If the instrument has several slanting beams (like the ADCPs), each beam observation will observe a different cross-section of the wake, thus providing some

information about the missing dimension. Multiple 2D instruments in a line could also be used to cover all three dimensions.

3.1.2 Turbulence sensors

Microstructure shear probes (MSPs) are turbulence sensors using shear probes and fast response temperature sensors to observe high frequency velocity shear *in situ*, from which ε can be calculated (Wolk et al., 2002, Lucas et al., 2014). MSP profilers are free-falling sensor platforms equipped with MSPs, falling at a speed of approximately 1 m s^{-1}. There are currently no published studies using MSP profilers to observe turbulent ship wakes, but they could theoretically be deployed in the wake from the wake-inducing ship or another vessel. The MSP profilers' main disadvantage with regards to turbulent wake studies, is the sparse spatiotemporal data (Lucas et al., 2014), as they only make a discrete vertical observation (1D).

3.1.3 Remote sensing

Remote sensing methodologies such as satellite or aerial drone imagery, provide *ex situ* observations of large horizontal spatiotemporal scales (2D) (**Paper I**), but they cannot capture the vertical dimension (Kouzoubov et al., 2014). Surface aperture radar (SAR) imagery of sea surface roughness, can be used for wake detection (Soloviev et al., 2010, Fujimura et al., 2016, Reed and Milgram, 2002), but does not provide information about the turbulent wake or its impact (Kouzoubov et al., 2014)(**Paper I**). However, high-resolution infra-red imagery provide data of sea surface temperature (SST), which can be used to observe thermal wakes (NDRC, 1946, Voropayev et al., 2012, Issa and Daya, 2014), from which information about the turbulent wake can be inferred (**Paper I**). Thermal wakes are a result of ship-induced water column mixing in a stratified water mass, and thus a proxy for the wake water and the longevity of the impact of the ship-induced turbulence (Voropayev et al., 2012).

Satellite imagery provides a snapshot in time over a large area, whereas drones can provide continuous observations with a higher spatial and temporal resolution. High resolution SST satellite data is temporally sparse, e.g. the Landsat 8 satellite passes every 16th day (USGS, 2023) and the Sentinel 2 satellite pair every 5 days (ESA, 2023). SST imagery is also less reliable in coastal areas due to land contamination (Gentemann et al., 2010), and requires cloud free conditions, which increases data scarcity in areas with a lot of cloud cover. Drones do not have these limitations but may be practically or legally restricted when operating at sea in areas with intense ship traffic. Nevertheless, compared to satellites, drones are more suitable for the spatiotemporal scales of turbulent wakes and are easier to combine with simultaneous underwater observations.

3.1.4 Adding tracers to the turbulent wake

An approach that has been used to study the dilution of discharges in the ship wake, is the release of a detectable tracer in the near wake, and then monitoring the spread and dilution over time (e.g. (Loehr et al., 2006, Katz et al., 2003, US-EPA, 2002, Byrne et al., 1988)). The tracer signal can then be used as a proxy of the wake water, analogous to the bubbles in acoustic measurements, and the spread of the tracer thus provide information about the wake extent. The dilution of the tracer is also related to the mixing of the wake water, and an effect of the ship-induced turbulence. This approach is therefore useful for estimating the impact of the turbulent wake on the dilution of pollutants but does not directly characterise the turbulent wake itself.

3.1.5 CTD observations of stratification

Water column stratification can both affect and be affected by the turbulent wake, and *in situ* observations of stratification are therefore central in characterising the turbulent wake. Stratification is measured using CTD-sensors, which measure salinity, temperature, and pressure, from which water density can be calculated. If vertical measurements (a profile) are made with high enough spatial resolution, they will provide information about the stratification's location, strength, and thickness. The main disadvantages of CTD-sensors when it comes to turbulent wake studies, is that the sensors need to be in direct contact with the water it is measuring. Hence continuous CTD observations of the entire wake passage is not feasible, since the wake inducing ship would strike any deployments inside the wake area. It is therefore difficult to use CTDs to observe the effect of ship-induced water column mixing, as the wake-mixing event occur on short time scales (**Paper III**).

3.1.6 Observing ship-wake impact on air-sea gas exchange

The bubbles and turbulence in the ship wake can affect air-sea gas-exchange in the wake region (Weber et al., 2005, Emerson and Bushinsky, 2016). Observing this potential impact requires observations of ship-wake related changes in the gas exchange-rate or concentration changes of gases in the water and/or atmosphere. However, observations of air-sea gas flux measurements is a field of its own, and outside the scope of this thesis. The subject has recently been reviewed by others (e.g. Wanninkhof et al. (2009), Bastviken et al. (2022)), hence only a brief overview of the most relevant methodological approaches related to turbulent wake observations will be presented here.

Water column concentrations can be sampled either using *in situ* sensors, or by taking water samples for laboratory analysis. Discrete water sampling in the turbulent wake is possible, but it is difficult to sample the near wake and to achieve a high spatiotemporal resolution. Available *in situ* sensors for O_2, CO_2, and CH_4, can be used and deployed in a similar way as the CTD sensors. The gas flux over the air-sea surface can be measured *in situ* using floating chambers, but as the they require calm conditions for reliable measurements (Bastviken et al., 2022), they are not ideal for observing the turbulent wake region. Atmospheric concentrations and flux of gases can be observed *in situ* using spectrophotometric instruments, such as cavity ring-down spectrometer (CRDS) (Beecken et al., 2015, Grönholm et al., 2021), or using micrometeorological approaches such as the eddy-covariance (EC) method (Wanninkhof et al., 2009, Thornton et al., 2020, Gutiérrez-Loza et al., 2019, Bastviken et al., 2022). CRDS have previously been used to observe air emissions from ships and can be made at a distance from the emission source (Beecken et al., 2015, Grönholm et al., 2021)(**Paper IV**), which is convenient with regards to turbulent wake studies. However, the concentration changes need to be within the instrument detection limit, and knowledge about the dispersion of the observed emission is needed to estimate the initial emission concentration (Bastviken et al., 2022). The EC method has been used to observe atmospheric fluxes of e.g. CH_4 and CO_2 at sea, but as it is not suitable for low concentrations or short time scales (< 1 h) (Wanninkhof et al., 2009, Thornton et al., 2020, Bastviken et al., 2022), the application for *in situ* wake measurements is limited.

3.1.7 Ship tracking (AIS)

An integral part of *in situ* observations of turbulent ship wakes is the ability to identify the ships inducing the wakes. Since 2002, the international maritime organisation (IMO) convention Safety of Life at Sea (SOLAS) (regulation V/19) require all passenger

vessels and large ships (> 300 GT) to have an Automatic Identification System (AIS). The AIS transmit information about the ship's identity, position, speed, and current operation, and is thus useful to gather vessel specific data during opportunistic observations of turbulent ship wakes (**Paper I**, **Paper III**). Still, many of the ship-specific parameters in the AIS data are entered manually and are not always reliable, hence there is a need for cross-validation. Although the AIS coverage is generally good, ships can turn off their transmitters and avoid being recorded (**Paper I**, **Paper III**, **Paper IV**).

3.2 SENSOR PLATFORMS RELEVANT FOR TURBULENT WAKE STUDIES

A sensor platform is the physical frame holding any or several of the instruments described in the previous section. Different platform types use different ways of deploying the sensors in the field, and the mode of deployment will impact which spatiotemporal scales that are possible to observe. Table 3 summarises the main features of three categories of *in situ* sensor platforms relevant for turbulent wake studies: profilers, mobile platforms, and stationary platforms. The profilers, such as CTDs and MSPs, are used to make vertical measurements and can provide a snapshot in time of the dept dimension. The mobile category includes all platforms which can move and thus observe any dimension (depth, width, or length), such as drones or ship-mounted systems. The stationary platforms will observe the same point or profile (which dimension depends on the configuration) and can often be deployed for a longer period of time than the other two categories.

The handheld profiler includes platforms/instruments small and light enough to be deployed by hand and from any vessel and could thus potentially be deployed in the near and intermediate wake. The winch deployed profiler (e.g., a CTD-rosette) is a larger system requiring a vessel equipped with a winch and can usually hold a large variety of sensors and water samplers. However, they cannot be deployed quickly enough to capture the near and intermediate wake. Moreover, when a larger vessel is needed for carrying the profiler, there is a risk of disturbing the observed wake, hence winch deployed profilers are unsuitable for turbulent wake observations. There are also intermediate profiling systems that can be deployed while the ship is moving, such as moving vessel profilers and yo-yoing profilers.

Mobile self-propelled platforms, such as autonomous underwater vehicles (AUVs) and remotely operated vehicles (ROVs), can be equipped with a variety of instruments depending on design, and can be operated in any dimension (depth, width, length). As these vehicles generally operate at a low speed (1–4 knots), they are not very suitable for cross-section or profile observations of the near and intermediate wake, where the turbulent wake characteristics change very rapidly.

The passive mobile platforms include drifters and towed or ship-mounted systems, where the latter is the most frequently used method to observe turbulent ship wakes (Ermakov and Kapustin, 2010, Loehr et al., 2001, Soloviev et al., 2012, Francisco et al., 2017, Kouzoubov et al., 2014, Marmorino and Trump, 1996, Stanic et al., 2009). Towing instruments alongside or across the turbulent wake, is an approach that has been used both in ship wake studies (Marmorino and Trump, 1996, Stanic et al., 2009) and in studies of the wakes of off-shore wind power structures (Schultze et al., 2020). A few studies have also observed the wake from the inside or side, but remained stationary

instead of moving along/across the wake (Soloviev et al., 2012, Francisco et al., 2017) (Kouzoubov et al., 2014). Another approach, used by Loehr et al. (2001), is the deployment of drifters with sensor strings inside the wake, which then follows and observe inside the wake as it drifts. Drifters and instruments towed behind the wake inducing ship can be deployed inside the near and intermediate wake, and ship-mounted acoustic instruments can observe the near wake from a distance. However, in the case of crossing the wake with a vessel equipped with instruments, it will be difficult to capture the near and possibly also intermediate wake.

Table 3.Summary of *in situ* sensor platforms able to hold acoustic instruments and conductivity, temperature, depth (CTD) sensors for stratification observations. The spatial resolution (res.) **Line** means that either a depth or width profile is possible, and **Profile** indicates that only a depth profile can be made. A continuous temporal resolution will add the length or width dimension to the wake observation. The wake resolution is given by the combination of the spatial and temporal resolution and a 3D observation is only possible if depth, width, and length can be observed simultaneously. The 2D wake resolution always corresponds to depth or width + length (i.e. time). The advantages, disadvantages and comments are based on the results of the appended papers and are further discussed in section 6.6.

	Handheld profiler (e.g., CastAway CTD, MSP)	**Winch deployed profiler (e.g., CTD & rosette)**	**Mobile, self-propelled (e.g., AUV, ROV, drones)**	**Mobile, passive (drifters) or towed/hull mounted**	**Stationary (e.g. moored or bottom mounted, sensor strings)**
Tested	Paper I, III, IV	no	no	no	Paper I, III
Temporal res.	Discrete	Discrete	Continuous	Continuous	Continuous
Spatial res. acoustic	Profile	Profile	Line/Area*	Line/Area*	Line/Area*
Wake res. acoustic	1D (depth)	1D (depth)	2D	2D/3D*	2D/3D*
Wake region acoustic	Far (intermediate)	Far	Far (intermediate)	Potentially any	Potentially any
Spatial res. CTD	Profile	Profile	Line	Point/Line**	Point/Line**
Wake res. CTD	1D (depth)	1D (depth)	2D/3D*	1D (time)/2D**	1D (time)/2D**
Wake region CTD	Far (potentially any)	Far	Far (intermediate)	Potentially any	Wake edge***
Advantages	Easy to quickly deploy from any vessel. High-resolution.	Possible to combine with multiple sensors and water sampling.	Flexible, can observe different dimensions.	Drifters can follow drifting wake. Sensors can be towed behind ship in near wake.	Long-term, bottom mounted can observe entire wake development.
Disadvantages	Difficult and dangerous to get in position fast enough to deploy in the near wake, unless sampled from wake-inducing ship, risking the instrument and propeller to collide.	Cannot deploy in intermediate and near wake. Vessel required which can induce turbulence in the upper surface layer.	Cannot deploy in near wake. Difficult to use in intensely trafficked areas and close to ships. Relatively slow, temporal mismatch between observati-ons within transect	Towing could affect the wake. Difficult to get high enough vertical resolution to capture changes in stratification (strings). Challenging to tow instruments in wake of a large ship.	Cannot deploy in wake region due to collision risk. Difficult to get high vertical resolution needed to capture changes in stratification.
Comment	Could complement observations by stationary platforms.	Not very suitable for wake studies due to ship disturbance.	Could complement a missing dimension of a stationary instruments.	Common approach, not long-term. Can potentially capture parts of the near wake	If wake drifts over mooring, a wake cross section can be observed.

*If a multibeam is used.

**Multiple 1D sensors combined can give an interpolated 2D view (line) of the wake.

***If deployed under the shipping lane, only the wake region deeper than the passing ship's draught can be observed, if deployed beside the shipping lane, only the sides (and not the centre line) of the wake can be observed.

Abbreviations: MSP (microstructure shear probe), AUV (autonomous underwater vehicle), ROV (remotely operated vehicle).

Stationary platforms, such as moored instruments (Trevorrow et al., 1994) or upward-facing instruments placed on the sea floor (**Paper I**, **Paper III**) (Weber et al., 2005), are suitable for long term monitoring of ship wakes. Instruments moored near or at the

surface, cannot be deployed where ships are passing, due to collision risk. Hence, surface platforms can only observe from the side of the wake, which is a limitation when it comes to CTD sensors. However, for acoustic instruments the platform can be deployed at a safe distance below or at the side of the ship route. A disadvantage of stationary platforms is that they need ships to pass close enough for a wake to be detected, as the platform cannot move to the wake. This requires either deployment in a location where ships are known to pass, like a shipping lane, or the use of designated ships inducing wakes in the vicinity of the instruments. The latter approach has been most common in previous studies using stationary platforms (Trevorrow et al., 1994, Weber et al., 2005).

3.3 USING MACHINE LEARNING FOR SHIP WAKE DETECTION

An in-depth description of ML and the different ways it can be used in turbulent wake studies, is beyond the scope of this thesis. This section will provide a brief overview of how ML can be used to analyse acoustic data, with respect to image classification.

ML models are useful when identifying statistically significant patterns in large datasets (LeCun et al., 2015, Malde et al., 2019, Guidi et al., 2020), such as detecting ship wakes in acoustic data (echograms) (**Paper II**). ML models have been developed for automatic identification of fish species in acoustic data (echograms) (Horne, 2000, Yassir et al., 2023), and a similar approach can be applied for ship wake detection. Automatic ship wake detection in echograms is related to image and pattern recognition, a task suitable for Convolutional Neural Networks (CNNs), which is a class of deep learning ML models (Krizhevsky et al., 2012). To train a state-of-the art CNN, a large dataset of labelled data is needed, which is challenging when data is limited (as in the case ship wakes). However, data scarcity can also be addressed using ML models, as the available data can be used to generate additional training data (Van Dyk and Meng, 2001). The data generation can be further improved by including an expert evaluation of the generated dataset, a so called expert-in-the-loop approach (Holzinger, 2016, Guo et al., 2016). This additional feedback from the expert to the algorithm can improve the training time and model accuracy.

3.4 MODELLING TURBULENT SHIP WAKES

An in-depth description of the modelling of turbulent ship wakes is outside the scope of this thesis, and has been reviewed in the recent thesis by Wall (2021). Here, a brief overview of different numerical and semiempirical model approaches relevant for turbulent wake studies will be presented, describing the main advantages and limitations.

Modelling the turbulent wake development is complex, and there is currently no numerical or semiempirical model able to capture its entire wake extent (Figure 2) (Wall and Paterson, 2020, Soomere, 2007, Golbraikh and Beegle-Krause, 2020). The near wake region has been described using high resolution computational fluid dynamic (CFD) models (Wall and Paterson, 2020, Brucker and Sarkar, 2010, Carrica et al., 1999, Wall, 2021)(**Paper III**, **Paper IV**) and semiempirical models (Golbraikh and Beegle-Krause, 2020, Chou, 1996). The wake turbulence and wake water dilution in the intermediate and far wake have been estimated using semiempirical models (Katz et al., 2003, Voropayev et al., 2012, Milgram et al., 1993, Dubrovin et al., 2011, Chou, 1996, Tennekes and Lumley, 1972).

3.4.1 CFD modelling

High-resolution CFD modelling, such as 3D Reynolds-averaging Navier-Stokes (3D RANS) models (Wall and Paterson, 2020, Fujimura et al., 2016, Wall, 2021)(**Paper III**) and Delayed Detached Eddy Simulation (DDES) models (Gritskevich et al., 2012, Esmaeilpour et al., 2016)(**Paper IV**), have been developed within the field of naval architecture, for the purpose of optimising propeller and hull design. As these models require large computational power (Wall and Paterson, 2020, Fujimura et al., 2016), it is not possible to expand the model for the entire wake extent, and only a few studies have run the model past 1–2 ship-lengths behind the propeller (Wall and Paterson, 2020, Brucker and Sarkar, 2010). There are also very few CFD studies of turbulent wakes of surface ships in stratified conditions (Wall and Paterson, 2020, Brucker and Sarkar, 2010), and it is a field currently in development (Wall and Paterson, 2020). The CFD model results are mainly validated using tank experiments with model-scale ships (e.g. (Carrica et al., 1999, Parmhed and Svennberg, 2006, Fu and Wan, 2011, Liefvendahl and Wikström, 2016)), and field measurements of turbulent ship wakes are scarce (Wall, 2021, Kouzoubov et al., 2014).

3.4.2 Semi-empirical models

Semi-empirical models can cover a large spatiotemporal range and overlap with the CFD models, thereby providing a bridge between the near and intermediate/far wake. However, they are simplified numerical models and are only valid for the vessels and conditions they have been validated for, which limits their applicability. Except for Voropayev et al. (2012), none of the previous semiempirical models were derived for stratified conditions, and only the model in Milgram et al. (1993) (based on data from Hoekstra and Ligtelijn (1991)), characterise the development of wake turbulence. The remaining semiempirical wake models have focused on describing the dilution of contaminants in the wake water (Golbraikh and Beegle-Krause, 2020, Katz et al., 2003, Chou, 1996, Lewis, 1985, Byrne et al., 1988), the wake water temperature (Voropayev et al., 2012), or the spatial expansion of the wake (Golbraikh and Beegle-Krause, 2020, Golbraikh et al., 2013, Dubrovin et al., 2011). Hence, there are currently no semiempirical models characterising turbulent wake development in stratified conditions.

3.4.3 Bridging the gap between the near and far wake

A few studies have combined near-wake and far-wake models, in order to cover the entire wake extent (Chou, 1996, Fujimura et al., 2016). Fujimura et al. (2016) used the results from the near 3D wake model as input in the second 3D model and was thereby able to model the entire wake extent. A similar approach, which requires less computational power, is the "2D + time" approach (Wall and Paterson, 2020), where a 2D cross section of the wake is modelled over time. The turbulence field from a CFD model of the near wake can then be used as input in an oceanic general circulation model (GCM), which can model the far field turbulent wake development in stratified conditions.

4 METHODS

In the appended papers, the turbulent wake development has been characterised using different sensor platforms, instrumentation, and numerical models, in order to capture different aspects of the turbulent wake and its impacts. A brief description and motivation of the methodological approach applied in each paper is presented here and detailed descriptions are provided in the appended papers. The *in situ* and *ex situ* field observations included in this thesis have been conducted at four different sites with intensive ship traffic in the Baltic Sea region (HELCOM, 2021) (Figure 8). The observations outside Saint Petersburg were made in summer 2011 and 2012 (**Paper IV**), the Gothenburg observations in late summer 2018 (**Paper I, Paper II**), and the Oresund measurements in August 2020 (**Paper III**). The different instruments and methodologies used to observe the turbulent wake development and its impact are illustrated in Figure 9.

Figure 8. Overview of the sites where field observations of the turbulent wake and its impact have been conducted. The back box indicates the shipping lane area north of Bornholm (Bornholm Strait) included in the satellite analysis.

4.1 PAPER I

The aim of Paper I was to characterise the magnitude and spatiotemporal scales of the turbulent wake, with a focus on wake extent. A bottom mounted Nortek Signature 500 kHz broadband ADCP (S500) was used to observe the vertical and temporal extent of the turbulent wake in a shipping lane outside Gothenburg, and a handheld SonTek CastAway®-CTD (Xylem, San Diego, California) was used to measure stratification at the time of instrument deployment and retrieval (Figure 8, Figure 9). The instrument was deployed for four weeks (28 August to 25 September 2018). The width and length of thermal ship wakes was observed in the Bornholm Strait shipping lane using SST satellite imagery from the Landsat 8 satellite (Figure 8, Figure 9). The ships inducing the observed wakes were identified using the Helsinki Commission (HELCOM) AIS database (HELCOM, 2018) and Marine Traffic (https://www.marinetraffic.com).

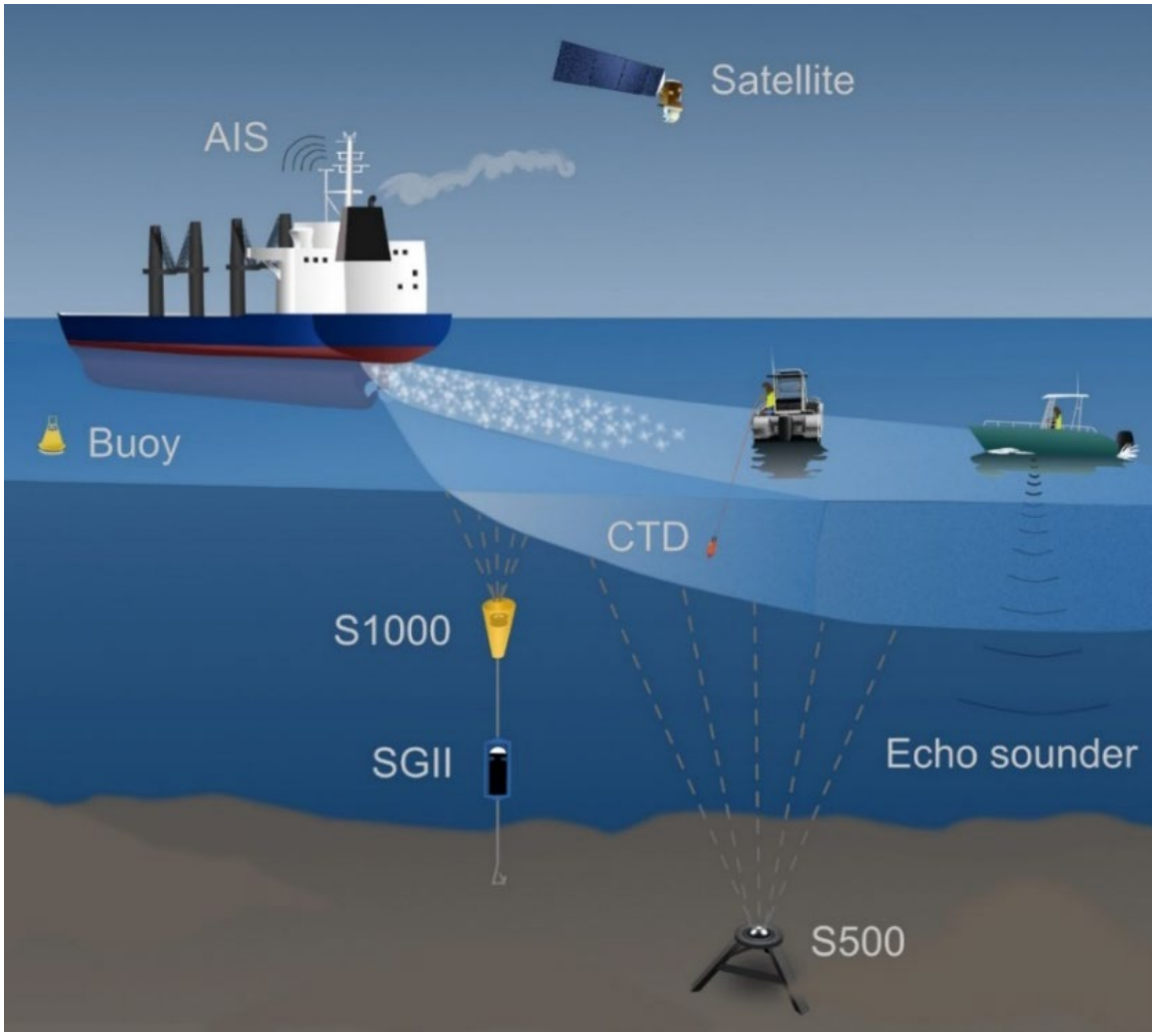

Figure 9. Schematic illustration of the *in situ* and *ex situ* observation methods used to characterise the turbulent wake. The CTD is a handheld conductivity, temperature, depth profiler. AIS is the ship's automatic identification system. S500 and S1000 (Signature 500 and 1000) are acoustic doppler current profilers (ADCPs), and SGII is a Sea Guard II ADCP. Note that the figure is not to scale.

The ship wakes in the ADCP data were manually identified and annotated from echograms. The vertical and temporal extent was estimated for both the bubble wake and the turbulent wake (ε wake), the latter calculated from the ADCP along beam velocities using the structure function method (Lucas et al., 2014). As the bow wave and hull of the wake inducing ship interfered with the velocity observations, the first 0.5–1 min after ship passage were excluded from the ε calculations. Thermal wake width and length was estimated from cloud free (< 23 %) satellite images from the IR and near-IR bands of Landsat 8. Automatic detection was used to identify ships in the satellite images and the thermal wakes were then manually digitalised. The thermal wake width was calculated using 400 m cross sections every 250 m along the wake length. An approximation of the vessel force (F, kg m s^{-2}) was calculated for each wake-inducing ship, according to Equation 2:

$$F = \rho_{sw} * B * T * s^2 \qquad \text{(Eq. 2)}$$

where B is the ship width [m], T is the ship draught [m], s is the ship speed [m s^{-1}], and ρ_{sw} the seawater density (1025 kg m^{-3}). F is proportional to ship drag and relates ship speed and size to the turbulent wake extent.

4.2 PAPER II

The manual annotation of ship wakes in the ADCP data in **Paper I** was time consuming, and the aim of **Paper II** was therefore to develop and test a deep learning model for automatic wake detection. The task was considered a classification problem, with the aim of identifying echogram images as either positive (with a wake) or negative (no wake/background). The study consisted of two parts, data collection and labelling (**Paper I**) and developing the deep learning model.

As the available training dataset was too small to train the deep learning model (165 positive wake samples from **Paper I**), additional augmented training data was generated from the original data, using a simple probabilistic Gaussian Mixture Model (GMM) (Reynolds, 2009). As the GMM required the acoustic data to be compressed before application, a simple CNN-based autoencoder trained on the ADCP dataset was used to preserve the wake patterns during compression. The output from the autoencoder was then further compressed using principal component analysis (PCA), and the GMM model was then fitted compressed data. The additional wake samples generated by the GMM were run inversely through the PCA model and autoencoder. The final augmented training dataset of comprised 1000 samples. As a step in the data generation, the augmented training dataset was approved by a domain expert (in this case, the same person who annotated the original data). This approach can speed up and increase the quality of the learning and is referred to as the expert-in-the-loop framework (Holzinger, 2016, Guo et al., 2016).

Two models were developed based on a small ResNet18 CNN model (He et al., 2016) with 18 convolutional layers. One model used the baseline ResNet18 architecture with a balanced training dataset. For the other model, robustness for an imbalanced training dataset was increased by adding an example reweighting technique (Ren et al., 2018). Five datasets of different percentage of positive samples were used to train the two models (50%, 20%, 10%, 5%, 2.5%) and their accuracy and False Negative Rate (FNR) was evaluated from 10 test runs. The models were also tested on an independent and noisy part of the original dataset.

4.3 PAPER III

The aim of **Paper III** was to quantify the turbulent wake extent and intensity and to study the interaction between stratification and the turbulent wake. In order to capture the turbulence in the near and far wake, *in situ* ADCP observations of the intermediate and far wake were combined with RANS CFD modelling of the near wake (first 30 s).

The field observations were conducted in the Oresund Strait (Oresund) (Figure 8), which is usually strongly stratified (Snoeijs-Leijonmalm and Andrén, 2017) and has an intensively trafficked narrow shipping lane (HELCOM, 2021). The setup was similar to **Paper I**, but in addition to the bottom mounted S500, a Nortek Signature 1000 kHz ADCP (S1000) and Aanderaa Sea Guard II ADCP (SGII) was also moored below the shipping lane at 20 and 30 m depth respectively (Figure 9). The distance between the S500 and the mooring was approximately 200 m, and they were deployed between August 19–31 in 2020. The water column stratification at the instrument location was measured daily during August 19–25, using a using a handheld CTD SonTek CastAway®-CTD (Xylem, San Diego, California) deployed from a small leisure boat. Opportunistic CTD measurements in ship wakes before and after passage were also

made, where the echosounder of the leisure boat was used to locate the bubble cloud of the ship wake. The wake-inducing ships were identified using the same HELCOM AIS database as in Paper I (HELCOM, 2018), and detailed vessel information was retrieved from the Sea-web Ships (2022) database.

The detection and analysis of the acoustic data was performed the same way as in **Paper I**, except the current velocities used in the ε calculations were not wave corrected. The observed ε decay rate was estimated by a linear fit to the logged mean ε values in the top 2–20 m of the water column, which were calculated every 30 s of the first 10 min of the ADCP wake.

CFD simulations of the turbulent wake were made for two generic Tanker and RoPax (Roll on passenger ferry) geometries, in stratified and non-stratified conditions. The two ship types were similar to ships present in the field observations in **Paper I**, **Paper III** (and **Paper IV**), and they were chosen due to their difference in hull design and propeller configuration, and as ship types of particular interest in the field observations. RoPax and similarly designed RoRo (roll-on roll-off) cargo vessels induced the largest wakes in **Paper I** and some of the largest in **Paper II**, whereas a tanker vessel caused a clear example of the interaction between the turbulent wake and stratification (see results and discussion in **Paper III**).

The RANS modelling was performed in full-scale, using the k-ω-SST turbulence model with wall functions (Menter et al., 2003) and the open source libraries of OpenFOAM (Weller et al., 1998). To include the effects of the propeller rotation, the model included resolved rotating propellers and a refinement box several ship lengths aft of the ship. The tanker had a grid mesh size of 33 M cells and the RoPax 30 M cells. As the RoPax had a twin-screw propeller, only half the hull was simulated with a symmetry plane. To save computational effort, the ship-induced waves were not resolved by the model, as they were considered less important for the turbulence in the near wake. A Boussinesq approximation model was used to model two stratified cases, corresponding to the *in situ* conditions in the field observations in August 19 and 21, 2020. The modelled time step represented less than 1° of propeller revolution, and the simulations were run longer than 30 s real time.

By combining field observations with the modelling results, the wake's total ship-induced ε was estimated for a Tanker and RoPax. Two ships of the same type and size as the modelled ships were chosen from the *in situ* observations. The observed ε in the far wake was then integrated over 2-–20 m depth and the first 10 minutes of the ADCP observations. The integrated ε values were multiplied with the ship speed, seawater water density, and wake width, to estimate the corresponding power of the total observed ε in kW. The total ε in the near wake was calculated the same way but using the simulated ε in the propeller centreline. The near- and far-wake estimates where then summed to get the total estimate for the entire wake.

4.4 PAPER IV

The aim of **Paper IV** was to investigate how ship passages and the turbulent wake impact the release of CH_4 to the atmosphere in an estuarine CH_4 rich area. The study consisted of two parts: field observations of ship-induced CH_4 emissions and CFD modelling of the pressure field and turbulence during a ship passage.

The field observations were conducted in the Neva Bay shipping lane outside Saint Petersburg (Figure 8), in the narrow dredged shipping lane channel 14 m deep and 120 m wide. The conditions in the Neva Bay are perfect for biogenic CH_4 production, as it is shallow, have a large input of organic matter, it is partly closed off by a dam structure, has low salinity (Telesh et al., 2008, Wallenius et al., 2021, Egger et al., 2018, Humborg et al., 2019), and high concentrations of CH_4 have been observed in the water (Schneider et al., 2014).

Atmospheric concentrations of CH_4 and CO_2 behind ship passages were observed using a G2304 Picarro CRDS, a method previously used to observe emissions from the ship's smokestack (plume) (Beecken et al., 2015) (**Paper IV**). Air-water flux measurements, wind observations, and CTD-measurements were also made. AIS data for the observed ships was logged continuously, and additional vessel information was retrieved from the Sea-web Ships database (Sea-web Ships, 2022). The observed CH_4 emissions were calculated assuming a similar dispersion of CH_4 and CO_2, using the Ship Traffic Emission Assessment Model (STEAM) (Jalkanen et al., 2009) to calculate the initial CO_2 emission from the ship's smokestack. A similar approach has previously been used to estimate emission factors for NO_x and SO_2 (Beecken et al., 2015). The frequency and magnitude of CH_4 emissions were quantified, the latter per ship passage and per day. All uncertainty estimates of the emission observations were calculated according to GUM (Guide to the Expression of Uncertainty in Measurement) ISO/IEC Guide 98-3:2008 (Joint Committee for Guides in Metrology, 2008).

An estimate of the ship-induced pressure change (ΔP) was calculated according to Bernoulli's principle, assuming negligible energy loss, according to Equation 3:

$$\frac{\rho}{2}(U_s^2 - U_0^2) = -\Delta P, \qquad \text{(Eq. 3)}$$

where U_0 is the ship speed, U_s is the water speed under the ship relative to the ship, and ρ is the water density. U_s depends on the cross-sectional area around the ship influenced by the ship's passage (w_0), and was estimated according to Equation 4:

$$U_s = U_0 \cdot \frac{w_0 \times h}{(w_0 \times h - w_s \times D)}, \qquad \text{(Eq. 4)}$$

where w_0 was estimated as the shipping lane channel width, w_s is the ship width, h is the water depth in the channel, and D is the ship draught.

The ship-induced pressure was also estimated using CFD simulations of two ship geometries in conditions similar to the Neva Bay shipping lane. The same generic Tanker and RoPax ship geometries in **Paper III,** was used in **Paper IV**. These two ship types were of particular interest in the CH_4 field observations as well, as RoPax ships often induced very large CH_4 emissions, whereas small tankers never induced any CH_4 emissions. The CFD simulations also provided information about the depth and intensity of the mixing in the turbulent wake.

The ship simulation was performed in full scale using DDES modelling and the k-ω-SST turbulence model with wall functions (Gritskevich et al., 2012) and using the open source libraries of OpenFOAM (Weller et al., 1998). The model included resolved rotating propellers and a refinement box, but did not resolve the waves generated by the ship. At the modelled speeds (10 and 12 knots), ship-induced surface waves are small, and were assumed not to contribute significantly to the pressure field on the sea floor.

The bathymetry area of the model was 700 x 550 m, with a water depth of 4 m with a channel in the middle, 14 m deep and 120 m wide. The mesh sizes were 22 M cells for the Tanker and 42 M cells for the RoPax, with cell sizes < 2 mm around the propeller and 10 cm in the wake region. The time step of the simulations corresponded to less than 0.05° of propeller revolution, and the models were run for up to 30 s real time.

5 RESULTS

In this chapter, the main results from the appended papers related to the thesis aim and research questions, are summarised. Each section provides relevant results from all appended papers.

5.1 TURBULENT WAKE EXTENT AND INTENSITY

Turbulent wake extent and intensity was observed and modelled in **Paper I** and **Paper III**. The focus of **Paper I** was on observing the turbulent wake extent and **Paper III** focused on characterising the turbulent intensity and decay. As the environmental conditions were different between the two study sites, the combined results provide information about the turbulent wake development for a large range of ship types in both stratified and non-stratified conditions.

5.1.1 Spatial and temporal extent

The wake depth and longevity for the field observations in the shipping lane outside Gothenburg and in Oresund, are presented in Figure 10 (**Paper I** and **Paper III**). The Gothenburg dataset includes the observed close passages, defined as passing within 3 ship widths of the instrument, and the Oresund data includes the observed passages with a visible echosounder signal. The ε wake depth was slightly larger than the bubble wake, and the observed depths were similar between locations and the two ADCP instruments (S500 and S1000). For the wake duration, on the other hand, there was a clear difference between the S500 and S1000, as the bubble wake duration was much shorter in the S1000 dataset compared to the S500. The S500 bubble wake duration was also longer compared to the ε wake and similar at both locations.

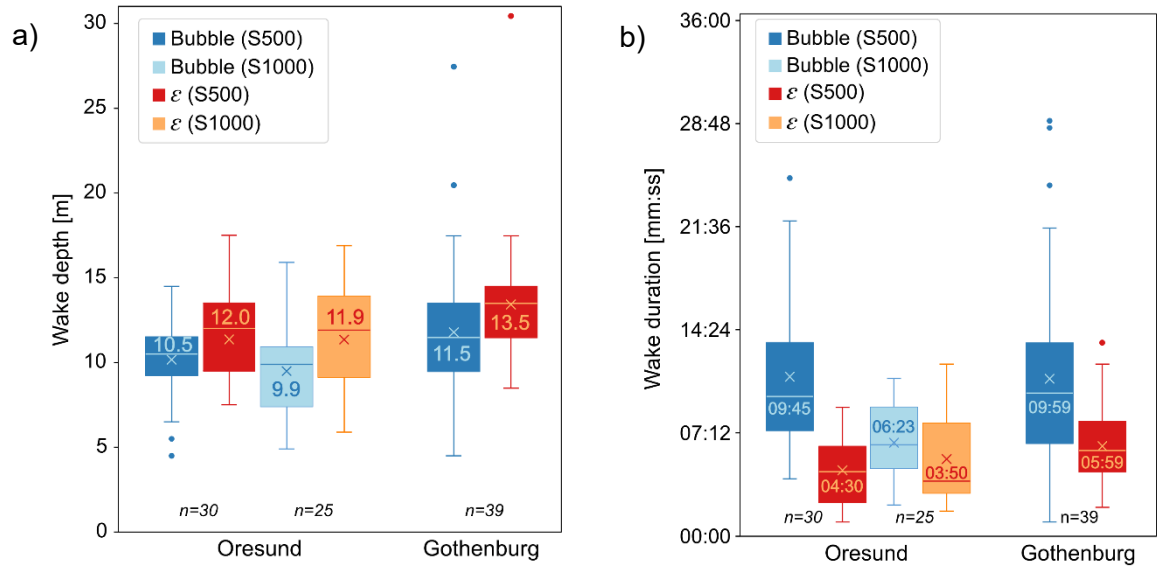

Figure 10. Bubble and ε wake depth [m] (a) and duration [mm:ss] (b) in the Oresund and Gothenburg field observations, from the S500 and S1000 instruments. Median values are indicated by the horizontal line and number, mean value is indicated by the x. The sample size (n) is indicated below each instrument and location. Blue colours indicate bubble wake observations and red/orange colours, ε wake observations. Note the difference in bubble wake duration between the S500 and S1000 instruments.

The Gothenburg sample size (n) was larger and comprised larger and faster vessels compared to the Oresund dataset. Still, there was no statistically significant correlation between vessel force (F) and wake depth or duration, at either of the sites or for the

combined dataset (R^2-values > 0.17). Apart from the slightly longer duration of the ε wake in the Gothenburg dataset (not statistically significant), there was no clear difference in wake extent between the sites, except that wakes deeper than 18 m did not occur in Oresund. From Figure 10, this difference in depth extent is not very clear, as the two very deep wakes (>18 m) in the Gothenburg dataset appear as outliers. However, in addition to the wakes in Figure 10, there were several cases where it was not possible to assign the wake to a single ship as two ships were passing at similar distance at the same time. Among these cases, four wakes exceeded 18 m depth. Thus, considering all the observed wakes, the Oresund wakes had a shallower maximum vertical extent compared to the Gothenburg dataset.

The bubble and ε wake depths and duration for the six ship types where $n > 3$ observed passages were investigated, and there was no clear difference between the ship types, for the entire dataset or between the two sites. However, the deepest observed wakes were from RoRo and RoPax ships. Moreover, in the Oresund dataset, the longest bubble wakes occurred when bubbles were "trapped" in the stratification, remaining up to 10 min after the rest of the bubble wake disappeared (see Figure 7 for example). In the Gothenburg dataset, however, the entire wake often remained for > 10 minutes (**Paper I**, supplementary material).

The ADCP instruments used in **Paper I-III** did not allow for quantification of the turbulent wake width. However, the maximum distance between the four slanted beams in the ADCPs is ca 20 m (S1000) and 30 m (S500) (at 25° angel and 30 m depth), hence for the passages where the wake was visible in all five beams, this distance indicates the minimum wake width. In the Oresund dataset, the bubbles and turbulence were visible in all five beams in a majority of the passages for both instruments. As 75 % of the Oresund ships were < 20 m wide, it indicates that wake width was frequently at least 50 % wider than the ship width. In the Gothenburg dataset the median ship width was 26.5 m, thus too close to the 30 m estimate to provide any useful information regarding the ship width. Nevertheless, in the Gothenburg dataset, ship wakes were frequently detected from ships passing at 2–6 ship widths distance, with one bubble wake being detected from a ship passing 55 ship widths (184 m) from the instrument. Hence, the observations from **Paper I** and **Paper III**, indicate that the turbulent and bubble wake width is 50–600 % wider than the ship.

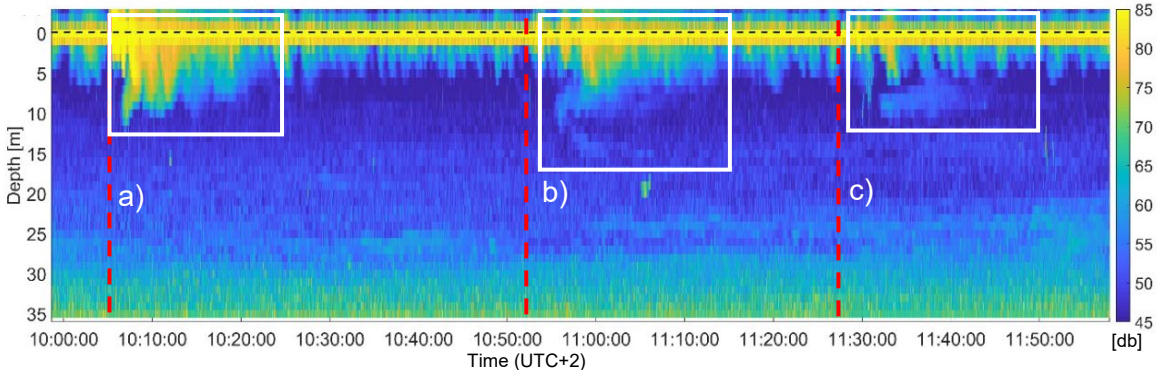

Figure 11. Signature 500 ADCP data of the signal strength from overpasses of R/V Svea. The dashed black line indicates the sea surface, and the red dashed lines indicate the passages of Svea. (a) is the passage right over the instrument (10:05 UTC+2), (b) 25 m east of the instrument (10:51 UTC+2), and (c) 50 m east of the instrument (11:28 UTC+2). The white boxes indicate the wake signal. The x-axis indicate time [hh:mm:ss] and the colour bar the signal strength in dB.

The wake width estimate of 0.5–6 ship widths, was in agreement with field observations of ship overpasses, where the bubble wake of a 15.8 m wide ship was detectable 50 m east of the S500 instrument (Figure 11) (results not included in the appended papers). The estimate was also in line with the satellite image analysis of thermal ship wakes in **Paper I,** which showed a median thermal wake width of 157.5 m, and that all observed wakes were > 100 m wide (Figure 10b in **Paper I**). The median thermal wake length was 13.7 km (34 minutes for a ship with a speed of 13 knots) and 25 % of the wakes were longer than 20.9 km (Figure 10a in **Paper I**). The temperature decrease caused by the ship-induced turbulent mixing could thus be observed for a longer time than the bubbles and turbulence itself.

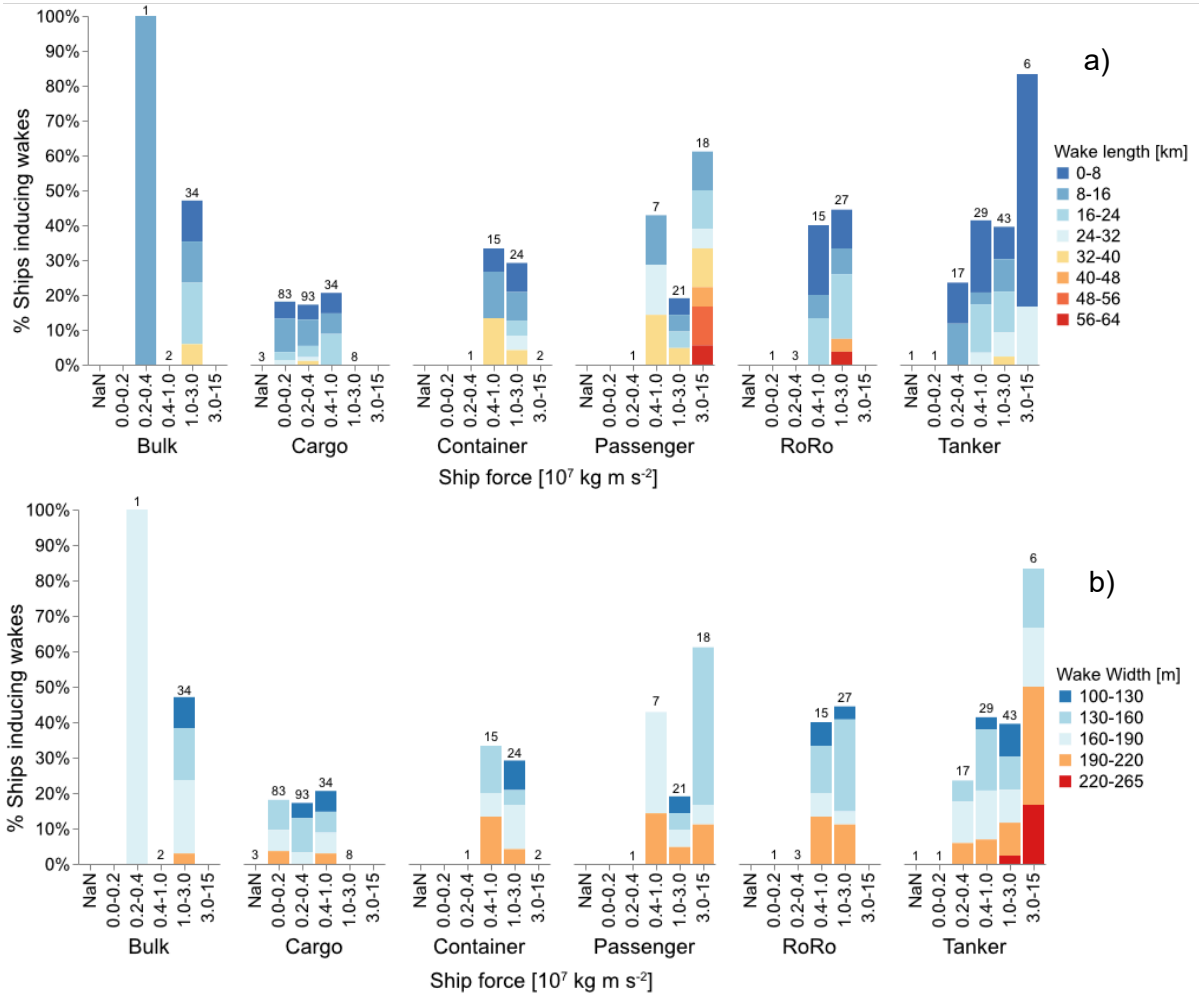

Figure 12. Satellite thermal wake length (a) and width (b) per ship type, for different ship force categories. The passenger category includes Cruise and RoPax ships. The y-axis indicates the percentage of passages for each category that induced a detectable thermal wake. The x-axis indicates the ship force, which is dependent on ship speed, draught, and width. The number above each bar indicates the samples size (n), and no number means no passage in that category. The colours indicate the wake width/length, where blue shades are smaller/shorter values and red shades are large values.

The thermal wake widths and lengths were also analysed with respect to ship length, speed, draught, width, force, and type, where the force results are presented in Figure 12 (the force estimate is defined in the methods section). The sample size for the different categories varied greatly (the numbers above each bar), hence the results should be interpreted with caution. The Cargo ships induced detectable thermal wakes least frequently (< 30 % of the passages), and they also had few/no passages in the large

force categories (1–3 and 3–15 [10^7 kg m s^{-2}]). Passenger (Cruise and RoPax), Tanker and Bulk ships with high force induced detectable wakes most frequently (50–85 % of the passages). Of the observed ships, the widest thermal wakes were induced by Tanker ships with a large force (Figure 12) and width (40–60 m wide, data not shown). No similar relationship between wake width and large force/ship width was found for any other ship type. The longest wakes (32–64 km) were induced by Passenger and RoRo ships with a large force. There were indications that a large force also increased the wake length for the Tanker and Bulk categories, but no reliable conclusions can be drawn, due to the skewed number of passages in each force category. Hence, no general relationship between ship force and thermal wake length and width was found among the ship types.

The CFD simulations of the Tanker and RoPax ε wake showed that during the initial 30 s, the wake did not widen much beyond the ship width, and there was no major difference between the stratified and non-stratified cases (**Paper III,** Figure 16 and Supplementary Figure 11–13). Likewise, there were there were no clear differences in ε wake depth between the stratified and non-stratified cases, but some small differences between the ship types. The Tanker ε wake reached ~11 m at 30 s (5 m below draught) and the RoPax ~14 m after 25 s (7 m below draught) (**Paper III** Figure 16 and Supplementary Figure 12–13).

5.1.2 Turbulence intensity

The observed decay of ε for all passages with visible echosounders in all five beams, for both Gothenburg and Oresund, are presented in Figure 13 (**Paper I**, **Paper III**). The R^2-values for the linear function fitted to the logged data was 0.46 for Oresund and 0.42 for Gothenburg and within the 95 % confidence interval of the dataset mean. The observed Gothenburg ε decay rate was slightly higher compared to the Oresund (Figure 13). The difference was expected, as both the sampled vessels and hydrographic conditions differed between the sites. The observed ε values were similar for all the nine Oresund vessels, which had comparable draughts, but were of varying lengths, widths, speeds, and types. This contrasted with the six Gothenburg vessels, which also had similar ε values, but were all induced by RoRo or RoPax vessels with similar dimensions and speed. When comparing the ε decay rate for only the RoRo/RoPax vessels between the two sites (Figure 13, Supplementary Figure 9a in **Paper III**) the Oresund values and decay rate was still lower, indicating that the observed difference in ε decay rate was not due to differences in observed ship types. When comparing the ε decay rate and values for all ship types in the Oresund dataset, there was no clear difference between the ship types (Supplementary Figure 9a in **Paper III**).

The Tanker and RoPax CFD stratified model outputs for mean ε over 2–20 m depth, are also included in the Oresund Figure 13a for comparison (**Paper III**). In the Gothenburg figure (Figure 13b), the same model output is included, but for a homogenous water mass. As the field observations start 30 s to 1 min aft of the rudder, a 30 s delay have been added to the field observations to illustrate the time relationship between the model result and field observations. The modelled ε decay rate (-7/3) was much larger than the observed decay rates (approximately -3/5), but at the time of convergence the modelled and observed ε values were in good agreement for both sites, especially for the Tanker simulation. The initial 30 s of the wake are thus the most turbulent, with a ε decay rate close to -7/3, which is in line with previous studies (Wall and Paterson, 2020, Brucker and Sarkar, 2010) (**Paper III**). The non-stratified model cases had higher

maximum intensities than the stratified cases, but after ~10 s the values converged, and the decay rate was similar for both cases (Figure 13, Figure 15 in **Paper III**). The modelled maximum ε intensities were ~2 orders of magnitude larger than the highest observed values, with the RoPax values being ca 2 times larger than the tanker (Figure 13, Figure 15 in **Paper III**). The high ε intensities in the RoPax wake also covered a larger area compared to the Tanker ε wake (Figure 16 and Supplementary Figure 12–13 in **Paper III**), which was expected considering the RoPax's twin propellers and larger engine power.

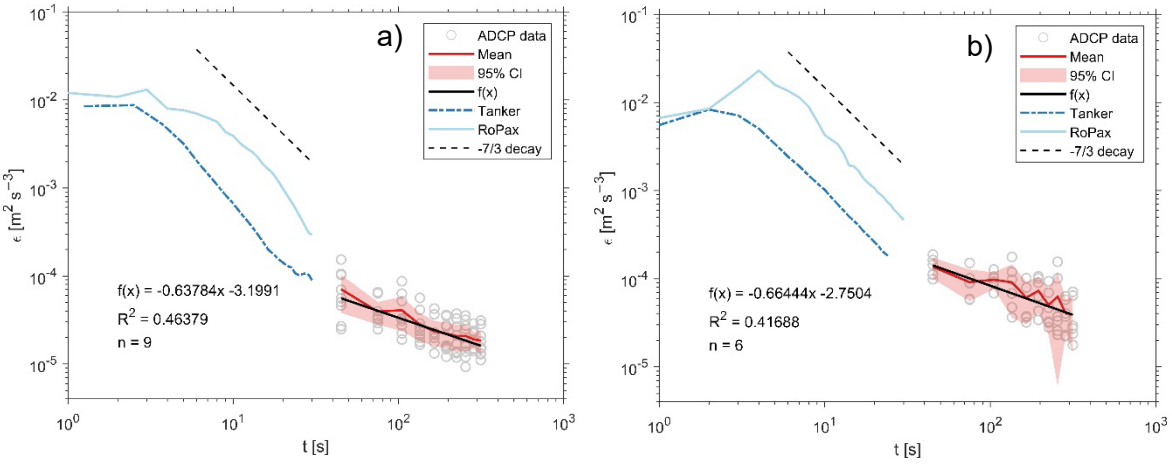

Figure 13. The observed mean exponential decay of turbulent kinetic energy dissipation rate (ε) for the top 2–20 m of the water column, for all ships with a visible echosounder in all 5 beams (S500) in (a) Oresund and (b) Gothenburg. The x-axis shows the time in seconds. The ADCP data points are indicated by circles, the red line is the dataset mean, and the red area indicates the 95 % confidence interval (CI). The black line is a linear function f(x) fitted to the logged data. The CFD model output of mean ε over 2–20 m depth from the rudder position (10^0) and 30 s onwards for the Tanker (dark blue dash dotted line) and RoPax (light blue line). The Oresund model output is for stratified conditions (200819 case) and the Gothenburg data is for a homogenous water mass. As the field observations start 0.5–1 min aft of the rudder, a 30 s delay have been added to the field observations to illustrate the time relationship between the model result and field observations. The (-7/3) ε decay rate is included for comparison (black dashed line).

In both the S500 and S1000 data in Oresund, ≥ 50 % of the passages clearly induced ε levels above $2.5 \cdot 10^{-4}$ m^2 s^{-3} lasting for ≥ 30 s. The modelling results also indicate that during the first 30 s of the wake, the ε values mostly exceed $2.5 \cdot 10^{-4}$ (Figure 13). Few of the S500 passages had ε values exceeding $1 \cdot 10^{-3}$ m^2 s^{-3}, and the duration of the occurrences of ε values above the threshold level were mostly very short (30 s–1 min). All but one of the S1000 passages exceeding the threshold were > $1 \cdot 10^{-3}$ m^2 s^{-3} and had a longer duration compared to the S500 wakes (2–10 min). The values exceeding the threshold levels appear over the entire wake depth. The ship-induced ε values occurring at the pycnocline, reaches deeper and are more intense than for the observed wind generated turbulence (Supplementary Figure 10 in **Paper III**). In general, the S1000 data recorded higher ε values compared to the S500 instrument.

The integrated observed total ε in the turbulent wake of a Tanker and RoPax, corresponded to power estimates of 450 ± 7 kW and 3148 ± 25 kW, respectively. 90–95 % of the total estimate was from the modelled near wake. The estimated power corresponded to 13 % (RoPax) and 19 % (Tanker) of the installed engine power of the *in situ* vessels.

5.2 INTERACTION BETWEEN TURBULENT SHIP WAKES AND STRATIFICATION

The field observations clearly showed that the turbulent wake development was impacted by the stratification and/or currents, with a decreased vertical extent and increased horizontal spread (**Paper III**). The modelling results did not show the same vertical restriction of the wake during stratified conditions (**Paper III**); however, they only simulate the first 30 s of the wake, and the field observations indicate that the deepest part of the wake often occurs later than 30 s after passage (**Paper I**, **Paper III**).

The ε and bubble wake were observed to penetrate below the stratification on several occasion in the Oresund dataset (25 % in S500 and 36 % in S1000) (**Paper III**), and during one passage in the Gothenburg dataset when stratification observations were available (**Paper I** and **Paper III**). In the Oresund ADCP observations, there were clear indications of ship-induced turbulence entraining water from below the stratification (**Paper III**). This observation was supported by the CFD modelling results (**Paper III**), which showed an increased density above the stratification after the ship passage, especially for the RoPax case (Figure 17 in **Paper III**).

The thermal ship wakes detected in the satellite analysis of SST, provide another concrete example of ship-induced entrainment, as the thermal wakes are the result of ship-induced vertical mixing in a stratified water mass (**Paper I**). The satellite analysis of SST showed that thermal wakes were both frequent and extensive, with a temperature decrease of up to 1 °C in the thermal wake, compared to the surrounding water.

Ship-induced internal waves were frequently noted in the Oresund dataset, and occasionally in the Gothenburg dataset (**Paper I** and **Paper III**). Internal waves were induced both by ships passing close to the instrument (with visible bubble and turbulent wake), and by ships up to 100–350 m away (without a visible bubble or turbulent wake). The model results also showed that the ship passages induced large vertical movement of the water masses, visible as diapycnal displacements (Supplementary Figures 15–17, **Paper III**).

5.3 QUANTIFYING SHIP-INDUCED METHANE EMISSIONS

In the Neva Bay field study, large and frequent ship-induced CH_4 emissions were observed and quantified (**Paper IV**). Container, Cruise, and RoPax vessels had the largest CH_4 emissions and triggered emissions most frequently (56–77 % of the cases) (**Paper IV**). The estimated total CH_4 emission from the observed section of the Neva Bay shipping lane, was 117.0 kg day^{-1}, corresponding to a CH_4 flux of 0.179 g m^{-2} day^{-1} (or 11.14 mmol m^{-2} day^{-1}).

The analysis of the parameters governing the ship-induced methane emissions, indicated that ship draught, length, speed, and ΔP, had threshold values that when exceeded will often trigger a methane emission (**Paper IV**). Ships > 250 m long, with a draught > 8 m, and speed > 12 knots, frequently induced methane emissions, and few emissions were triggered by ships < 125 m long, with draughts < 5 m, and with a speed < 9 knots (**Paper IV**). The ΔP was not measured directly in **Paper IV**, but the modelled pressure field and the calculated estimate of ΔP were in good agreement, both indicating a threshold value for emission-triggering between 30–60 mbar. The calculated and modelled ΔP in **Paper IV** was in the same range as the observed ship-induced ΔP in **Paper III**, which was ~15–20 mbar at 34 m depth.

There was a weak correlation between the observed CH_4 emissions magnitude and the calculated ΔP, a R^2-value of 0.474 for a fitted exponential curve (Extended Data Fig. 6d, **Paper IV**). The largest CH_4 emissions were induced by ships faster than 12 knots, but there was no statistically significant correlation between ship speed and emission magnitude. No correlation was found between emission magnitude and the ship draught, ship length, or the time since the last ship passage.

The modelling results showed that the RoPax-induced pressure field covered a larger area and that these vessels induced larger vertical velocities, compared to the Tanker (**Paper IV**). For both ships, a large part of the water column in the wake region was affected by high ε levels and vertical velocities (**Paper IV**).

5.4 USING MACHINE LEARNING FOR AUTOMATIC DETECTION OF SHIP WAKES IN ADCP DATA

The evaluation of the developed deep learning-based expert-in-the-loop framework for automatic wake detection in ADCP data, showed that for a balanced training dataset with 50 % positive samples, the baseline ResNet18 model had an average accuracy of 93.4 % ± 1.80 %, when classifying ship wakes in acoustic data with low noise levels (**Paper II**). The false negative rate (FNR) for the same case was 9.87 ± 3.28 %. A majority of the erroneously classified wake samples were due to false negatives, hence the model seldom classified non-wakes as wakes, but did not identify all of the wake samples. The model was accuracy in classifying wakes in noisy acoustic data, was low, with a mean accuracy score of 60.6 % and FNR of 38.06. When using unbalanced training datasets with fewer positive samples (≤ 10 %), both models performed worse, but the reweighted ResNet18 model was more robust than the baseline model.

6 DISCUSSION

The results presented in this thesis are the outcome of interdisciplinary collaboration, comprising a divers set of methodological approaches and field observations. The unique dataset of *in situ* turbulent wake observations in the far wake, combined with CFD modelling of the near wake, provide the basis for a characterisation of the turbulent wake from an environmental impact perspective. The limitations an implication of the presented results will be discussed in this chapter, in relation to the main objectives and research questions.

6.1 LARGE VARIATION IN TURBULENT WAKE EXTENT AND INTENSITY

The S500 median values of the observed turbulent wake extent and intensity were in good agreement between the Gothenburg and Oresund sites. The exception was the ε wake duration and intensity, which were a bit longer and higher in the Gothenburg dataset (Figure 10 and Figure 13). The S1000 observations were similar to the S500, except the median bubble wake longevity, which was considerably shorter (06:23 min) for the S1000 compared to the S500 (~10 min) (Figure 10). There are several potential explanations to the higher ε wake intensities observed at the Gothenburg site: differences in the observed vessel types and speeds, difference in hydrographic conditions, or a methodological difference. The ships observed outside Gothenburg were slightly larger and faster compared to the Oresund dataset, but no correlation was found between ship size/speed and wake intensity (Figure 13). The modelling results, on the other hand, showed that the larger RoPax vessel induced higher ε intensities compared to the smaller Tanker (Figure 13, **Paper III**). The results are thus inconclusive regarding whether the higher intensities in Gothenburg are caused by the difference in observed ship types. The other two explanations are also plausible, and possibly interconnected. The Oresund wakes did not penetrate as deep as the Gothenburg wakes (Figure 10, **Paper I** and **Paper III**) and at multiple occasions an horizontal wake spread was observed, a phenomenon likely caused by the strong stratification and/or currents in Oresund (**Paper III**). If the wake spreads horizontally instead of vertically, the calculated mean ε value for each ADCP beam would decrease, as a smaller portion of the 2–20 m depth interval would contain the wake. Hence, the observed lower ε values in Oresund do not necessarily mean that the total wake turbulence was lower, it could also be a methodological artefact of only estimating the mean ε for a vertical profile.

The total power estimate from the integrated ε values in the near and far turbulent wake, indicated that 90–95 % of the dissipation occurred in the near wake (the modelled first 30 s), for both the Tanker and RoPax. This has implications for the potential impact of the ship-induced turbulence. As it usually takes more than 30 s for the turbulent wake to reach its maximum depth, the most intense turbulence might not reach the same depths as have been observed in the far wake, and potentially never reach deep enough to directly impact the stratification. There are also methodological implications for turbulent wake characterization. If most of the dissipation occurs in the near wake, CFD modelling of the near wake could provide a sufficient estimate of the total turbulent intensities. However, the estimated power only corresponded to 13 % (RoPax) and 19 % (Tanker) of the installed engine power, which is about one third of the expected energy loss between the engine power and thrust power delivered to the propeller (usually 55–70 % of the engine power) (Xing et al., 2020). This discrepancy indicates

either that a large part of the propeller thrust power is removed from the system in other ways than through dissipation, or that the methodological approach used to estimate the wake ε does not capture all the wake dissipation. RoPax vessels are expected to have a higher discrepancy between installed engine power and propeller thrust power, as for passenger ships, the hotel load represents 30–40 % of the total engine load (Micoli et al., 2021, Brækken et al., 2023). Still, this does not account for the large difference, but it explains why the Tanker had a higher percentage than the RoPax. Energy losses due to ship-induced waves or an increase in the water's potential energy due to vertical mixing, are also possible ways in which energy could leave the system, but they were not quantified in the appended papers. There are several potential methodological explanations to the discrepancy. Firstly, the near wake ε estimate only included a 1 m wide section behind the propeller centerline. This simplification was made as a conservative estimate of the wake ε, as there was a rapid decline in ε values to either side of the centreline (**Paper III**, Supplementary Figure 12). An estimate of ε in the entire wake region would be more accurate and could potentially account for some of the energy loss. Secondly, there are several potential explanations related to the ADCP measurements. The top 2 m of the water column could not be observed by the ADCP and were therefore excluded from the analysis and unaccounted for. In addition, there background noise was high in the ADCP observations, which made it impossible to separate the wake ε from the ambient ε, hence the lower intensities in the far wake region were not included in the estimate. In addition, the vertical resolution of the ADCP measurements could be too low to capture all the turbulent length scales in the wake region, when using the structure function method. Moreover, there could be residual currents and large-scale turbulence, which had not yet dissipated during the first 10 minutes of the far wake.

The ε wake depth estimate was quite coarse, as the resolution of the ADCP bins (0.5 and 1 m for S500 and S1000) meant that the calculated ε estimates only captured intense turbulent eddies of vertical eddy scales larger than 2–3 m. Still, the estimates give an indication of the wake depth magnitude and variation but wake depth differences less than 1–2 m should not be considered significantly different. The CFD simulations of the ε wake depth were in line with the field observations, with the Tanker wake reaching ~11 m after 30 s and the RoPax ~14 m after 25 s (**Paper III**). However, the model results should not be considered an estimate of the maximum wake depth, as the field observations show that the deepest part of the turbulent wake often occurs more than 30 s after ship passage, sometimes several minutes later (**Paper I**, **Paper III**) (Golbraikh and Beegle-Krause, 2020).

There are no previous field studies of the turbulent wake extent of full-scale ships, but the median observed bubble wake depths and duration, were in the same range as observed in previous studies (see references in Table 1). However, the deepest wakes in the Gothenburg dataset were 18–30.5 m, and the largest wake depth was more than 10 m deeper than any previous observations (Table 1). Two previous studies observed bubble wake depths of 18 m (Soloviev et al., 2010, Loehr et al., 2001), and US-EPA (2002) observed dyed wake water reaching 18 m depth. The ships in these three studies were much larger compared to the other field studies (Table 1), with the exception of Soloviev et al. (2012). The ships observed in Oresund were all > 70 m long (median 103.5 m) and 75 % of the ships had draughts > 5 m (median 6 m). Thus, so far, wake depths of ≥ 18 m has only been observed for ships > 70 m long and with draughts > 5.5 m.

The observed thermal wake lengths were up to one order of magnitude longer compared to previous model estimates of 30 ship lengths (Voropayev et al., 2012), though wake temperature differences lasting more than an hour has previously been observed in the field (NDRC, 1946). The observed thermal wake width (median 157.5 m, range 100-265 m) was in the same range as previously observed wake widths for a large cruise vessel (100–250 m) (Gilman et al., 2011). The extent of the thermal wakes in the satellite analysis were detectable for much longer than the wake turbulence and bubbles (**Paper I**), indicating that effect/impact of the turbulent wake operates on different spatiotemporal scales than the turbulent wake itself. The results of the satellite image analysis also indicate that the wake water (at least the surface water) does not mix with the surrounding water for an extended period of time (median 38 min/13.7 km, 25 % > 20.9 km) (**Paper I**), which is important to consider with regards to spread and dilution of contaminants in the wake and in shipping lanes.

Several of the deepest observed wakes in the Gothenburg dataset were induced by double passages and were not included in the analysis as it was not possible to assign the wake to a single ship (**Paper I**). Apart from the data in Figure 10, four additional wakes with depths ≥ 18 m, were observed in Gothenburg. Hence, the analysis of the entire dataset, including double passages, implies that very deep wakes (≥ 18 m) are not extreme outliers, but is within the normal variability. Furthermore, as most of the double passages were ships escorted by pilot vessels or tugboats, not including double passages in the analysis could lead to a systematic bias, discriminating the largest ships, as larger ships more often need tug assistance. If the instrument had been placed outside the area where tug and pilot assistance was needed, this bias could have been avoided. The accidental double passage, when two ships pass at a similar distance from the instrument, could still occur, but would probably not occur systematically for a specific ship type/size and thus not bias the dataset in the same way.

Both sites had a large variability in the observed wake extent, indicating that natural variability of the turbulent wake development was high. The variation was high both within each site (Figure 10) and among ships of similar size and type. In addition, the wake depth varied over time and space within each wake. The variation in wake extent presented in this thesis, is comparable to the range of observed extents among all previous studies (Table 1).This is to be expected, as the sample size and variation of ship types, ship sizes, and hydrographic conditions, were much larger in the papers included in this thesis, compared to all previous studies combined. In the dataset used for the wake extent analysis (Figure 10), a total of 94 passages, 79 individual ships, and 17 different ship types were included. The grand total for all previous studies were 19 different ships of ~8 ship types, where NDRC (1946) had the largest sample size with 5 individual ships of two different Naval ship types (Table 1). Similar to the results in this thesis, NDRC (1946) noted that it was difficult to repeat the same experiment with the same result, even in favourable weather conditions, indicating a large variation when sampling in the field with varying hydrographic conditions. Likewise, Trevorrow et al. (1994) observed a large variation in bubble wake depth and intensity over the wake cross section, for repeated passages with the same vessel.

The large variation in wake extent could be caused either by the varying conditions between each passage, or the intermittent nature of the wake, which causes a variability in wake depth and width within each wake. When using a method of observation which does not resolve the entire wake development (vertically, horizontally, or temporally), it

is difficult to know if the deepest or most turbulent part of the wake was included in the observation. The ADCP used in this study only measured the wake along five discrete beams, and it is possible that different parts of the wake were measured in every passage, potentially causing sampling inconsistency and contributing to the variation. To minimise this source of variation, only the wakes with a visible echosounder in at least 3 beams were included in the ε decay rate calculation. The presence of the echosounder (and hull) is an indication that the ship is passing right over the instrument, hence the ADCP should be observing along or close to the centreline of the turbulent wake and any variation should be linked to differences in wake development, not sampling inconsistency. Still, the observed within wake variability in wake extent and intensity could potentially be reduced with a different experimental design, for example combining multiple instruments to observe the wake in 3D. In summary, one of the main conclusions of the wake extent and intensity analysis is that for field observations of full-scale ships, there is a large variation in turbulent wake development, and extreme values might be overlooked if the ship and wake sample size is too small or homogenous.

6.2 SHIP-RELATED PARAMETER GOVERNING THE TURBULENT WAKE DEVELOPMENT

Surprisingly, no significant correlation between vessel force and wake depth, width, or duration was found in the field observations, indicating that vessel force was not a main governing factor for wake extent (depth and duration) (Figure 12, **Paper I**, **Paper III**). Similarly, no correlation between either ship length, draught, speed, or type, and wake depth, width, or duration was found (Figure 12, **Paper I**, **Paper III**). The observed ε intensities were similar between ship types within the same site (Figure 13, **Paper I, Paper III**), which further indicates that vessel type, size and speed, did not significantly impact the wake characteristics. The model results showed that during the initial 25–30 s of the wake development, the larger RoPax vessel induced a wider and deeper wake compared to the Tanker, in both homogenous and stratified conditions (**Paper III**). These results indicate that in the near wake, the ship size and speed impact the turbulent wake development, but in the far and intermediate wake region, the wake development is not primarily governed by ship type.

Hoekstra and Aalbers (1997) observed similar turbulent intensity for different ship types in their model study. The observed lack of correlation between wake extent, and ship size/speed, contrasts to the assumptions and results of previous numerical and empirical estimates of wake development (Katz et al., 2003, Golbraikh and Beegle-Krause, 2020, Reed and Milgram, 2002, Milgram et al., 1993, Hoekstra and Ligtelijn, 1991, Lewis, 1985, Benilov et al., 2001). All of these previous studies found good agreement between field/model scale observations of wake development, and numerical models estimating the wake extent based on ship speed, draught and/or width. However, none of these studies considered stratified conditions, and as it is well known that stratification impacts the turbulent wake development (Lin and Pao, 1979, Brucker and Sarkar, 2010, Jacobs, 2020, Merritt, 1972), the difference in hydrographic conditions is a plausible explanation to the diverging results. The results presented in in this thesis indicate that in the intermediate and far wake region, hydrography have a larger influence on wake development than any single ship-specific parameter. Another possible interpretation of the results is that in relation to the large sample variation, the

sample size was too small to properly resolve the ship-specific variation. Still, the dataset included in this thesis is much larger than in any previous study, and consists of *in situ* observations, unlike most publicly available turbulent wake studies. Thus, although variable, the dataset presented in this thesis provides a realistic representation of the actual wake development, which evidently is both variable and complex.

For the observed ship-wake related temperature differences and methane emissions, there were some indications that ship size and speed could play an important role, but the results were inconclusive. The thermal wake width for Tanker vessels and the thermal wake length for Passenger ships increased with increasing force (Figure 12), however, the other five analysed ship types did not exhibit this relationship. The difference in sample size and distribution between the ship types makes it difficult to draw any definite conclusions, but both Tanker, Passenger, and Cargo ships had similar sample size and distribution, yet there was no uniform pattern among them. For the ship-induced methane emissions (**Paper IV**), there were clear indications of ship size, speed, and pressure threshold levels, above which methane emissions were usually triggered. However, the likelihood or magnitude of the emissions did not scale with increasing size, speed, or pressure, and some of the largest ships induced comparatively small methane emissions. Thus, no ship-related factor could clearly be shown to govern or predict the thermal wake extent or the magnitude of ship-induced methane emissions. Consequently, the results presented in this thesis indicate that in natural conditions, especially in stratified waters, the turbulent wake development is very complex and not governed by any principal (ship-specific) parameter. Moreover, that previous semiempirical estimates of contaminant dilution and dispersion, are not representative for the conditions investigated in this thesis.

6.3 INTERACTION BETWEEN STRATIFICATION AND THE TURBULENT WAKE

In the Oresund field study (**Paper III**), there were frequent observations of turbulent wakes penetrating the stratification and entraining water from below the thermocline to the upper surface layer (**Paper III**). The entrainment increased the density of the wake water above the stratification (**Paper III**), which along with the stratification, affects the turbulent wake development by decreasing the vertical extent and increasing the horizontal extent. The modelling results in **Paper III** also showed an increase in water density above the thermocline after ship passage, especially for the RoPax. The model results in **Paper III** did not indicate that the vertical development was restricted by the stratification during the initial 30 s of the wake, nor an increased horizontal spread. However, the field observations indicate that the deepest part of the wake occur later than 30 s, hence it is likely that the model results does not capture the region of the wake where stratification and entrainment impact the wake development the most.

The results presented in this thesis are the first field observations of this process, which has previously been observed in model scale laboratory experiments and numerical modelling (Lin and Pao, 1979, Brucker and Sarkar, 2010, Jacobs, 2020, Merritt, 1972). Loehr et al. (2001) observed an asymmetric horizontal expansion of the wake during field measurements, but this was more likely due to the strong current shear and not entrainment, as it was only observed at one side of the wake in the direction of the current. Jacobs (2020) modelled propeller wakes in a stratified fluid, and also found that the propeller would create mixing across the stratification, as well as entrain water from

the side of the wake. Merritt (1972) released dye in turbulent wakes in both stratified and non-stratified conditions and observed the same entrainment effect in the stratified wakes. They also found a decreased vertical spread and increased horizontal spread and, furthermore, noted that the dye in the thin stratified wake appeared to dilute more slowly compared to the unstratified case.

Due to lack of frequent observations of the stratification in the Gothenburg field study, there were only a few turbulent wake observations where the stratification was known. For those observations there were two turbulent wakes observed to reach far below the stratification (up to 10 m below) (**Paper** I). For both occasions, the ship draught was deeper than the stratification depth, and there were no observations of the increased horizontal spread and decreased vertical spread. Moreover, the penetration depth of the Gothenburg wakes was generally deeper, as the Oresund wakes only reached a few meters below the stratification (**Paper III**). This difference between the sites was likely related to the difference in stratification and current velocities, as Oresund had a deeper and stronger stratification and higher current velocities (**Paper III**). However, due to the low number of observations with a known and weak stratification, it was not possible to determine at which stratification depth and strength the wake development begin to be significantly affected by the stratification.

In addition to the ADCP observations of the turbulent wake itself, the thermal wakes observed in the satellite analysis in **Paper I,** is a detectable effect of ship-induced entrainment across a thermocline. Consequently, the results presented in this thesis clearly shows that in areas with intense ship traffic, ship-induced vertical mixing will frequently induce entrainment across the thermocline for stratification depths down to at least 12 m. Furthermore, the temperature signal from the ship-induced entrainment is detectable up to 60 km behind the ship (median 13.7 km). Hence, in areas with intense ship traffic, ship-induced entrainment has the potential to increase the nutrient availability and primary production in the upper surface layer, during periods where there is a strong stratification, and the surface layer is depilated of nutrients.

Ship-induced internal waves were also frequently observed in both datasets, although more often in the Oresund dataset (**Paper III**). Similar field observations have previously been made by Watson et al. (1992), who found that stronger stratification and larger ships (180 m long) induced higher amplitude waves. The higher frequency of internal waves in Oresund could thus be due to a stronger stratification, but as the stratification was not known for most of the Gothenburg dataset, this could not be concluded with certainty. The result by Watson et al. (1992) was partly reflected in the Oresund and Gothenburg observations, as several of the largest detected internal waves were induced by very large ships (> 300 m long) (**Paper III**, data not shown). Still, ships of all observed sizes induced internal waves (**Paper III**). Ship-induced internal waves were not studied in detail in this work, and future studies are needed to further investigate their spread and potential impact on vertical mixing.

6.4 ENVIRONMENTAL IMPACT OF THE TURBULENT WAKE

The observed thermal and turbulent wake extents indicate that in areas with intense ship traffic, like the Bornholm shipping lane (**Paper I)** and Oresund (**Paper III)**, a large part of the shipping lane area will be affected by a ship's turbulent wake. Based on the observed thermal wake extents in **Paper I**, 5.8–11.5 % of the Bornholm shipping

lane area would be affected by thermal wakes at any given time. These results indicate that ship-induced turbulence occur at spatiotemporal scales large enough to motivate consideration when assessing and monitoring impacts from shipping on a local and regional level.

The observed and modelled ε (section 4.1.2, **Paper I**, **Paper III**) frequently exceeded $2.5{\cdot}10^{-4}$ $m^2\,s^{-3}$ for 45 s, an exposure shown to increase mortality in copepods (Bickel et al., 2011) and diatoms (Garrison and Tang, 2014). The field samples by Bickel et al. (2011) showed a higher percentage of copepod carcases in the shipping lane (34 %), compared to an undisturbed area outside the shipping lane (~5–6 %). This observation was further supported by laboratory experiments, where the number of dead copepods increased with increasing turbulent intensities. Increased plankton mortality can affect local nutrient availability, as the dead plankton can either be remineralised and release nutrients in the upper surface layer, or sink and remove nutrients from the upper surface layer (Garrison and Tang, 2014, Bickel et al., 2011). In addition, there is a possibility that areas with intense ship traffic, such as shipping lanes, could become barriers for plankton connectivity.

The modelled and observed ship-induced ε levels penetrated deeper (5–15 m) and was 1–3 order of magnitude more intense than naturally occurring wind-induced turbulence (10^{-5} $m^2\,s^{-3}$) (**Paper III**) (Umlauf and Burchard, 2003, Fuchs and Gerbi, 2016, Franks et al., 2022). In the surf zone, higher ε values have been observed, ranging from 10^{-5}–10^{-3} $m^2\,s^{-3}$ (Fuchs and Gerbi, 2016), even reaching 10^{-1} $m^2\,s^{-3}$ at wind speeds > 10 m s^{-1} (Gemmrich and Farmer, 2004). Observations of surface ocean turbulence from the Baltic Sea, have occasionally found ε values > $5{\cdot}10^{-5}$ $m^2\,s^{-3}$, but only during limited time periods and never below 7 m depth (Lass et al., 2003, Zülicke et al., 1998). Thus, at any depth below the breaking wave zone, i.e. 1–2 significant wave heights from the surface (Umlauf and Burchard, 2003), the conditions within the turbulent wake are highly unnatural. Hence, in areas with intense ship traffic, ship-induced turbulence will be an unnatural disturbance in the surface ocean, which should be considered a type of energy pollution.

The observed ship-induced CH_4 emissions (**Paper IV)**, demonstrate that ship passages and the turbulent wake can impact air-sea gas exchange. The emissions were likely ebullition events triggered by the ship-induced pressure changes, and though the relative contribution of the turbulent wake could not be determined, it was likely smaller than the pressure effect. The observed CH_4 fluxes of 11.14 mmol m^{-2} day^{-1} in the Neva Bay shipping lane, indicate that shipping lanes in estuarine and coastal areas are potential hot-spots for ship-induced CH_4 emissions (**Paper IV**). The observed flux is comparable with known large aquatic sources, such as freshwater reservoirs and dams (Deemer et al., 2016, Maeck et al., 2013), lakes (Deemer et al., 2016), estuarine mudflats (Chen et al., 2017, Shalini et al., 2006), and CH_4 ebullition hotspots on the Arctic continental shelf (Thornton et al., 2020). Hence, future estimates of CH_4 emissions in coastal/estuarine areas with intense ship traffic or shipping lanes, should include observations in the ship-affected areas. This suggestion is likely contrasting current sampling behaviour, as shipping lanes are generally avoided during field observations, in fear of contamination and for practical and safety reasons. Still, as all of the major ports in the world (UNCTAD, 2022) are located in shallow waters with CH_4-rich sediments (Zang et al., 2020, Sun et al., 2018, Mao et al., 2022, Borges et al., 2016, Liu et

al., 2022, Jing et al., 2016), the contribution of ship-induced CH_4 emissions to the global aquatic CH_4 budget should be further investigated.

To assess the impact of ship-induced turbulence from all ship passages, in a geographical region, it would be advantageous to integrate an estimate of the turbulent wake impact in existing regional oceanographic biogeochemical models. The combined effect from frequently occurring local events, such as entrainment of nutrient rich water to the surface layer, are difficult to observe *in situ*. Using a modelling approach to assess nutrient input, the cumulative impact from small but frequent entrained volumes of nutrient rich water could be estimated. Regional oceanographic models have been used to assess the impact of the wind and water wake from offshore wind farms (Daewel et al., 2022). However, the spatial and temporal resolution of such models is currently too low to capture the turbulent wake. A simplified estimate of the turbulent wake effects with regards to nutrient input, would be to estimate and sum the total volume of water entrained for each ship passage. However, as the effect from the turbulence itself would not be considered, the estimate would not include the potential effects from stratification-wake interactions, such as internal waves and a potential deepening of the mixed layer due to ship-induced vertical mixing.

6.5 THE IMPACT OF TURBULENT WAKES IS INTERMITTENT AND IS EASILY OVERLOOKED

The large variability in the observed wake extent and intensity, highlights the need for large sample sizes, as the extreme values would likely have been missed if only a limited number of passages had been observed. Knowledge about the variability and extreme values is important, especially when considering the environmental impact. ε intensity is a concrete example where it is important to know the extreme values, since there are known threshold values above which plankton morality is increased (Bickel et al., 2011, Garrison and Tang, 2014). If the observations were averaged over a long time period or a large depth, the averaged values might mask the occurrence of high-intensity periods Moreover, if only a few ship wakes were sampled, the highest values might not be missed altogether. The observation of ship-induced CH_4 emissions is another example of scale-dependency. The observed CH_4 emissions had a short duration, but large magnitude and occurred frequently. However, it is necessary to measure in the right place (in the shipping lane which is usually avoided) and at the right time, or ships as a methane emission-source would have been overlooked. Previous studies have highlighted the challenges associated with observing CH_4 emissions, which are related to the spatiotemporal patchiness of emission/ebullition events (Deemer et al., 2016, Lohrberg et al., 2020, Bastviken et al., 2022). Moreover, the methodological challenges mentioned by Bastviken et al. (2022), in relation to CH_4 flux observations, are similar to the challenges for turbulent wake observations. In short, there is a need to observe multiple spatiotemporal scales simultaneously and the scale of interest lies within the range 0–2 km. The methodological challenges in observing ship-induced turbulence and its impacts in natural conditions, is likely one reason to why ship-induced turbulence from an environmental impact perspective has received little attention until now.

6.6 METHODS DISCUSSION

In this thesis ε was used as a measure of the wakes' turbulent intensity and induced water column mixing, and was calculated using the structure function method (Lucas et

al., 2014) (see details in **Paper I** and **Paper III**). When the current velocity observations are made with a vertical resolution of 1 m (as in **Paper I** and **Paper III**) the structure function method only captures very strong turbulence with vertical eddy scales larger than 2–3 m. This creates a discrepancy between the estimated and actual turbulence, as the small-scale turbulence is not captured. However, as the ship-induced turbulence is very strong and cause large eddies, this loss has been assumed to be comparatively small. Still, the higher levels of ε observed by the S1000 instrument in **Paper III**, indicates that the turbulent length scales are too small for the S500 to make a correct estimate of the dissipation rate. As the S1000 instrument was moored, the higher ε could also be due to increased noise caused by the instrument's movements. Thus, further studies are needed to resolve the cause of the higher observations in S1000, and to evaluate which frequency that are most suitable for estimating the wake turbulence.

Another limitation of using current velocities to estimate turbulence, which has been observed in in **Paper I** and **Paper III,** is that the ship hull, bow wave, and echosounder interfere with the ADCP velocity observations (Figure 7). This makes the first 30 s to 1 min of the turbulent wake observations useless for calculating ε, hence turbulence in the near wake region cannot be estimated using ADCPs (Figure 3b). A microstructure shear prober can be used to capture fine scale turbulence, both at the surface and in the near wake. Still, it will only provide a profile for a single point, and the temporal wake development will thus be low-resolution even if multiple profiles are made. Moreover, to observe the near wake, the profiler needs to be deployed into the wake from the wake-inducing vessel itself. This is because it is very difficult to get in position with another vessel close enough to measuring the near wake (1–2 ship lengths behind the vessel/within the first 30–60 seconds after passage) (Figure 3b) (Kouzoubov et al., 2014)(**Paper III**). In addition, if a separate ship is used to observe the turbulent wake, there is a risk of "turbulence contamination" from the observing ships wake (Franks et al., 2022, Lass et al., 2003). An alternative would be to measure the wake directly from the wake inducing vessel, which is feasible for a smaller vessel, but more challenging when observing wakes from large commercial ships as the ones included in the appended papers. These practical challenges also apply to other type of profilers and can be exemplified by the CTD observations in ship wakes in **Paper III**. The opportunistic CTD observations made in the turbulent wakes of passing ships (**Paper III**), were not a suitable method for observing the ship-induced vertical mixing in the Oresund. This was related to the strong stratification, as the mixing event in the wake was only detectable for a short time before the newly mixed water was re-stratified (**Paper III**) (Lindholm et al., 2001).

For the short time periods needed to observe the ship-induced mixing event, continuous *in situ* CTD measurement would be advantageous. However, a high spatiotemporal resolution of the sensors would be needed to observe changes in the stratification (**Paper III**). Moreover, as CTD sensors need to be in direct contact with the water in the wake region, they cannot be used to observe the turbulent wake, as the string/buoy/mooring would be in the way of the wake-inducing ship. Hence, many of the conventional oceanographic methods used to observe hydrographic features and turbulence, are challenging or even impossible to use when observing the turbulent wake.

CFD modelling can complement in situ observations, as it can simulate the initial part of the near wake region which is so difficult to observe. A CFD model can also be used to test different scenarios, to investigate how different ship types, ship speeds, and stratifications, impact the turbulent wake development. Such tests can be a supplement in the interpretation of complex and noisy field observations, from which the most important governing factors can be difficult to define. Field observations also provide information when interpreting the CFD results, especially regarding the representativeness and scope of the modelled cases. One example is the maximum extent of the turbulent wake. The simulations in **Paper III** and **Paper IV** were run for ca 30 s in full-scale and real time, but the field observations show that the deepest part of the turbulent wake often occur more than 30 s aft of the vessel (**Paper I**, **Paper III**) (Golbraikh and Beegle-Krause, 2020). Thus, the model needs to run for run for several minutes, and for a larger domain, to ensure that the vertical wake development is fully resolved. In contrast, the estimate of the total wake turbulence indicates that CFD models of the near wake are suitable for estimating the turbulent wake intensities, as a large portion of the wake turbulence dissipates within the initial 30 s of the wake. In summary, a methodological approach where field observations are combined with CFD modelling, can provide valuable information when characterising the turbulent wake development.

The results in **Paper IV**, indicate that the observed ship-induced CH_4 emissions were likely triggered by a combination of pressure changes and the turbulent wake. Future studies should combine underwater observations of pressure, the turbulent wake, and CH_4 bubbles (ebullition), as it would increase the mechanistic understanding of the emissions. Using an acoustic instrument for ebullition detection would be ideal, as it can be used to observe the turbulent wake as well. The effect of bubbles and turbulence on air-sea gas exchange is a field of its own, but shipping lanes should be considered as having different conditions compared to undisturbed water, especially in shallow and/or stratified areas where turbulent wakes have the potential to impact the exchange (**Paper IV**).

6.7 IMPLICATIONS FOR FIELD OBSERVATIONS IN TURBULENT WAKES AND SHIPPING LANES

The hydrographic conditions will impact the turbulent wake development, and thereby also the dispersion and dilution of contaminants in the wake. Hence, when sampling contaminant concentrations in shipping lanes or ship wakes, it is necessary to know the hydrographic conditions in order to plan an appropriate sampling design. In stratified conditions, the entrainment of deeper water leads to a deeper and horizontal spread of the wake, and sampling at the surface might completely miss the wake water. Moreover, in stratified waters the wake may have a larger horizontal spread in relation to the shipping lane compared to non-stratified condition. Likewise, dispersions models should consider different types of wake development for stratified and non-stratified conditions and include spreading at and from different depths. For example, the well-established STEAM model used to estimate the spatiotemporal dispersion of different types of contaminants from shipping, currently assumes that all direct discharges from ships to the water are deposited at the sea surface (Jalkanen et al., 2021). This is despite the fact that many of the discharge points on the ship, are located a few meters below surface. As

current velocity and direction vary over depth, the depth at which the wake water distributes will impact the continued dispersion.

The results presented in this thesis, have implications for field observations in shipping lanes, and especially for observations from ships traveling along major shipping lanes (i.e. FerryBox systems), as there is a high likelihood that the sampled water is from the wake of another ship. As the thermal wake was observed to be up to 1°C colder compared to the surrounding water, a large difference considering that the general uncertainty of seawater temperature measurements is in the order of 0.0025°C (e.g. (Schmidt et al., 2016)). Sampling in a thermal wake would hence not be representative for the surrounding water and would significantly increase the sampling uncertainty (**Paper I**). Although the 1°C temperature difference was observed at the surface, the extensive longevity of the thermal wake (estimated median duration 34 min, max 1 h 42 min) indicates that the temperature change was not only in a shallow surface layer, but in the entire wake region. This is supported by the ADCP observations and model results of ship-induced entrainment, as they indicate a change in the entire wake, not only at the surface. Consequently, the impact of ship-induced turbulence should be considered when collecting and interpreting FerryBox data.

7 CONCLUSIONS

This thesis provides new insights regarding turbulent wake development for full-scale ships in naturally stratified waters. The applied interdisciplinary methodological approach, of combining *in situ* observations of the far wake with CFD modelling of the near wake, made it possible to characterise the extent and intensity for the entire turbulent wake. The extensive dataset of turbulent wake observations highlights the large natural variability, and the complexity of turbulent wake development in natural conditions. The spatiotemporal scales of the turbulent wake are challenging to observe and model and the environmental impact from ship-induced turbulence is therefore easily overlooked. The wake characterisation presented in this thesis, is a first step towards assessing the environmental impact of ship-induced turbulence in surface layer of the coastal ocean.

7.1 ANSWERS TO THE RESEARCH QUESTIONS

Objective 1: *To review, test, and develop suitable methodologies and approaches for detecting and characterising turbulent ship wakes and their impact.*

RQ1a: Which available methodologies are suitable for observing turbulent ship wakes and their impact?

During the work with this thesis, a large set of methods and methodological approaches has been tested and developed. The results have shown that ADCP current measurements can be used to estimate ε in the turbulent wake, and that the estimated levels are in good agreement with CFD modelling estimates. Bottom-mounted, upward-facing ADCPs placed under the shipping lane are suitable to observe the vertical and temporal extent of the wake and the interaction between the turbulent wake and stratification. However, the horizontal wake extent was not well captured by a single ADCP, but using multiple ADCPs or a multibeam would likely be able to capture the horizontal extent below surface. SST satellite images were used to observe the spatial extent at sea surface, but a drone would likely be more suitable, as it could more easily be combined with below-surface observations. Due to the interference from the ship echosounder and bow wave, the ADCP observations cannot be used to estimate the initial ~30 s of the turbulent wake development. Therefore, CFD modelling was successfully used to estimate the turbulent wake development for the first 30 s of the wake. When there is a strong stratification, it is challenging to observe any ship-induced changes in stratification using CTD instruments deployed into the wake from the surface, as the buoyancy frequency of the wake water is so high it re-equilibrates before a CTD instrument can be deployed.

RQ1b: To which extent can machine learning models be trained to accurately detect ship wakes in acoustic data, with only a limited dataset to train on?

The developed machine learning model for detecting ship wakes in acoustic data was able to accurately detect ship wakes, except for noisy datasets affected by large waves or migrating plankton. Hence, until a larger training dataset is available, expert annotation and analysis of the acoustic dataset is still needed for noisy data, but the developed machine learning algorithm can help detect a large portion of the wakes.

Objective 2: *Characterise the turbulent wake development with respect to spatiotemporal scales and turbulent intensity, for stratified and non-stratified conditions, using in situ observations and modelling.*

RQ2a: What is the spatiotemporal extent and intensity of turbulent ship wakes?

The observed median ε wake depths were ~12–13 m, and median wake longevities ranged from 4–6 minutes for the ε wake. The maximum observed turbulent wake dimensions were 30 m deep and ~15 min long. The median thermal wake width was 157.5 m and 13.7 km long. The longest observed thermal wake was 62.5 km. The ε-decay rate in the near wake was close to -7/3, and the far wake decay rate was ca -3/5. The observed maximum ε intensities in the far wake were ~10^{-4} m^2 s^{-3}, and the maximum modelled ε intensities in the near wake were ~10^{-2} m^2 s^{-3}.

RQ2b: What are the effects of the interaction between the ship's turbulent wake and stratification?

Ship-induced entrainment of water from below the thermocline, was observed *in situ* and modelled. In addition, satellite images of SST showed frequent and long-lasting thermal wakes, which is concrete evidence of ship-induced entrainment and vertical mixing. The observed entrainment has implications for nutrient cycling and hydrography, in areas with intense ship traffic, but assessment of that impact was beyond the scope of this thesis and should be addressed in future studies. The field observations indicate that a strong stratification reduced the vertical extent of the wake and increased the horizontal extent of the wake, which is in line with previous experimental and numerical modelling studies. Ship-induced internal waves were also frequently observed, more so at the strongly stratified Oresund study site.

Objective 3: *Quantify the impact of ship passages in coastal shipping lanes with respect to energy pollution and ship-induced methane emissions.*

RQ3a: How does the quantity and distribution of ship-induced turbulent mixing compare to the natural wind driven mixing?

The ship-induced turbulent kinetic energy dissipation rate (ε) was 1-3 orders of magnitude higher than generally observed in the upper surface layer, and in the same order of magnitude as in the surf/wave zone at the sea surface. The turbulent wake penetrates much deeper than the surf zone, and the deeper parts of the wake region thus constitutes a very unnatural environment of elevated turbulence.

RQ3b: Which ship related and natural processes govern the magnitude and frequency of ship-induced methane emissions in coastal/estuarine shipping lanes?

Large and frequent CH_4 emissions triggered by ship-passages where observed. The main trigger was likely the ship-induced pressure change at the sea floor. The modelling results indicated that the ship-induced turbulence could reach the sea floor and thus potentially increase the air-sea gas exchange. Larger and faster ships induced large CH_4 emissions more frequently, hence size and speed limitations could be a potential mitigation to reduce the emission.

7.2 CONTRIBUTIONS TO THE FIELD

1) A characterisation of the turbulent wake extent and intensity based on an extensive and unique dataset of *in situ* observations combined with CFD modelling, for stratified and non-stratified conditions

2) Estimates of the energy pollution from ship-induced turbulence in the surface ocean in shipping lanes

3) Novel observations and quantification of ship-induced methane release in shallow coastal shipping lanes

4) The first steps in resolving some of the complexities related to wake development in natural waters

5) Contributing to the discussion of scale-dependence and the need to consider the relevant scales

6) Constitutes the first comprehensive work focusing on characterising the turbulent wake from an environmental impact perspective

8 FUTURE OUTLOOK

Future studies of the turbulent wake should continue to include different spatiotemporal scales when observing and simulating the wake development and impact. The governing parameters for the turbulent wake development should be furthered studied, as the large variation in the observed turbulent wakes have not been fully explained within the work of this thesis. The characteristics of turbulent wake development in stratified waters, should be integrated in modelling estimates of pollution dispersion. The ship-induced internal waves should be further investigated, especially in relation to their potential contribution to diapycnal mixing. The impact of ship-induced turbulence on plankton should also be further studied, and especially with regards to the impact of shipping lanes on connectivity and biogeochemical cycles. The processes governing ship-triggered CH_4 emissions should be further investigated, and include *in situ* observations of pressure, and CH_4 flux/ebullition from the sediment to the atmosphere. The modelling estimate of the wake development should be further expanded, for example by using CFD model output of the near wake as input in a 2D+time general circulation model, which could work as an intermediate step between CFD models and regional oceanographic models.

9 REFERENCES

Andersson, K., Brynolf, S., Lindgren, J.and Wilewska-Bien, M. 2016. Shipping and the Environment - Improving Environmental Performance in Marine Transportation.

Balcombe, P., Brierley, J., Lewis, C., Skatvedt, L., Speirs, J., Hawkes, A.and Staffell, I. 2019. How to decarbonise international shipping: Options for fuels, technologies and policies. Energ. Convers. Manage., 182, 72-88.

Bange, H. W., Bartell, U. H., Rapsomanikis, S.and Andreae, M. O. 1994. Methane in the Baltic and North Seas and a reassessment of the marine emissions of methane. Global Biogeochemical Cycles, 8, 465-480.

Bastviken, D., Wilk, J., Duc, N. T., Gålfalk, M., Karlson, M., Neset, T.-S., Opach, T., Enrich-Prast, A.and Sundgren, I. 2022. Critical method needs in measuring greenhouse gas fluxes. Environmental Research Letters, 17, 104009.

Beecken, J., Mellqvist, J., Salo, K., Ekholm, J., Jalkanen, J. P., Johansson, L., Litvinenko, V., Volodin, K.and Frank-Kamenetsky, D. A. 2015. Emission factors of SO2, NOx and particles from ships in Neva Bay from ground-based and helicopter-borne measurements and AIS-based modeling. Atmos. Chem. Phys., 15, 5229-5241.

Benilov, A., Bang, G., Safray, A.and Tkachenko, I. Ship wake detectability in the ocean turbulent environment. 23rd Symposium on Naval Hydrodynamics, 2001 Val de Reuil, France.

Bickel, S. L., Malloy Hammond, J. D.and Tang, K. W. 2011. Boat-generated turbulence as a potential source of mortality among copepods. Journal of Experimental Marine Biology and Ecology, 401, 105-109.

Bonaglia, S., Rütting, T., Kononets, M., Stigebrandt, A., Santos, I. R.and Hall, P. O. 2022. High methane emissions from an anoxic fjord driven by mixing and oxygenation. Limnology and Oceanography Letters, 7, 392-400.

Borges, A. V., Champenois, W., Gypens, N., Delille, B.and Harlay, J. 2016. Massive marine methane emissions from near-shore shallow coastal areas. Scientific reports, 6, 1-8.

Borges, A. V., Speeckaert, G., Champenois, W., Scranton, M. I.and Gypens, N. 2018. Productivity and Temperature as Drivers of Seasonal and Spatial Variations of Dissolved Methane in the Southern Bight of the North Sea. Ecosystems, 21, 583-599.

Brækken, A., Gabrielii, C.and Nord, N. 2023. Energy use and energy efficiency in cruise ship hotel systems in a Nordic climate. Energy Conversion and Management, 288, 117121.

Brenner, S., Thomson, J., Rainville, L., Torres, D., Doble, M., Wilkinson, J.and Lee, C. 2023. Acoustic Sensing of Ocean Mixed Layer Depth and Temperature from Uplooking ADCPs. Journal of Atmospheric and Oceanic Technology, 40, 53-64.

Brucker, K. A.and Sarkar, S. 2010. A comparative study of self-propelled and towed wakes in a stratified fluid. Journal of Fluid Mechanics, 652, 373-404.

Bussmann, I., Brix, H., Flöser, G., Ködel, U.and Fischer, P. 2021. Detailed patterns of methane distribution in the German Bight. Frontiers in Marine Science, 8, 728308.

Byrne, C. D., Law, R. J., Hudson, P. M., Thain, J. E.and Fileman, T. W. 1988. Measurements of the dispersion of liquid industrial waste discharged into the wake of a dumping vessel. Water Research, 22, 1577-1584.

Carrica, P., Bonetto, F., Drew, D.and Lahey Jr, R. 1998. The interaction of background ocean air bubbles with a surface ship. International journal for numerical methods in fluids, 28, 571-600.

Carrica, P. M., Drew, D., Bonetto, F.and Lahey, R. T. 1999. A polydisperse model for bubbly two-phase flow around a surface ship. International Journal of Multiphase Flow, 25, 257-305.

Chen, X., Schäfer, K. V.and Slater, L. 2017. Methane emission through ebullition from an estuarine mudflat: 2. Field observations and modeling of occurrence probability. Water Resour. Res, 53, 6439-6453.

Chou, H.-T. 1996. On the dilution of liquid waste in ships' wakes. Journal of Marine Science and Technology, 1, 149-154.
Colbo, K., Ross, T., Brown, C.and Weber, T. 2014. A review of oceanographic applications of water column data from multibeam echosounders. Estuarine, Coastal and Shelf Science, 145, 41-56.
Corbett, J. J., Fischbeck, P. S.and Pandis, S. N. 1999. Global nitrogen and sulfur inventories for oceangoing ships. Journal of Geophysical Research: Atmospheres, 104, 3457-3470.
Daewel, U., Akhtar, N., Christiansen, N.and Schrum, C. 2022. Offshore wind farms are projected to impact primary production and bottom water deoxygenation in the North Sea. Communications Earth & Environment, 3, 292.
Deemer, B. R., Harrison, J. A., Li, S., Beaulieu, J. J., DelSontro, T., Barros, N., Bezerra-Neto, J. F., Powers, S. M., Dos Santos, M. A.and Vonk, J. A. 2016. Greenhouse gas emissions from reservoir water surfaces: a new global synthesis. Bioscience, 66, 949-964.
Duarte, C. M., Chapuis, L., Collin, S. P., Costa, D. P., Devassy, R. P., Eguiluz, V. M., Erbe, C., Gordon, T. A., Halpern, B. S.and Harding, H. R. 2021. The soundscape of the Anthropocene ocean. Science, 371.
Dubrovin, K., Golbraikh, E., Gedalin, M.and Soloviev, A. 2011. Turbulent viscosity variability in self-preserving far wake with zero net momentum. Physical Review E, 84, 027302.
Egger, M., Lenstra, W., Jong, D., Meysman, F. J. R., Sapart, C. J., van der Veen, C., Röckmann, T., Gonzalez, S.and Slomp, C. P. 2016. Rapid Sediment Accumulation Results in High Methane Effluxes from Coastal Sediments. PLOS ONE, 11, e0161609.
Egger, M., Riedinger, N., Mogollón, J. M.and Jørgensen, B. B. 2018. Global diffusive fluxes of methane in marine sediments. Nature Geoscience, 11, 421-425.
Emerson, S.and Bushinsky, S. 2016. The role of bubbles during air-sea gas exchange. J. Geophys. Res.-Oceans, 121, 4360-4376.
Ermakov, S. A.and Kapustin, I. A. 2010. Experimental study of turbulent-wake expansion from a surface ship. Izv. Atmos. Ocean. Phy+, 46, 524-529.
ESA. 2023. Sentinel-2 overview [Online]. European Space Agency (ESA). Available: https://www.esa.int/Applications/Observing_the_Earth/Copernicus/Sentinel-2_overview [Accessed July 20 2023].
Esmaeilpour, M., Martin, J. E.and Carrica, P. M. 2016. Near-field flow of submarines and ships advancing in a stable stratified fluid. Ocean Engineering, 123, 75-95.
European Parliament 2008. Directive 2008/56/EC of the European Parliament and of the Council of 17 June 2008 establishing a framework for community action in the field of marine environmental policy (Marine Strategy Framework Directive). Official Journal of the European Union L, 164, 19-40.
Francisco, F., Carpman, N., Dolguntseva, I.and Sundberg, J. 2017. Use of Multibeam and Dual-Beam Sonar Systems to Observe Cavitating Flow Produced by Ferryboats: In a Marine Renewable Energy Perspective. J. Mar. Sci. Eng., 5, 30.
Franks, P. J. S., Inman, B. G., MacKinnon, J. A., Alford, M. H.and Waterhouse, A. F. 2022. Oceanic turbulence from a planktonic perspective. Limnology and Oceanography, 67, 348-363.
Fredriksson, S. T., Arneborg, L., Nilsson, H., Zhang, Q.and Handler, R. A. 2016. An evaluation of gas transfer velocity parameterizations during natural convection using DNS. Journal of Geophysical Research-Oceans, 121, 1400-1423.
Fu, H.and Wan, P. 2011. Numerical simulation on ship bubbly wake. J. Mar. Sci. Appl., 10, 413-418.
Fu, M., Liu, H., Jin, X.and He, K. 2017. National- to port-level inventories of shipping emissions in China. Environmental Research Letters, 12, 114024.
Fuchs, H. L.and Gerbi, G. P. 2016. Seascape-level variation in turbulence-and wave-generated hydrodynamic signals experienced by plankton. Progress in Oceanography, 141, 109-129.
Fujimura, A., Soloviev, A., Rhee, S. H.and Romeiser, R. 2016. Coupled Model Simulation of Wind Stress Effect on Far Wakes of Ships in SAR Images. IEEE T. Geosci. Remote, 54, 2543-2551.

Gabel, F., Lorenz, S.and Stoll, S. 2017. Effects of ship-induced waves on aquatic ecosystems. Sci. Total Environ., 601-602, 926-939.
Garrison, H. S.and Tang, K. W. 2014. Effects of episodic turbulence on diatom mortality and physiology, with a protocol for the use of Evans Blue stain for live–dead determinations. Hydrobiologia, 738, 155-170.
Gemmrich, J. R.and Farmer, D. M. 2004. Near-surface turbulence in the presence of breaking waves. Journal of Physical Oceanography, 34, 1067-1086.
Gentemann, C. L., Wentz, F. J., Brewer, M., Hilburn, K.and Smith, D. 2010. Passive Microwave Remote Sensing of the Ocean: An Overview. In: Barale, V., Gower, J. F. R. & Alberotanza, L. (eds.) Oceanography from Space: Revisited. Dordrecht: Springer Netherlands.
Gilman, M., Soloviev, A.and Graber, H. 2011. Study of the far wake of a large ship. J. Atmos. Ocean. Tech., 28, 720-733.
Golbraikh, E.and Beegle-Krause, C. 2020. A model for the estimation of the mixing zone behind large sea vessels. Environmental Science and Pollution Research, 27, 37911-37919.
Golbraikh, E., Eidelman, A.and Soloviev, A. 2013. On helical behavior of turbulence in the ship wake. Journal of Hydrodynamics, Ser. B, 25, 83-90.
Gritskevich, M. S., Garbaruk, A. V., Schütze, J.and Menter, F. R. 2012. Development of DDES and IDDES formulations for the k-ω shear stress transport model. Flow Turbulence and Combustion, 88, 431.
Grönholm, T., Mäkelä, T., Hatakka, J., Jalkanen, J.-P., Kuula, J., Laurila, T., Laakso, L.and Kukkonen, J. 2021. Evaluation of Methane Emissions Originating from LNG Ships Based on the Measurements at a Remote Marine Station. Environmental Science & Technology, 55, 13677-13686.
Guidi, L., Fernandez Guerra, A., Canchaya, C., Curry, E., Foglini, F., Irisson, J.-O., Malde, K., Marshall, C. T., Obst, M., Ribeiro, R. P., Tjiputra, J.and Bakker, D. C. E. (2020). Big Data in Marine Science. Alexander, B., Heymans, J. J., Muñiz Piniella, A., Kellett, P. & Coopman, J. [Eds.]. Future Science Brief 6 of the European Marine Board, Ostend, Belgium.
Guo, X., Yu, Q., Li, R., Alm, C. O., Calvelli, C., Shi, P.and Haake, A. An expert-in-the-loop paradigm for learning medical image grouping. Pacific-Asia Conference on Knowledge Discovery and Data Mining, 2016. Springer, 477-488.
Gutiérrez-Loza, L., Wallin, M. B., Sahlée, E., Nilsson, E., Bange, H. W., Kock, A.and Rutgersson, A. 2019. Measurement of air-sea methane fluxes in the Baltic Sea using the eddy covariance method. Frontiers in Earth Science, 7, 93.
Gülzow, W., Rehder, G., Schneider v Deimling, J., Seifert, T.and Tóth, Z. 2013. One year of continuous measurements constraining methane emissions from the Baltic Sea to the atmosphere using a ship of opportunity. Biogeosciences, 10, 81-99.
Halpern, B. S., Frazier, M., Afflerbach, J., Lowndes, J. S., Micheli, F., O'Hara, C., Scarborough, C.and Selkoe, K. A. 2019. Recent pace of change in human impact on the world's ocean. Scientific reports, 9, 11609.
Hassellöv, I., Larsson, K.and Sundblad, E. (2019). Effekter på havsmiljön av att flytta över godstransporter från vägtrafik till sjöfart. Rapport nr 2019:5. Rapport nr 2019:5.
He, K., Zhang, X., Ren, S.and Sun, J. Deep Residual Learning for Image Recognition. 2016 IEEE Conference on Computer Vision and Pattern Recognition (CVPR), 27-30 June 2016 2016. 770-778.
HELCOM (2010). Maritime Activities in the Baltic Sea—An Integrated Thematic Assessment on Maritime Activities and Response to Pollution at Sea in the Baltic Sea Region, Balt. Sea Environ. Proc. No. 123. Helsinki, Finland.
HELCOM (2018). HELCOM Assessment on maritime activities in the Baltic Sea 2018. Baltic Sea Environment Proceedings No.152. Helsinki, Finland.
HELCOM. 2021. HELCOM Map and Data Service [Online]. Available: https://maps.helcom.fi/website/mapservice/ [Accessed 11 October 2021].

HELCOM. 2023. HELCOM Map and Data Service [Online]. Available: https://maps.helcom.fi/website/mapservice/ [Accessed 26 July 2023].
Hoekstra, M.and Aalbers, A. Macro wake measurements for a range of ships. Proc. 21st Symp. Naval Hydrodyn, 1997. 278-290.
Hoekstra, M.and Ligtelijn, J. 1991. Macro wake features of a range of ships. MARIN Rep**,** 410461-1.
Hofmann, H., Federwisch, L.and Peeters, F. 2010. Wave-induced release of methane: Littoral zones as source of methane in lakes. Limnology and Oceanography*,* 55**,** 1990-2000.
Holzinger, A. 2016. Interactive machine learning for health informatics: when do we need the human-in-the-loop? Brain Informatics*,* 3**,** 119-131.
Horne, J. K. 2000. Acoustic approaches to remote species identification: a review. Fisheries Oceanography*,* 9**,** 356-371.
Humborg, C., Geibel, M. C., Sun, X., McCrackin, M., Mörth, C.-M., Stranne, C., Jakobsson, M., Gustafsson, B., Sokolov, A.and Norkko, A. 2019. High emissions of carbon dioxide and methane from the coastal Baltic Sea at the end of a summer heat wave. Frontiers in Marine Science*,* 6**,** 493.
Inall, M. E., Toberman, M., Polton, J. A., Palmer, M. R., Green, J. A. M.and Rippeth, T. P. 2021. Shelf Seas Baroclinic Energy Loss: Pycnocline Mixing and Bottom Boundary Layer Dissipation. Journal of Geophysical Research: Oceans*,* 126**,** e2020JC016528.
IPCC 2022. Summary for Policymakers. In*:* Shukla, P. R., Skea, J., Slade, R., Khourdajie, A. A., Diemen, R. V., Mccollum, D., Pathak, M., Some, S., Vyas, P., Fradera, R., Belkacemi, M., Hasija, A., Lisboa, G., Luz, S. & Malley, J. (eds.) Climate Change 2022: Mitigation of Climate Change. Contribution of Working Group III to the Sixth Assessment Report of the Intergovernmental Panel on Climate Change. Cambridge, UK and New York, NY, USA: Cambridge University Press.
Issa, V.and Daya, Z. A. 2014. Modeling the turbulent trailing ship wake in the infrared. Applied Optics*,* 53**,** 4282-4296.
Jacobs, C. T. 2020. Modelling a Moving Propeller System in a Stratified Fluid Using OpenFOAM. Fluids*,* 5**,** 217.
Jalkanen, J. P., Brink, A., Kalli, J., Pettersson, H., Kukkonen, J.and Stipa, T. 2009. A modelling system for the exhaust emissions of marine traffic and its application in the Baltic Sea area. Atmos. Chem. Phys.*,* 9**,** 9209-9223.
Jalkanen, J. P., Johansson, L., Wilewska-Bien, M., Granhag, L., Ytreberg, E., Eriksson, K. M., Yngsell, D., Hassellöv, I. M., Magnusson, K., Raudsepp, U., Maljutenko, I., Styhre, L., Winnes, H.and Moldanova, J. 2020. Modeling of discharges from Baltic Sea shipping. Ocean Science Discussions*,* 2020**,** 1-54.
Jalkanen, J. P., Johansson, L., Wilewska-Bien, M., Granhag, L., Ytreberg, E., Eriksson, K. M., Yngsell, D., Hassellöv, I. M., Magnusson, K., Raudsepp, U., Maljutenko, I., Winnes, H.and Moldanova, J. 2021. Modelling of discharges from Baltic Sea shipping. Ocean Science*,* 17**,** 699-728.
Jing, H., Cheung, S., Zhou, Z., Wu, C., Nagarajan, S.and Liu, H. 2016. Spatial Variations of the Methanogenic Communities in the Sediments of Tropical Mangroves. PLOS ONE*,* 11**,** e0161065.
Joint Committee for Guides in Metrology 2008. Evaluation of measurement data—Guide to the expression of uncertainty in measurement. JCGM*,* 100**,** 1-116.
Jürgensen, C. Vertical mixing due to ship traffic and consequences for the Baltic Sea. Report from IABSE Colloquium, Nyborg, Denmark, 1991. 187-194.
Katz, C. N., Chadwick, D. B., Rohr, J., Hyman, M.and Ondercin, D. 2003. Field measurements and modeling of dilution in the wake of a US navy frigate. Mar. Pollut. Bull.*,* 46**,** 991-1005.
Kelpšaite, L., Parnell, K. E.and Soomere, T. 2009. Energy pollution: the relative influence of wind-wave and vessel-wake energy in Tallinn Bay, the Baltic Sea. Journal of Coastal Research**,** 812-816.

Kouzoubov, A., Wood, S.and Ellem, R. Acoustic imaging of surface ship wakes. INTER-NOISE and NOISE-CON Congress and Conference Proceedings, 2014. Institute of Noise Control Engineering, 3685-3694.
Krizhevsky, A., Sutskever, I.and Hinton, G. E. 2012. Imagenet classification with deep convolutional neural networks. Advances in neural information processing systems, 25, 1097-1105.
Lass, H. U., Prandke, H.and Liljebladh, B. 2003. Dissipation in the Baltic proper during winter stratification. Journal of Geophysical Research: Oceans, 108.
Lavery, A. C., Chu, D.and Moum, J. N. 2010. Observations of Broadband Acoustic Backscattering From Nonlinear Internal Waves: Assessing the Contribution From Microstructure. IEEE Journal of Oceanic Engineering, 35, 695-709.
LeCun, Y., Bengio, Y.and Hinton, G. 2015. Deep learning. Nature, 521, 436-444.
Leppäranta, M.and Myrberg, K. 2009. Physical oceanography of the Baltic Sea, Springer Science & Business Media.
Lewis, R. E. 1985. The dilution of waste in the wake of a ship. Water Research, 19, 941-945.
Liang, J.-H. 2020. Studying the Role of Gas Bubbles on Air-Sea Gas Transfer Using Computer Models. In: Vlahos, P. & Monahan, E. C. (eds.) Recent Advances in the Study of Oceanic Whitecaps: Twixt Wind and Waves. Cham: Springer International Publishing.
Liefvendahl, M.and Wikström, N. (2016). Modelling and simulation of surface ship wake signatures, Report FOI-R--4344--SE. Stockholm. ISSN: xx. ISBN: xx. doi.
Lin, J.-T.and Pao, Y.-H. 1979. Wakes in stratified fluids. Annual Review of Fluid Mechanics, 11, 317-338.
Lindholm, T., Svartström, M., Spoof, L.and Meriluoto, J. 2001. Effects of ship traffic on archipelago waters off the Långnäs harbour in Åland, SW Finland. Hydrobiologia, 444, 217-225.
Liu, S., Gao, Q., Wu, J., Xie, Y., Yang, Q., Wang, R., Zhang, J.and Liu, Q. 2022. Spatial distribution and influencing mechanism of CO2, N2O and CH4 in the Pearl River Estuary in summer. Sci. Total Environ, 846, 157381.
Loberto, A. 2007. An Experimental study of the mixing performance of boat propellers. Queensland University of Technology.
Loehr, L., Mearns, A.and George, K. (2001). Initial report on the 10 July 2011 study of opportunity: currents and wake turbulence behind cruise ships.
Loehr, L. C., Beegle-Krause, C.-J., George, K., McGee, C. D., Mearns, A. J.and Atkinson, M. J. 2006. The significance of dilution in evaluating possible impacts of wastewater discharges from large cruise ships. Mar. Pollut. Bull., 52, 681-688.
Lohrberg, A., Schmale, O., Ostrovsky, I., Niemann, H., Held, P.and Schneider von Deimling, J. 2020. Discovery and quantification of a widespread methane ebullition event in a coastal inlet (Baltic Sea) using a novel sonar strategy. Scientific reports, 10, 4393.
Lucas, N., Simpson, J., Rippeth, T.and Old, C. 2014. Measuring turbulent dissipation using a tethered ADCP. J. Atmos. Ocean. Tech., 31, 1826-1837.
Lundevall-Zara, M., Lundevall-Zara, E.and Brüchert, V. 2021. Sea-air exchange of methane in shallow inshore areas of the Baltic Sea. Frontiers in Marine Science, 8, 657459.
Maeck, A., DelSontro, T., McGinnis, D. F., Fischer, H., Flury, S., Schmidt, M., Fietzek, P.and Lorke, A. 2013. Sediment Trapping by Dams Creates Methane Emission Hot Spots. Environmental Science & Technology, 47, 8130-8137.
Maeck, A., Hofmann, H.and Lorke, A. 2014. Pumping methane out of aquatic sediments–ebullition forcing mechanisms in an impounded river. Biogeosciences, 11, 2925-2938.
Malde, K., Handegard, N. O., Eikvil, L.and Salberg, A.-B. 2019. Machine intelligence and the data-driven future of marine science. ICES Journal of Marine Science.
Mao, S.-H., Zhang, H.-H., Zhuang, G.-C., Li, X.-J., Liu, Q., Zhou, Z., Wang, W.-L., Li, C.-Y., Lu, K.-Y., Liu, X.-T., Montgomery, A., Joye, S. B., Zhang, Y.-Z.and Yang, G.-P. 2022. Aerobic oxidation of methane significantly reduces global diffusive methane emissions from shallow marine waters. Nature communications, 13, 7309.

Marmorino, G.and Trump, C. 1996. Preliminary side-scan ADCP measurements across a ship's wake. J. Atmos. Ocean. Tech., 13, 507-513.
Mattson, M. D.and Likens, G. E. 1990. Air pressure and methane fluxes. Nature, 347, 718-719.
Menter, F. R., Kuntz, M.and Langtry, R. Ten years of industrial experience with the SST turbulence model. Proceedings of the fourth international symposium on turbulence, heat and mass transfer, 2003 Antalya, Turkey. Begell House, 625-632.
Merritt, G. E. 1972. Wake laboratory experiment. CAL NOSC-5047-A-2, Cornell Aeronaut Lab, Buffalo, NY.
Micoli, L., Coppola, T.and Turco, M. 2021. A Case Study of a Solid Oxide Fuel Cell Plant on Board a Cruise Ship. J. Mar. Sci. Appl., 20, 524-533.
Middelburg, J. J., Nieuwenhuize, J., Iversen, N., Høgh, N., de Wilde, H., Helder, W., Seifert, R.and Christof, O. 2002. Methane distribution in European tidal estuaries. Biogeochemistry, 59, 95-119.
Milgram, J., Skop, R. A., Peltzer, R. D.and Griffin, O. M. 1993. Modeling short sea wave energy distributions in the far wakes of ships. Journal of Geophysical Research: Oceans, 98, 7115-7124.
Millefiori, L. M., Braca, P., Zissis, D., Spiliopoulos, G., Marano, S., Willett, P. K.and Carniel, S. 2021. COVID-19 impact on global maritime mobility. Scientific reports, 11, 18039.
Moldanová, J., Fridell, E., Matthias, V., Hassellöv, I.-M., Eriksson, M., Jalkanen, J.-P., Tröeltzsch, J., Quante, M., Johansson, L.and Majutenko, I. (2018). Information on completed BONUS SHEBA project. Hamburg, Germany.
Muchowski, J., Umlauf, L., Arneborg, L., Holtermann, P., Weidner, E., Humborg, C.and Stranne, C. 2022. Potential and Limitations of a Commercial Broadband Echo Sounder for Remote Observations of Turbulent Mixing. Journal of Atmospheric and Oceanic Technology, 39, 1985-2003.
Myllykangas, J.-P. 2020. Methane processes in the coastal sediments and water column of the Baltic Sea. Doctoral thesis, University of Helsinki.
Myllykangas, J.-P., Hietanen, S.and Jilbert, T. 2020. Legacy Effects of Eutrophication on Modern Methane Dynamics in a Boreal Estuary. Estuaries and coasts, 43, 189-206.
NDRC 1946. The Physics of Sound in the Sea. United States Office of Scientific Research and Development, National Defense Research Committee, Division 6. Washington, D.C.
Nilsson, M.M., Kononets, M., Ekeroth, N., Viktorsson, L., Hyl!en, A., Sommer, S., Pfannkuche, O., Almroth-Rosell, E., Atamanchuk, D., Andersson, J.H., Roos, P., Tengberg, A., Hall, P.O.J. 2019. Organic carbon recycling in Baltic Sea sediments – an integrated estimate on the system scale based on in situ measurements. Mar. Chem. **20**, 81–93.
Nilsson M., A. Hylén, N. Ekeroth, M. Kononets, L. Viktorsson, E. Almroth-Rosell, P. Roos, A. Tengberg & P.O.J.Hall 2021. Particle shuttling and oxidation capacity of sedimentary organic carbon on the Baltic Sea system scale: Marine Chemistry, **232**, 1-10.
Parmhed, O.and Svennberg, U. 2006. Simulering av luftbubblor och ytvågor runt ytfartyg, Repot FOI-R-2217-SE. Tumba.
Popper, A. N.and Hawkins, A. 2016. The effects of noise on aquatic life II, Springer.
Reed, A. M.and Milgram, J. H. 2002. Ship wakes and their radar images. Annual Review of Fluid Mechanics, 34, 469.
Reissmann, J. H., Burchard, H., Feistel, R., Hagen, E., Lass, H. U., Mohrholz, V., Nausch, G., Umlauf, L.and Wieczorek, G. 2009. Vertical mixing in the Baltic Sea and consequences for eutrophication–A review. Progress in Oceanography, 82, 47-80.
Ren, M., Zeng, W., Yang, B.and Urtasun, R. 2018. Learning to Reweight Examples for Robust Deep Learning. In: Jennifer, D. & Andreas, K. (eds.) Proceedings of the 35th International Conference on Machine Learning. Proceedings of Machine Learning Research: PMLR.

Rippeth, T. P., Lincoln, B. J., Kennedy, H. A., Palmer, M. R., Sharples, J.and Williams, C. A. J. 2014. Impact of vertical mixing on sea surface pCO2 in temperate seasonally stratified shelf seas. Journal of Geophysical Research: Oceans, 119, 3868-3882.

Rippeth, T. P., Wiles, P., Palmer, M. R., Sharples, J.and Tweddle, J. 2009. The diapcynal nutrient flux and shear-induced diapcynal mixing in the seasonally stratified western Irish Sea. Continental Shelf Research, 29, 1580-1587.

Rosentreter, J. A., Borges, A. V., Deemer, B. R., Holgerson, M. A., Liu, S., Song, C., Melack, J., Raymond, P. A., Duarte, C. M.and Allen, G. H. 2021. Half of global methane emissions come from highly variable aquatic ecosystem sources. Nature Geoscience, 14, 225-230.

Roth, F., Sun, X., Geibel, M. C., Prytherch, J., Brüchert, V., Bonaglia, S., Broman, E., Nascimento, F., Norkko, A.and Humborg, C. 2022. High spatiotemporal variability of methane concentrations challenges estimates of emissions across vegetated coastal ecosystems. Global Change Biology, 28, 4308-4322.

Römer, M., Riedel, M., Scherwath, M., Heesemann, M.and Spence, G. D. 2016. Tidally controlled gas bubble emissions: A comprehensive study using long-term monitoring data from the NEPTUNE cabled observatory offshore Vancouver Island. Geochemistry, Geophysics, Geosystems, 17, 3797-3814.

Saunois, M., Stavert, A. R., Poulter, B., Bousquet, P., Canadell, J. G., Jackson, R. B., Raymond, P. A., Dlugokencky, E. J., Houweling, S.and Patra, P. K. 2020. The global methane budget 2000–2017. Earth system science data, 12, 1561-1623.

Schmidt, H., Wolf, H.and Hassel, E. 2016. A method to measure the density of seawater accurately to the level of 10− 6. Metrologia, 53, 770.

Schneider, B., Gülzow, W., Sadkowiak, B.and Rehder, G. 2014. Detecting sinks and sources of CO2 and CH4 by ferrybox-based measurements in the Baltic Sea: Three case studies. Journal of Marine Systems, 140, 13-25.

Schultze, L. K. P., Merckelbach, L. M., Horstmann, J., Raasch, S.and Carpenter, J. R. 2020. Increased Mixing and Turbulence in the Wake of Offshore Wind Farm Foundations. Journal of Geophysical Research: Oceans, 125, e2019JC015858.

Sea-web Ships. 2022. IHS Markit. Available: https://maritime.ihs.com [Accessed 8 December 2022].

Shakhova, N., Semiletov, I., Leifer, I., Sergienko, V., Salyuk, A., Kosmach, D., Chernykh, D., Stubbs, C., Nicolsky, D.and Tumskoy, V. 2014. Ebullition and storm-induced methane release from the East Siberian Arctic Shelf. Nature Geoscience, 7, 64-70.

Shalini, A., Ramesh, R., Purvaja, R.and Barnes, J. 2006. Spatial and temporal distribution of methane in an extensive shallow estuary, south India. Journal of Earth System Science, 115, 451-460.

Situ, R.and Brown, R. J. 2013. Mixing and dispersion of pollutants emitted from an outboard motor. Marine Pollution Bulletin, 69, 19-27.

Smirnov, A., Celik, I.and Shi, S. 2005. LES of bubble dynamics in wake flows. Computers and Fluids, 34, 351-373.

Snoeijs-Leijonmalm, P.and Andrén, E. 2017. Biological oceanography of the Baltic Sea, Dordrecht, Netherlands, Springer Science & Business Media.

Soloviev, A., Gilman, M., Young, K., Brusch, S.and Lehner, S. 2010. Sonar measurements in ship wakes simultaneous with TerraSAR-X overpasses. IEEE T. Geosci. Remote, 48, 841-851.

Soloviev, A., Maingot, C., Agor, M., Nash, L.and Dixon, K. 2012. 3D sonar measurements in wakes of ships of opportunity. J. Atmos. Ocean. Tech., 29, 880-886.

Somero, R., Basovich, A.and Paterson, E. G. 2018. Structure and Persistence of Ship Wakes and the Role of Langmuir-Type Circulations. Journal of Ship Research, 62, 241-258.

Soomere, T. 2005. Fast ferry traffic as a qualitatively new forcing factor of environmental processes in non-tidal sea areas: a case study in Tallinn Bay, Baltic Sea. Environmental Fluid Mechanics, 5, 293-323.

Soomere, T. 2007. Nonlinear Components of Ship Wake Waves. Applied Mechanics Reviews, 60, 120-138.

Soomere, T.and Kask, J. 2003. A specific impact of waves of fast ferries on sediment transport processes of Tallinn Bay. Proc. Estonian Acad. Sci. Biol. Ecol*,* 52**,** 319-331.
Stanic, S., Caruthers, J. W., Goodman, R. R., Kennedy, E.and Brown, R. A. 2009. Attenuation measurements across surface-ship wakes and computed bubble distributions and void fractions. IEEE J. Oceanic Eng*.,* 34**,** 83-92.
Steinle, L., Maltby, J., Treude, T., Kock, A., Bange, H. W., Engbersen, N., Zopfi, J., Lehmann, M. F.and Niemann, H. 2017. Effects of low oxygen concentrations on aerobic methane oxidation in seasonally hypoxic coastal waters. Biogeosciences*,* 14**,** 1631-1645.
Stigebrandt, A. 2001. Physical oceanography of the Baltic Sea. A systems analysis of the Baltic Sea. Springer.
Stranne, C., Mayer, L., Jakobsson, M., Weidner, E., Jerram, K., Weber, T. C., Anderson, L. G., Nilsson, J., Björk, G.and Gårdfeldt, K. 2018. Acoustic mapping of mixed layer depth. Ocean Science*,* 14**,** 503-514.
Sun, M. S., Zhang, G. L., Ma, X., Cao, X. P., Mao, X. Y., Li, J., Ye, W. W.and Liu, S. M. 2018. Dissolved methane in the East China Sea: Distribution, seasonal variation and emission. Marine Chemistry*,* 202**,** 12-26.
Swedish Maritime Administration. 2015. Fartygstrafik år 2015 – ALLA fartyg som bär transponderutrustning [Online]. Swedish Maritime Administration. Available: https://sjofartsverket.se/Sjofart/Sjotrafikinformation/Trafikflodesstatistik-fartyg/ [Accessed April 7 2021].
Telesh, I. V., Golubkov, S. M.and Alimov, A. F. 2008. The Neva Estuary Ecosystem. In*:* Schiewer, U. (ed.) Ecology of Baltic Coastal Waters. Berlin, Heidelberg: Springer Berlin Heidelberg.
Tennekes, H.and Lumley, J. L. 1972. A firs Course in Turbulence*,* Cambridge, Massachusetts, and London, England, Massachusetts Institute of Technology.
Thornton, B. F., Prytherch, J., Andersson, K., Brooks, I. M., Salisbury, D., Tjernström, M.and Crill, P. M. 2020. Shipborne eddy covariance observations of methane fluxes constrain Arctic sea emissions. Science Advances*,* 6**,** eaay7934.
Thorpe, S. A. 2007. An introduction to ocean turbulence*,* New York, Cambridge University Press.
Togneri, M., Lewis, M., Neill, S.and Masters, I. 2017. Comparison of ADCP observations and 3D model simulations of turbulence at a tidal energy site. Renewable Energy*,* 114**,** 273-282.
Trevorrow, M. V., Vagle, S.and Farmer, D. M. 1994. Acoustical measurements of microbubbles within ship wakes. Journal of the Acoustical Society of America*,* 95**,** 1922-1930.
Umlauf, L.and Burchard, H. 2003. A generic length-scale equation for geophysical turbulence models. Journal of Marine Research*,* 61**,** 235-265.
UNCTAD (2022). Review of maritime transport 2022, Navigating stormy waters, UNCTAD/RMT/2022. New York. ISSN: xx. ISBN: xx. doi.
US-EPA (2002). Cruise Ship Plume Tracking Survey Report. Washington, D.C. ISSN: xx. ISBN: xx. doi.
USGS. 2023. Landsat 8 [Online]. United States Geological Survey (USGS). Available: https://www.usgs.gov/landsat-missions/landsat-8 [Accessed July 20 2023].
Van Dyk, D. A.and Meng, X.-L. 2001. The art of data augmentation. Journal of Computational and Graphical Statistics*,* 10**,** 1-50.
von Deimling, J. S., Greinert, J., Chapman, N. R., Rabbel, W.and Linke, P. 2010. Acoustic imaging of natural gas seepage in the North Sea: Sensing bubbles controlled by variable currents. Limnology and Oceanography: Methods*,* 8**,** 155-171.
Voropayev, S., Nath, C.and Fernando, H. 2012. Thermal surface signatures of ship propeller wakes in stratified waters. Physics of Fluids*,* 24**,** 116603.
Wall, D.and Paterson, E. 2020. Anisotropic RANS Turbulence Modeling for Wakes in an Active Ocean Environment. Fluids*,* 5**,** 248.
Wall, D. J. 2021. Anisotropic Turbulence Models for Wakes in an Active Ocean Environment*.* Virginia Tech.

Wallenius, A. J., Dalcin Martins, P., Slomp, C. P.and Jetten, M. S. 2021. Anthropogenic and environmental constraints on the microbial methane cycle in coastal sediments. Frontiers in microbiology, 12, 631621.
Wanninkhof, R., Asher, W. E., Ho, D. T., Sweeney, C.and McGillis, W. R. 2009. Advances in Quantifying Air-Sea Gas Exchange and Environmental Forcing. Annual Review of Marine Science, 1, 213-244.
Watson, G., Chapman, R. D.and Apel, J. R. 1992. Measurements of the internal wave wake of a ship in a highly stratified sea loch. Journal of Geophysical Research: Oceans, 97, 9689-9703.
Weber, T., Wiseman, N. A.and Kock, A. 2019. Global ocean methane emissions dominated by shallow coastal waters. Nature communications, 10, 4584.
Weber, T. C., Lyons, A. P.and Bradley, D. L. 2005. An estimate of the gas transfer rate from oceanic bubbles derived from multibeam sonar observations of a ship wake. Journal of Geophysical Research (Oceans), 110.
Weller, H. G., Tabor, G., Jasak, H.and Fureby, C. 1998. A tensorial approach to computational continuum mechanics using object-oriented techniques. Computers in physics, 12, 620-631.
Wiles, P. J., Rippeth, T. P., Simpson, J. H.and Hendricks, P. J. 2006. A novel technique for measuring the rate of turbulent dissipation in the marine environment. Geophysical Research Letters, 33.
Wilkinson, J., Maeck, A., Alshboul, Z.and Lorke, A. 2015. Continuous seasonal river ebullition measurements linked to sediment methane formation. Environmental Science & Technology, 49, 13121-13129.
Wolk, F., Yamazaki, H., Seuront, L.and Lueck, R. G. 2002. A new free-fall profiler for measuring biophysical microstructure. Journal of Atmospheric and Oceanic Technology, 19, 780-793.
Xing, H., Spence, S.and Chen, H. 2020. A comprehensive review on countermeasures for CO2 emissions from ships. Renewable and Sustainable Energy Reviews, 134, 110222.
Yang, J., Zhang, G.-L., Zheng, L.-X., Zhang, F.and Zhao, J. 2010. Seasonal variation of fluxes and distributions of dissolved methane in the North Yellow Sea. Continental Shelf Research, 30, 187-192.
Yassir, A., Jai Andaloussi, S., Ouchetto, O., Mamza, K.and Serghini, M. 2023. Acoustic fish species identification using deep learning and machine learning algorithms: A systematic review. Fisheries Research, 266, 106790.
Zang, K., Zhang, G., Zhao, H., Xu, X., Zheng, N., Wang, J.and Zhang, G. 2020. Multiple factors dominate the distribution of methane and its sea-to-air flux in the Bohai Sea in summer and autumn of 2014. Marine Pollution Bulletin, 154, 111049.
Zülicke, C., Hagen, E.and Stips, A. 1998. Dissipation and mixing in a coastal jet: A Baltic Sea case study. Aquatic Sciences, 60, 220-235.